CELLULAR SENESCENCE IN SKELETAL MUSCLE REGENERATION, AGEING AND DISEASE

Victoria Moiseeva

TESI DOCTORAL UPF / 2022

Thesis supervisors

Dr. Pura Muñoz Cánoves

Dr. Eusebio Perdiguero Santamaría

DEPARTMENT OF MEDICINE AND LIFE SCIENCES

Universitat Pompeu Fabra Barcelona

To my beloved family,

ACKNOWLEDGEMENTS

5 de la mañana, hora habitual de repentina inspiración para los que no tenemos ritmo circadiano, o los “búhos” como dirían en mis tierras natales. Solo que esta vez es más especial y emocionante, estoy escribiendo los agradecimientos de mi tesis. Inevitablemente, es el momento de recapitular y revivir lo más memorable, lo cual me lleva a todos vosotros, la gran familia Puralab.

No hay palabras para transmitir lo importantes que habéis sido para mí cada uno de vosotros. Desde el momento en el que he llegado al laboratorio me he sentido acogida y por ello os estaré eternamente agradecida. Llevaba un tiempo sin sentirme así. Sois un gran grupo, con gente inteligente, capaz y divertida. Estar a vuestro lado me ha hecho crecer muchísimo, ¡Gracias!

A Mireia, ¡mi reina de corazones! Desde el momento en el que te conocí supe que eras una gran persona. Solo se me ocurre lo más bonito al pensar en ti. No sé expresar lo afortunada que me siento de haber compartido estos años contigo y lo especial que es poder terminar esta etapa juntas. Nos hemos podido enfrentar juntas a lo más complicado, y eso lo ha hecho todo menos duro (al menos para mi). Te mereces lo mejor en la vida y espero que sea así en adelante. ¡Gracias por todos los momentos en los que has estado a mi lado (y por despertarme aquel día que casi perdemos el tren en Madrid)! ¡Te quiero un montón!

A Val, mi “espaguetti” favorita. Sin tu apoyo, sesiones de vóley y cafés esto no sería igual. Eres la voz de la razón cuando quiero que arda el edificio (gracias a ti no lo he quemado aún). ¡Gracias por escucharme siempre que lo necesitaba y apoyarme durante este proceso tan tedioso!

A Verita, no sabría agradecerte todo lo que me has ayudado en estos años. Para mi has sido la hermana mayor, que ha velado por mi todo el tiempo que he pasado en el laboratorio. ¡Gracias por toda la ayuda, apoyo, barbacoas en el huerto, las expresiones en checo y la risa contagiosa que me iba alegrando el día!

A Eva, por tu manera de ser y por transmitirme confianza en el día a día. La amante de los gatos, sushi y buena cerveza. No hay cerveza suficiente en el mundo para agradecerte toda tu ayuda y lo mucho que ha significado para mí, pero intentaré compensarlo al menos un poquito =)

A Andrés, la persona con la que puedes mantener conversaciones interesantes sobre cualquier temática. No hace falta decir lo mucho que me has ayudado durante mi tesis, tanto a nivel de trabajo como de ánimos. Ahora nos toca intercambiar los papeles, ¡ánimo, que ya casi estás allí!

A Antonio S., la persona más sigilosa y curiosa del grupo y mi primer contacto con alguien del grupo. Gracias por el tour de bienvenida y por compartir tu conocimiento y ayuda siempre que lo necesitaba y bromas de "russki". ¡Muchas gracias!

A Aida Beà, la compañera de aventuras peligrosas alemanas, la cinnamon rolls and bikes lover; Aida, "La doctora Hielo"; Alex, el que tiene el poder de desaparecer/aparecer como Cheshire y sacar la pareja de Aces 5 veces seguidas; Aina, la chocolatera y la gran capi de "Los hijos de Pura"; Jessica, la persona cuya paciencia y experiencia es de admirar; Oleg, la mente curiosa y poco convencional; Marina, la persona con el asombroso poder de arreglarlo todo, por muy complicado que sea; Laurins, la mami y la persona más acogedora y cálida del grupo; Mercé, la fuente del conocimiento científico y de cualquier otro tipo; cuando sea mayor, quiero ser como tú! ¡Gracias por todo!

A todos los demás compañeros y compañeras de trabajo, gente con la que he compartido experiencias inolvidables: Kostya, Claudia, Guillem, Miguel, María, Alejandra, Alejandro, Javi, Antonio M, Jacob, Pedro, Mónica, Joan, Johanna, Jesús, Yacine, Xiaotong, Silvia, Nacho, José, Ángela, Anna, Marta, Sonia, William, ¡Muchas gracias!

A la unidad de citometría, Alex, Erika, Eva y Oscar, por vuestro conocimiento y conversaciones entretenidas durante el maravilloso ratito de sorting. ¡Gracias!

Al equipo campeón "Spiking Neurons", por los partidos de volei más intensos de la historia del BVPRBB tournament. ¡Gracias!

A mis tutores, Pura y Eusebio. Aún recuerdo el día de mi entrevista, 22 de mayo del año 2016. Ese día supe qué quería hacer y dónde. Salí de la entrevista y sólo podía

pensar en las ganas que tenía de empezar mi tesis en este laboratorio. Era la persona más inspirada del mundo gracias a lo que me transmitisteis aquel día. ¡Gracias por darme esta gran oportunidad, espero haber cumplido lo que prometía!

A Ricard, por ser tan buen amigo desde hace tantísimo tiempo. La persona que ha podido resolver mis dudas incluso cuando yo no podía. Por escucharme y apoyarme siempre. ¡Gracias!

A mi fuente de apoyo incondicional, mi Nyuf que ha estado allí en lo bueno y en lo malo. La persona que da media vuelta y viene a por mí en los momentos más desesperados sin pedírselo, porque me conoce tan bien. El que me manda detalles para animarme cuando el mundo se me cae encima. El que me espera hasta pasada la medianoche en el laboratorio y mucho más. Gracias por compartir mi carga durante tanto tiempo, sé que no ha sido fácil. ¡Gracias por ser tú, t'estimo!

Моей любимой семье, моим самым близким и дорогим. Вы мои корни, люди, которые создали меня и воспитали меня такой какая есть. Я посвящаю эту работу и все мои успехи вам, чтобы вы продолжали мною гордиться, как делали это всегда. Люблю бесконечно!

Ваша дочка, внучка и сестра.

ABSTRACT

Skeletal muscle regeneration requires coordination between muscle stem cells and local-niche cells. In this thesis, we identify senescent cells as novel integral components of the regenerative process. Using a new sorting protocol and single-cell techniques, we isolated *in vivo* senescent cells from damaged muscles and identified three main senescent populations arising from major niche components. A deeper transcriptomic approach of the three major populations isolated from young and geriatric animals at two stages of muscle regeneration unveiled high transcriptomic heterogeneity in the senescent cells and their SASP, with conserved cell identity traits. Senescent cells are generated in response to high oxidative stress and DNA damage during the early regeneration stages. Further pathway analysis identified two universal senescence hallmarks (inflammation and fibrosis) across cell types, regeneration time and ageing. Senescent cells create an "aged-like" inflamed niche, which mirrors inflammation associated with ageing (inflammageing) through their SASP even in young mice. Interactome analysis unveiled unproductive functional interactions between senescent cells and muscle stem cells, blunting muscle stem cell expansion and regeneration. Reduction of senescent cells by pharmacological and genetic approaches accelerates muscle regeneration in young and geriatric mice and ameliorates the disease progression in dystrophic mice. Conversely, transplantation of senescent cells delays regeneration. Targeting the SASP of senescent cells through CD36 neutralization was sufficient to induce accelerated muscle recovery, uncovering CD36 potential as senomorphic *in vivo*. Our results provide a novel technique for isolating *in vivo*-generated senescent cells, defining a senescence blueprint for muscle and uncovering the role of senescent cells in distinct muscle contexts. As senescent cells also accumulate in human muscles, our findings open a potential avenue towards improving muscle repair throughout life.

Keywords: senescence, ageing, muscle stem cells, muscle regeneration, SASP, CD36, inflammageing.

RESUMEN EN CASTELLANO

La regeneración del músculo esquelético requiere la precisa coordinación entre las células madre musculares y las células del nicho local. En esta tesis, hemos identificado a las células senescentes como nuevos componentes integrales del proceso regenerativo. Usando un nuevo protocolo de clasificación y técnicas de secuenciación de células individuales, hemos aislado células senescentes de músculos regenerantes *in vivo* y hemos identificado tres poblaciones senescentes derivadas de los principales componentes celulares del nicho. Tras realizar un análisis transcriptómico profundo de estas tres poblaciones, aisladas de animales jóvenes y geriátricos en dos etapas de la regeneración muscular, hemos determinado que existe una alta heterogeneidad entre los tres tipos de células senescentes y su SASP (fenotipo secretorio de las células senescentes), conservando cada una de ellas los rasgos de identidad celular. Hemos demostrado que las células senescentes se generan durante las primeras etapas de la regeneración muscular en respuesta a la elevación del estrés oxidativo y del daño al ADN. El análisis de las rutas diferencialmente expresadas, identificó dos características universales de la senescencia comunes a los tres tipos celulares, a los dos tiempos de regeneración y a las dos edades: la inflamación y la fibrosis. Las células senescentes, a través de su SASP, generan a su alrededor un nicho inflamado, parecido a la inflamación asociada al envejecimiento (“inflammageing”), incluso en ratones jóvenes. Análisis transcriptómico de las interacciones celulares, reveló la existencia de rutas de señalización improductivas entre las células senescentes y las células madre musculares, que tienen como consecuencia una frenada en su expansión y en la regeneración muscular. Reducción del número de células senescentes mediante técnicas farmacológicas o genéticas induce la aceleración de la regeneración muscular tanto en ratones jóvenes como en geriátricos, y mejora la progresión de la enfermedad en ratones distróficos. Por contra, trasplante de células senescentes retrasa la regeneración. La reducción del SASP mediante neutralización del receptor CD36 induce también la aceleración de la recuperación muscular. Nuestros resultados han proporcionado una nueva técnica para aislar células senescentes *in vivo*, han permitido definir las células senescentes del músculo y su papel en distintos contextos musculares en ratones. Dado que hemos observado que las células senescentes también se acumulan en los músculos de seres humanos, nuestros hallazgos abren la puerta a posibles estrategias terapéuticas para mejorar la reparación muscular a lo largo de la vida.

Palabras clave: senescencia, envejecimiento, regeneración muscular, células madre musculares, CD36, fenotipo secretorio asociado a la senescencia.

PREFACE

The work presented in this Doctoral Thesis was supported by a Predoctoral Fellowship from the Programa de Formación de Personal Investigador (Secretaría de Estado de Investigación, Desarrollo e Innovación, Ministerio de Economía y Competitividad) and was done in the Cell Biology Group at the Department of Medicine and Life Sciences of the Pompeu Fabra University (MELIS-UPF) in Barcelona.

This thesis provides a first to date transcriptomic data of *in vivo*-generated senescent cells and a newly established protocol for isolation of senescent cells from a complex tissue. Additionally, our work describes the contribution of senescent cells to the regenerative process of young, old and dystrophic organisms. This knowledge may help to develop therapeutic strategies to ameliorate the disease progression and accelerate the regeneration in both young and old organisms. Part of this Thesis has been submitted for publication.

TABLE OF CONTENTS

ACKNOWLEDGEMENTS V

ABSTRACT XI

RESUMEN EN CASTELLANO XV

PREFACE XIX

TABLE OF CONTENTS 1

LIST OF ABBREVIATIONS 7

INTRODUCTION 13

1. SKELETAL MUSCLE AND ITS REGENERATION 15
1.1 Function and repair capacity 15
1.2 Cells that participate in muscle regeneration 17
1.3 Muscle regeneration in ageing 22
1.4 Pathological muscle regeneration and Duchenne muscular dystrophy 24

2. CELLULAR SENESCENCE 26
2.1 Hallmarks of senescent cells 26
2.2 The senescence-associated secretory phenotype 27
2.3 Function of senescent cells 30
2.4 Role of senescence in muscle regeneration, ageing and disease 34
2.5 Role of CD36 in cellular senescence 36

OBJECTIVES 39

RESULTS 43

1. KINETICS OF CELLULAR SENESCENCE IN REGENERATING MUSCLE TISSUE 45

2. TRANSCRIPTOMIC CHARACTERIZATION OF ISOLATED SENESCENT CELLS FROM DAMAGED MUSCLE TISSUE 48
2.1 Establishment of an isolation protocol for senescent cells 48

2.2 Transcriptomic atlas of senescent cells in regenerating muscle..... 50
2.3 A novel method for separating distinct types of senescent cells *in vivo* ... 54
2.4 Senescent cells retain their homeostatic identity while gaining lineage-inappropriate traits in old age 58
2.5 Tissue injury drives senescence by inducing severe oxidative stress and DNA damage in a subset of niche cells 62
2.6 Ageing primes niche cells for exacerbated injury-induced senescence 64
2.7 Two major shared hallmarks define senescent cells across cell types, stages of regeneration, and lifespan..... 66

3. ROLE OF SENESCENT CELLS IN MUSCLE REGENERATION 69
3.1 Role of senescent cells in muscle regeneration at young and geriatric age 69
3.2 Role of senescent cells in chronic muscle disease 73
3.3 Senescent cells impact their microenvironment by secreting their SASP...76
3.4 Senescent cells block muscle stem cell expansion through the SASP paracrine actions 80
3.4 Role of the CD36 in the regulation of the SASP and muscle regeneration. 85

DISCUSSION 93

CONCLUSIONS..... 107

MATERIALS AND METHODS 111

REFERENCES..... 129

SUPPLEMENTARY INFORMATION.....151

LIST OF ABBREVIATIONS

#

γH2Ax - gamma H2A histone family member X

17-DMAG - 17-dimethylaminoethyl-amino-17-demethoxygeldanamycin

53BP1 - p53-binding protein 1

A

AKT - protein kinase B

ATM - ataxia telangiectasia mutated

Aβ - amyloid-beta

B

Bcl - B-cell lymphoma

bFGF - basic fibroblast growth factor

bHLH - basic helix-loop-helix

BRD4 - bromodomain-containing protein 4

BrdU – bromodeoxyuridine

C

C/EBPβ - CCAAT/enhancer-binding protein beta

C_{12}FDG - 5-dodecanoylaminofluo-rescein di-β-d-galactopyranoside

CCF - cytosolic chromatin fragments

CCL - C-C motif ligand

CCN1 - cellular communication network factor

CCR2 - C-C motif chemokine receptor 2

CD - cluster of differentiation

cGAS - cyclic GMP–AMP synthase

CHK2 - checkpoint kinase 2

CPM - counts per million

CTX - cardiotoxin

CX3CR1 - C-X3-C motif chemokine receptor 1

CXCL - C-X-C motif ligand family

D

D-dasatinib

DAB - 3,3′-Diaminobenzidine

DAMPs - damage-associated molecular patterns

DAPI - 4,6-diaminido-2-phenylindole

9

DDR – DNA damage response

DE – differentially expressed

DMD – Duchenne muscular dystrophy

DMEM - Dulbecco's Modified Eagle's medium

DMSO - dimethyl sulfoxide

DPI - days post-injury

E

ECM - extracellular matrix

ECs - endothelial cells

EDL - extensor digitorum longus

EdU - ethynyl-labelled deoxyuridine

EGF - epidermal growth factor

ER - endoplasmic reticulum

EVs - extracellular vesicles

F

FACS - fluorescence-activated cell sorting

FAPs - fibro-adipogenic progenitors

FBS - foetal bovine serum

FDR – false discovery rate

FGF2 - fibroblast growth factor 2

FMO - fluorescence minus one

FSC - forward scatter

G

G-CSE - granulocyte colony-stimulating factor

GATA4 - GATA binding protein 4

GC - gastrocnemius

GCV - ganciclovir

GDF - growth differentiation factor

GFP - green fluorescent protein

GMD - galactose-modified duocarmycin

GSEA - gene set enrichment analysis

H

H&E - haematoxylin and eosin

H3K27 - acetylated histone H3 Lys27

HMGB2 - high mobility group box 2

HSP90 - heat shock protein 90

HSV-TK - herpes simplex virus 1 thymidine kinase

I

IFNγ - interferon gamma
IGF-1 - insulin-like growth factor 1
IL - interleukin
IL-4R - interleukin 4 receptor
iNOS - inducible nitric oxide synthetase

J

JAK - Janus kinase 2

L

L-R – ligand-receptor
LINE-1 - long-interspersed element 1
Lmnb1 - lamin B1
Ly6C - lymphocyte antigen 6C

M

MCs - myeloid cells
MIF - macrophage migration inhibitory factor
MLL1 - mixed-lineage leukaemia 1
MMPs - matrix metalloproteinases
mRFP - monomeric red-fluorescent protein
MRFs - muscle regulatory factors
mTOR - mammalian target of rapamycin
Myf5 - myogenic factor 5
MyoD - myogenic differentiation antigen

N

NAC - N-acetylcysteine
NAD - nicotinamide adenine dinucleotide
NBS1 - Nijmegen breakage syndrome 1
NCAM - neural cell-adhesion molecule
NFκB - nuclear factor kappa-light-chain-enhancer of activated B cells
NK – natural killer
NOTCH1 - neurogenic locus notch homolog protein 1
NR - nicotinamide riboside
NTX – notexin

O

oxLDL - oxidized low-density lipoprotein
OXR1 - oxidation-resistant 1

P

p38MAPK - mitogen-activated protein kinase p38
PAI-1 - plasminogen activator inhibitor 1
Pax - paired-box transcription factor
PBS - phosphate buffered saline
PCA - principal component analysis
PDGF-AA - platelet-derived growth factor AA
PDGFRα - platelet-derived growth factor receptor alpha
PGE2 - prostaglandin E2
PI3K - phosphatidylinositol 3-kinase

Q

Q - quercetin
QA – quadriceps

R

RelA - v-rel avian reticulo-endotheliosis viral oncogene homolog A
ROS - reactive oxygen species
RPKM - reads per kilobase per million mapped reads

S

SA-β-gal - senescence-associated β-galactosidase
SAHF - senescence-associated heterochromatin foci
SASP - senescence-associated secretory phenotype
Sca-1 - stem cell antigen 1
scRNA-seq - single-cell RNA sequencing
SCs - satellite cells

SERPINs - serine/cysteine proteinase inhibitors
sIL6R - soluble interleukin-6 receptor alpha
SMMCs - smooth muscle-mesenchymal cells
SSC – side scatter
SPIA - signalling pathway impact analysis
STAT - signal transducer and activator of transcription
STING - stimulator of interferon genes

T

TA – tibialis anterior
TCF4 - transcription factor 4
TF – transcription factor
TGFβ - transforming growth factor beta
TGFβR1 - transforming growth factor beta receptor 1
TIMPs - tissue inhibitors of metalloproteinases
TMM - trimmed mean of M-values
TNFα - tumour necrosis factor alpha
tPA - tissue plasminogen activator
TPM - transcripts per million
Tregs - regulatory T-cells
TUNEL - terminal deoxynucleotidyl transferase biotin-dUTP nick end labelling

U

UMAP - uniform manifold approximation and projection
uPA - urokinase-type plasminogen activator
uPAR - urokinase-type plasminogen activator receptor

W

WISP1 - WNT1-inducible-signalling pathway protein 1
WT - wild-type

INTRODUCTION

1. SKELETAL MUSCLE AND ITS REGENERATION

1.1 Function and repair capacity

Skeletal muscle is one of the largest organ systems in the human body, comprising around 40% of the total mass[1,2]. Skeletal muscle significantly contributes to many functions of the body. The main roles of the tissue are to maintain posture and provide power and locomotive capacity to the individual, by converting chemical energy into mechanical energy[2]. Thus, skeletal muscle fitness impacts the social activity and functional independence of the individuals, highly influencing their quality of life. From a metabolic point of view, skeletal muscle serves as a storage of amino acids and carbohydrates, participates in the body thermoregulation, and contributes to the regulation of glucose levels in the blood[2,3]. Skeletal muscle is a highly adaptable tissue capable of undergoing hypertrophy upon resistance training or atrophy in case of lack of usage, ageing, or disease[3,4]. Importantly, reduced muscle mass has been linked to an impaired ability of the body to respond to stress and chronic disease[2,5]. Therefore, either restoring the integrity of muscle tissue after injury or protecting it from the ageing-related decline has been of great interest.

In normal physiological conditions, skeletal muscle is a stable tissue, with a very low turnover[6]. Homeostatic skeletal muscle presents a highly organized structure, mainly composed of bundles of longitudinally aligned multinucleated cells named myofibers (Figure 1)[7,8].

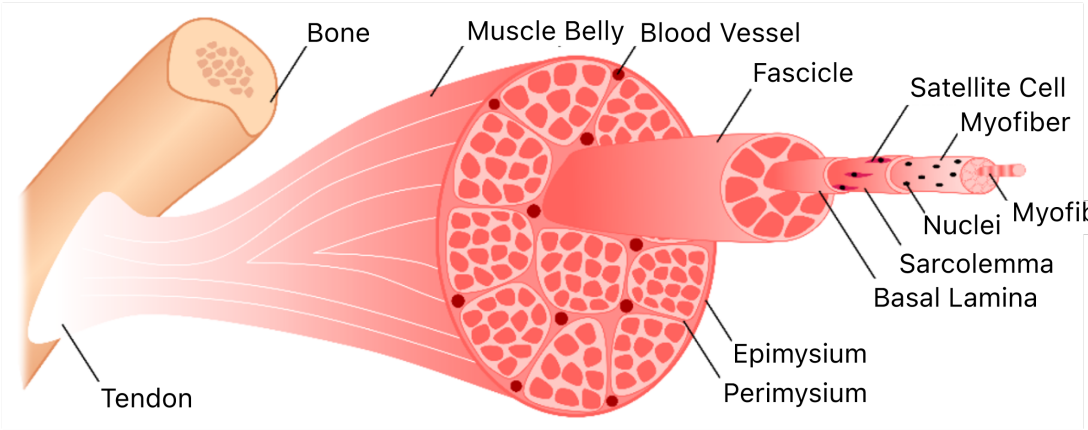

Figure 1. Structure of skeletal muscle.
Each myofiber is enveloped by endomysium (also called basement membrane or basal lamina). A thick layer of extracellular matrix (ECM), named perimysium, envelops several myofibers to form a fascicle. Finally, the outer layer of connective tissue, termed epimysium, envelops several fascicles and connects the muscle tissue and tendons. Adapted from: www.dr-ramon.com.

Myofibers are composed of myofibrils that contain actin and myosin filaments, which are responsible for muscle contraction. Bundles of myofibers form fascicles, and bundles of fascicles form the muscle, with each layer successively wrapped into layers of extracellular matrix (ECM), which gives support to the myofibers and envelops them with nerves and blood vessels within the muscle structure. Due to their considerable length, myofibers have numerous myonuclei that fulfil the high demand for protein synthesis. Importantly, myonuclei are postmitotic cells, meaning that they are not able to divide to produce new myonuclei[9]. Myofibers are generated by the fusion of myogenic precursor cells, named myoblasts, during embryonic and foetal muscle formation[10]. Although myofibers are the major component of the skeletal muscle, up to 15 distinct muscle-resident populations have been described by single-cell RNA-seq approaches in mice and human biopsies[11–16], including satellite cells (SCs), fibro-adipogenic progenitors (FAPs), endothelial cells (ECs), tenocytes, B and T cells, glial cells, and macrophages (Figure 2).

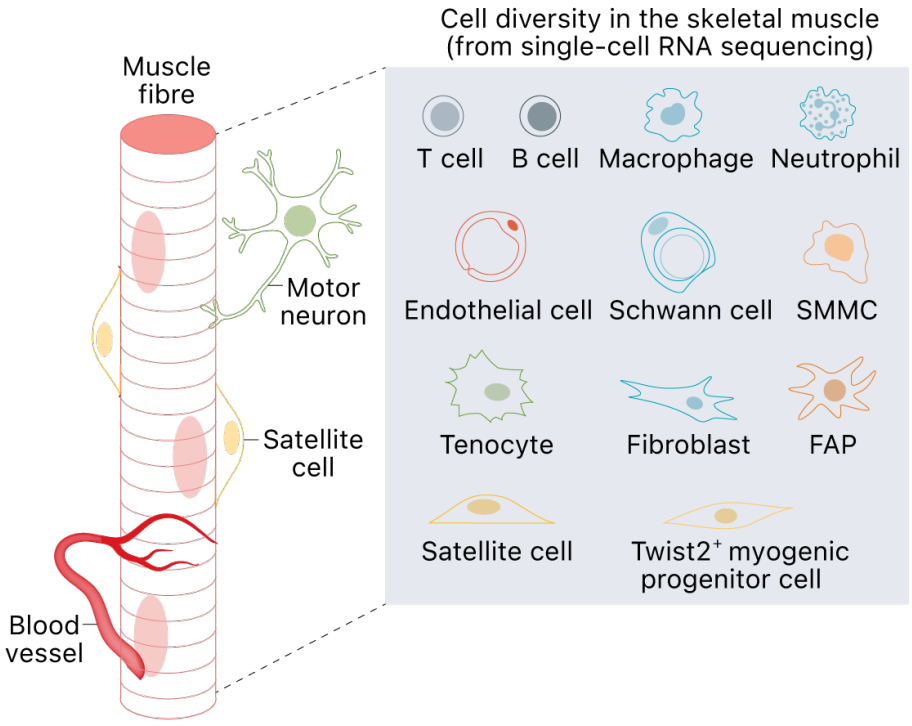

Figure 2. Muscle-resident populations identified by scRNA-seq approaches.
Distinct populations residing in homeostatic skeletal muscle tissue. SMMCs, smooth muscle-mesenchymal cells; FAP, fibro-adipogenic progenitors. Adapted from: Sousa-Victor et al., 2022[17].

Precise coordination between all these components is essential for the correct muscle function, with any external or internal perturbations resulting in its loss[18]. Luckily, skeletal muscle possesses a remarkable ability to regenerate following an insult, with only a few weeks needed for the muscle to restore its initial structure[9].

1.2 Cells that participate in muscle regeneration

After an injury, a series of events must occur in a timely-regulated manner to achieve successful regeneration of the muscle tissue[19]. Currently, the most commonly used injury models to study muscle regeneration include myotoxic agents (such as cardiotoxin [CTX] and notexin [NTX]), chemicals like barium chloride and physical procedures, including freeze injury. Five main phases of muscle regeneration can be distinguished after a sterile acute injury: degeneration-necrosis, inflammation, regeneration, tissue remodelling/maturation and re-innervation/functional recovery (Figure 3)[20].

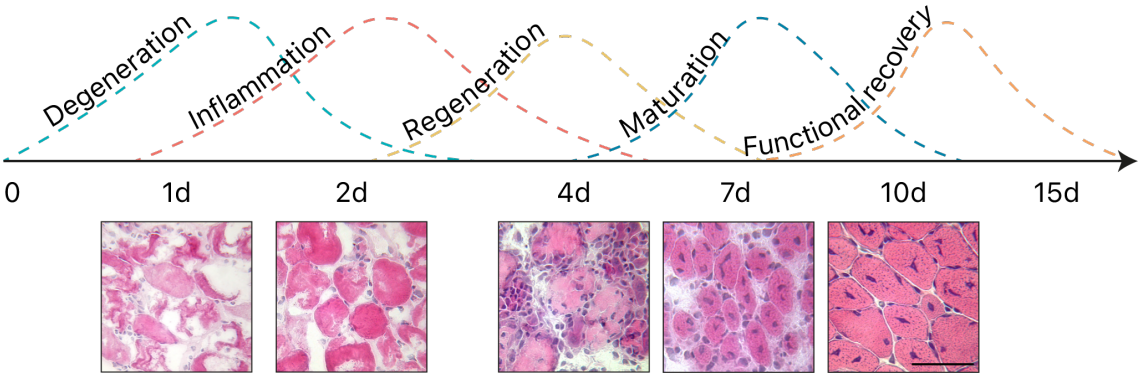

Figure 3. Stages of skeletal muscle regeneration.
Five interrelated and time-dependent stages of regeneration occur in response to injury, named degeneration, inflammation, regeneration, maturation and functional recovery. Injury triggers necrosis of myofibers and sterile inflammation, with infiltration of immune cells in the site of the lesion. Inflammation activates muscle stem cells, which together with other stem cells and precursors regenerate the tissue. The maturation stage is accompanied by matrix rearrangement and angiogenesis. The last step of muscle restoration is characterized by reconstitution of neuromuscular connections needed for correct muscle function. Representative images of haematoxylin and eosin (H&E) staining in mouse muscle sections at indicated time points are shown. Adapted from: Arnold et el., 2007[21].

The stages of muscle regeneration depend on the correct functioning and precise coordination of different muscle resident cells. For the scope of my thesis, I will focus on the major populations involved in the regenerative process, SCs, FAPs and myeloid cells (MCs), in the following section.

Satellite cells.

SCs reside between the basal lamina and sarcolemma of the myofibers and can be identified by the expression of the paired-box transcription factors Pax3 and Pax7, cluster of differentiation protein 34 (CD34), cell surface attachment receptor α7-integrin and neural cell-adhesion molecule (NCAM), among others[22,23]. Although small local damage to the myofiber can be restored by the myonuclei itself[24], muscle stem cells are absolutely required for correct muscle restoration upon any injury resulting in necrosis and *de novo* myofiber formation[25]. SCs are normally in a quiescent state in resting muscle but have the ability to activate, proliferate, differentiate and fuse to form new myofibers in response to an injury, a process called myogenesis (Figure 4)[6,26]. This process is tightly regulated by the expression of the muscle-specific basic helix-loop-helix (bHLH) transcription factor family (muscle regulatory factors, or MRFs), comprising myogenic differentiation antigen (MyoD), myogenic factor 5 (Myf5), Myogenin and MRF4[27–29]. In response to stress, quiescent SCs experience a rapid cell cycle re-entry, indicating a highly modulated and primed for activation state[30,31]. Activation of SCs occurs with upregulation of MyoD and subsequent generation of myoblasts, expressing low Pax7 and high MyoD levels.

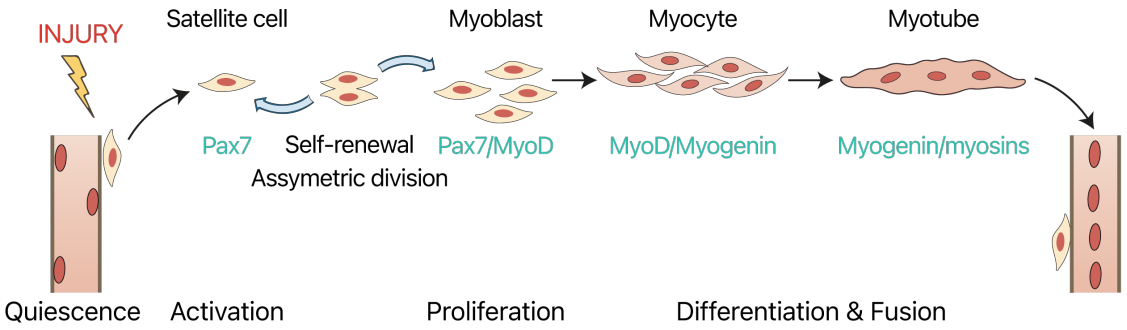

Figure 4. Schematic overview of SCs-driven myogenesis.
Quiescent SCs activate and proliferate upon injury. Symmetric division leads to myoblasts generation, while asymmetric division produces one committed (myoblast) and one self-renewing daughter. Thereafter, myoblasts differentiate into myocytes and fuse to form myotubes and myofibers. Adapted from Segalés et al., 2016[32].

Importantly, SCs proliferation has a dual role: generating committed cells to form new myofibers, and replenishing the stem cell pool[6,33,34]. When SCs perform symmetrical division, identical progeny with stem cell properties is produced. Otherwise, with an asymmetrical division of SCs, a single SC produce a daughter cell with self-renewing properties (with $Pax7^{High}/MyoD^{Low}$ expression) and a committed cell (with $Pax7^{Low}/MyoD^{High}$ expression). When this balance is impaired,

the pool of SCs is exhausted, leading to impaired muscle homeostasis and an inability to correctly regenerate the muscle tissue upon future injuries[34–36]. Following the SC expansion peak at 5-7 days post-injury (DPI), myoblasts differentiate into myocytes, which are characterized by late markers of the myogenic program, such as Myogenin and MRF4. The differentiated cell can either fuse to an existing myofiber or alternatively fuse to each other to generate *de novo* myofiber, which transiently expresses embryonal myosin heavy chain (eMHC) protein[37]. Interestingly, other cell populations with myogenic capacities have been described in skeletal muscle, including myoendothelial cells, $PW1^+$ interstitial cells, $CD133^+$ cells, $Twist2^+$ progenitor cells[38–41]. However, these cells are not sufficient to rescue muscle regeneration following SCs depletion and their exact role in myogenesis is yet to be determined. Thus, SCs ablation studies show that SCs have an irreplaceable role in adult myogenesis[42–45]. Nonetheless, other cell types are also needed for the correct muscle restoration, since their deletion is sufficient to induce a substantial delay in regeneration or even no regeneration at all.

Myeloid cells

The degeneration/necrosis phase is characterized by necrosis of myofibers, uncontrolled ionic flux, compromised plasmalemma and unfunctional organelles, after which a release of damage-associated molecular patterns (DAMPs) causes an inflammatory response and recruitment of the MCs to the site of lesion[46]. The first sensor of innate immunity is the complement system, which acts immediately after injury, allowing the immune response toward damaged tissue[47,48]. One of the earliest immune responses toward injury is degranulation of resident mast cells, with the release of pro-inflammatory cytokines, such as tumour necrosis factor alpha (TNFα), interferon gamma (IFN-γ) and interleukin 1 beta (IL-1β), which recruits peripheral neutrophils to the injured area[47,49,50]. Infiltrating neutrophils subsequently release enzymes and oxidative factors to facilitate the clearance of debris. Being a large source of reactive oxygen species (ROS), neutrophils contribute to the myofibers' degradation, temporarily worsening the muscle damage in some occasions[50,51]. However, more importantly, neutrophils further promote the inflammatory response by secreting IL-1, IL-6, IL-8 and soluble interleukin-6 receptor alpha (sIL6R), which induces monocyte and macrophage infiltration[52–54]. Macrophages initiate the second inflammatory response during muscle regeneration, becoming the predominant inflammatory cell type at 2 DPI[20].

Macrophages are identified by CD11b, F4/80, CD45, lymphocyte antigen 6C (Ly6C) and CD206, among other markers, and are a heterogeneous population, although their origin and distinctions are still controversial[21,54,55]. Both resident and blood monocyte-derived macrophages can be found at the site of the lesion. The latter can be classified based on the Ly6C and chemokine receptors C-C motif chemokine receptor 2 (CCR2) and C-X3-C motif chemokine receptor 1 (CX3CR1) expression. It has been proposed that Ly6C^{High} monocytes are recruited due to their high CCR2 levels to the damaged site, where they differentiate into the pro-inflammatory macrophages[56]. These types of macrophages remove muscle debris, secrete large amounts of pro-inflammatory cytokines, recruit T cells to the lesion, and promote muscle stem cells' proliferation (Figure 5). Importantly, depletion of pro-inflammatory macrophages results in impaired myoblasts' proliferation, persistent necrotic tissue and severe fibrosis[57–59].

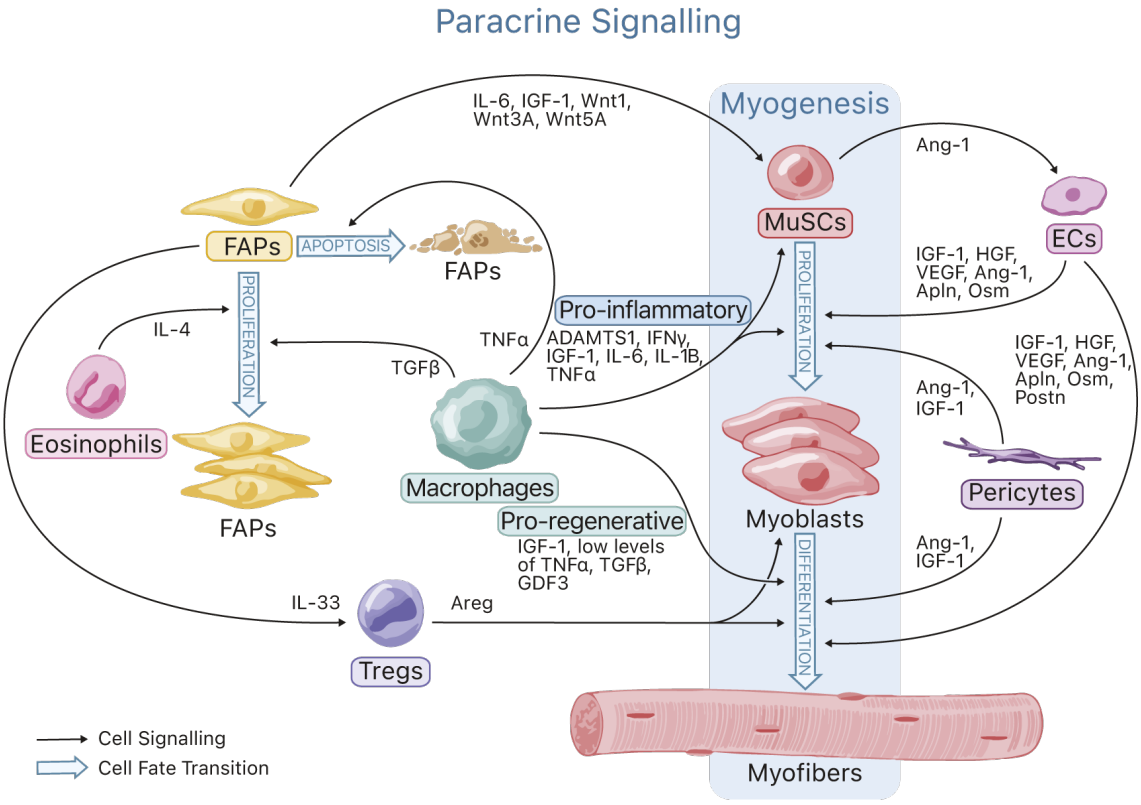

Figure 5. Paracrine signalling between SCs and cells of the regenerative niche. Muscle regeneration is a dynamic and highly coordinated process. Distinct muscle-residing populations participate in the regulation of the myogenic process by paracrine secretion of cytokines and growth factors. Adapted from Wosczyna and Rando, 2018[60].

Ly6C^{Low} monocytes, which have low CCR2 levels, then initiate the third wave of inflammation and differentiate into pro-regenerative, anti-inflammatory macrophages[61]. Functionally, these macrophages stimulate the differentiation of

muscle stem cells, by secreting IL-4, insulin-like growth factor 1 (IGF-1) and ECM proteins[21,53]. Ly6C^{High} and Ly6C^{Low} macrophages are not mutually exclusive, coexisting at the same time in the regenerating muscle and with the pro-inflammatory to pro-regenerative switch occurring gradually in time[62]. Of note, compromised pro-inflammatory to pro-regenerative switch results in reduced myogenin levels and impaired fibers' growth[63,64]. Thus, both types of macrophages regulate different stages of myogenesis in a timely precise manner.

Fibro-adipogenic progenitors

Although new myofiber generation relies on SCs, other interstitial cells are required for correct muscle formation. Such is the case of FAPs, which are mesenchymal stem cells able to undergo adipogenesis, fibrogenesis, chondrogenesis, and osteogenesis under specific conditions[65–69]. FAPs can be identified by the expression of platelet-derived growth factor receptor alpha (PDGFRα), stem cell antigen 1 (Sca-1) and transcription factor 4 (TCF4) specific markers[66,70,71]. FAPs rapidly increase upon injury, reaching their maximal numbers at 3-4 DPI[72,73]. Thereafter, the number of FAPs gradually returns to basal levels by a strong apoptotic response[73]. Conditional ablation experiments showed that FAP-depleted skeletal muscle presented prolonged necrosis and did not regenerate as efficiently as the normal skeletal muscle upon acute injury. However, these deficiencies can be rescued by FAP transplantation, confirming the pivotal role of FAPs on muscle regeneration[74]. FAPs majorly contribute to the deposition of extracellular proteins needed for transitional ECM during muscle regeneration, participate in the necrotic debris clearance and influence other cell populations in regenerating muscle[75]. The crosstalk of FAPs with other cell populations, including immune cells, SCs, Schwann cells, and ECs, is highly complex[75]. FAPs promote inflammation at the early stages of regeneration by secreting high levels of chemokines and recruiting monocytes and neutrophils into the injured site[12,13,74,76]. Of note, FAPs participate in the regulation of the pro-inflammatory to pro-regenerative switch of macrophages, by secreting IL-10, a master effector cytokine that triggers the change in phenotype of macrophages[77,78]. It has also been suggested that regulatory T-cells (Tregs), which accumulate at later stages of regenerations (4-7 DPI), are modulated by FAPs through their IL-33 production[79,80]. However, FAPs are also influenced by the immune cells during muscle regeneration. For example, eosinophils, which peak at 24 hours post-injury, are the main producers of IL-4

during muscle regeneration, which is needed for correct FAP functioning. Mice lacking eosinophils, IL-4 or interleukin 4 receptor (IL-4R) present lower FAP proliferation, impaired phagocytosis capacity and overall delayed muscle regeneration[81]. On the other hand, monocytes/macrophages regulate apoptosis and cell fate decisions of FAPs during muscle regeneration. For example, TNFα and transforming growth factor beta (TGFβ), which are highly secreted by pro- and anti-inflammatory macrophages, respectively, have been proposed to be effectors of FAP apoptosis and survival during skeletal muscle regeneration[73,82]. IL-1α/β, produced by pro-inflammatory macrophages, inhibits adipogenic differentiation of FAPs, while IL-4 polarized anti-inflammatory macrophages promote adipocytes' formation[83,84]. Thus, cellular communication between immune cells and FAPs is necessary to avoid excessive accumulation of FAPs and fibrotic deposition, to promote the return to homeostasis.

Myogenesis is closely coordinated with ECM remodelling during muscle regeneration. Indeed, FAPs peak in number prior to the myogenic cells, suggesting that FAPs might have an upstream role in myogenesis regulation[65,75]. Mice with different strategies of FAP-depletion (in the PDGFRα/CreER-DTX model and mice treated with nilotinib, PDGFR inhibitor that leads to FAP apoptosis) present impaired expansion of myoblasts at 3 days post-injury and smaller fiber size at late stages of myogenesis[74,76,85]. Co-culture experiments showed that FAPs promote differentiation of myogenic cells and their subsequent fusion into myotubes[65,66,86]. Importantly, FAPs abundantly secrete paracrine factors during muscle regeneration. Cytokines, growth factors and factors, such as IL-6, follistatin, WNT1-inducible-signalling pathway protein 1 (WISP1) and IGF-1, were shown to induce the progression of different stages of myogenesis, indicating an important role of FAPs during muscle regeneration (reviewed in Molina et al., 2021[75]). Interestingly, myogenic cells also regulate FAP expansion and presence in regenerating muscle tissue, as shown in mice with conditional SCs ablation (Pax7/CreERT2-DTX mouse model)[45]. Overall, these data indicate that cellular and molecular interactions between FAPs and other populations, including SCs and immune cells, are complex and essential for successful muscle regeneration.

1.3 Muscle regeneration in ageing

Ageing is associated with the accumulation of damage at a molecular, cellular and tissue level, affecting all tissues in the organism, including skeletal muscle.

Common hallmarks of ageing include genomic instability, telomere attrition, epigenetic changes, cellular senescence, loss of proteostasis, mitochondrial dysfunction, stem cell exhaustion, deregulated nutrient sensing and altered intercellular communication[87]. With ageing, skeletal muscle experiences loss of mass and function, termed sarcopenia, associated with fall-related injuries, frailty, and mortality in the elderly[88]. Simultaneously, the pool of SCs suffers a numerical loss with age, dropping to approximately 50% of its capacity[89–91]. Moreover, the outstanding ability of the skeletal muscle to regenerate upon an injury also gradually declines with ageing. Numerous studies have been performed to unveil the reason behind it, mainly focusing on the SCs' function. It is now known that SCs experience some intrinsic and extrinsic changes with ageing (reviewed in Sousa-Victor et al., 2022[17]). Among the intrinsic ones, impaired autophagy (and mitophagy), accumulation of dysfunctional mitochondria, excessive ROS production, and deficient mechanisms to maintain genome integrity have been identified[92–94]. Consistent with this, SCs exhibit a lower capacity to activate and proliferate upon injury[89,95,96] and a higher susceptibility to apoptosis[97]. Moreover, aged SCs shift towards fibroblastic and adipogenic fates especially in diseased aged contexts, partly explaining increased fibrotic deposition in aged muscle[98–100]. Another phenomenon observed in aged SCs is their predisposition to enter a senescent state upon a stimulus. Cellular senescence is an irreversible cell cycle arrest that impedes the proliferation of SCs needed for muscle regeneration and as a consequence leads to delayed muscle regeneration[91,94]. In addition, age-associated extrinsic changes occur in the SCs niche, participating in the regenerative decline. For instance, the levels of fibroblast growth factor 2 (FGF2) increase with ageing, leading to spontaneous quiescence exit and impaired self-renewal of SCs, which progressively exhaust the stem cell pool[101]. Other examples include increased TGFβ and TNFα signalling, nuclear factor kappa-light-chain-enhancer of activated B cells (NFκB) overactivation and unbalanced Wnt/Notch signalling, which limit SCs self-renewal and proliferation during regeneration[17,98,102–105]. Importantly, other niche components undergo changes with ageing as well. Ageing is associated with reduced levels of WISP1 produced by FAPs[106]. Notably, proteomic studies unveiled FAPs as the major affected source of niche proteins during ageing[107]. One example is defective production of IL-33 by FAPs with ageing, which impairs Treg recruitment and regenerative efficiency and contributes to inflammageing[80]. Moreover, aged FAPs express lower levels of

growth differentiation factor 10 (GDF10), important for the maintenance of myofiber mass[76]. On the other hand, the aged immune system and exacerbated pro-inflammatory signalling through CCR2 contribute to the age-associated regenerative decline, negatively influencing myogenesis[108–110]. Of note, aged mice experience a delayed immune response with compromised pro-inflammatory to pro-regenerative switch of macrophages during muscle regeneration[109,111]. Thus, impaired muscle regeneration is a result of multiple dysregulated processes and players with ageing.

1.4 Pathological muscle regeneration and Duchenne muscular dystrophy

Duchenne muscular dystrophy (DMD) is a fatal, X-linked muscle degenerative disorder. Currently, DMD remains incurable, with a life expectancy between 20 and 40 years with optimal care[112]. DMD is caused by mutations in the dystrophin gene (*Dmd*), which lead to a lack of functional dystrophin protein. Loss of dystrophin leads to a high susceptibility to damage upon muscle contraction, resulting in functional loss and progressive wasting. During the first stage of disease, degenerated muscle is replaced by a regenerative process; however, in later stages, dead myofibers are replaced by fatty and fibrotic tissue. Because of the continuous degenerative–regenerative cycles in DMD, SCs proliferate in an attempt to restore the architecture of muscle tissue; however, they eventually lose their regenerative potential[113,114]. The absence of dystrophin leads to a compromised asymmetrical division of SCs, causing exhaustion of the SC pool[115]. In addition, SCs shift towards fibrogenic fate in muscle tissue of mdx mice, a most widely used model of DMD, losing their normal function[99,100]. Accumulation of the fibrotic tissue is a well-established feature of DMD. FAPs are the main source of the ECM synthesis, although muscular, endothelial and hematopoietic cells undergo fibrogenic conversion in the DMD context as well[65,66,99,100]. Several pharmacological strategies targeting FAPs ameliorated muscle fibrosis in the mdx mice[73,116]. Another important feature of DMD is a chronic inflammatory response due to constant regeneration/degeneration cycles. Macrophages and lymphocytes are the main immune populations infiltrating the skeletal muscle of mdx mice; however, eosinophils and neutrophils have also been detected[117]. Although immune cells are needed for muscle regeneration, persistent inflammatory response induces negative outcomes on the disease progression. In fact, pro-inflammatory macrophages contribute to the generation of ROS through inducible nitric oxide

synthetase (iNOS), elevating the levels of oxidative stress and triggering muscle fiber damage through nitric oxide-dependent cytotoxicity[54]. Importantly, dystrophic muscle is more vulnerable to oxidative damage, due to lower levels of glutathione, one of the most abundant and important antioxidants of the muscle tissue[118,119]. On the other hand, pro-regenerative macrophages, also present in the skeletal muscle of mdx mice, secrete IL-10 and TFGβ, contributing to fibrosis accumulation[120]. It is known that a precise pro-inflammatory to pro-regenerative switch is necessary for a fate decision of FAPs (proliferation and apoptosis); however, this balance is altered in the chronically regenerating muscle of the mdx mice. Thus, impaired regulation through TNFα and TGFβ signalling leads to FAP persistence and fibrosis development. Overall, chronic inflammation acts as a driver of fibrosis, with several cell populations involved in the process.

2. CELLULAR SENESCENCE

2.1 Hallmarks of senescent cells

Cellular senescence is defined as an irreversible cell cycle arrest, induced by cyclin-dependent kinase inhibitors, such as $p16^{INK4a}$ and $p21^{CIP1}$ [121,122]. Cellular senescence was first described by Hayflick and Moorehead in 1961, who observed the replicative decline of human diploid fibroblasts after a finite number of serial passages[123]. Senescent state can be induced by many different triggers, such as DNA damage, oxidative stress, and oncogene activation among others[124,125]. Senescent cells are highly heterogeneous and there is no unique and exclusive marker for their identification[126–128]. One commonly used senescence marker is Senescence Associated β-galactosidase (SA-β-gal) activity, which shows β-galactosidase activity at a suboptimal lysosomal pH (Figure 6)[129].

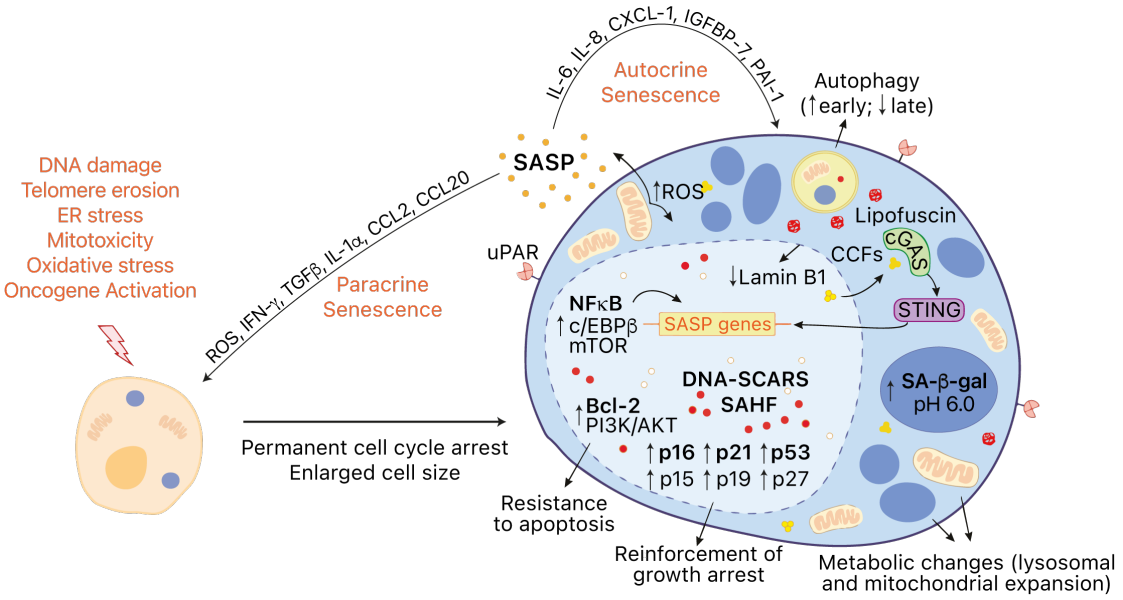

Figure 6. The hallmarks of cellular senescence.
Cellular senescence can be induced by different stimuli, including oncogene activation, DNA damage, telomere shortening, mitotoxicity and oxidative and endoplasmic reticulum (ER) stress. Senescent cells upregulate cell cycle inhibitors, $p16^{INK4a}$, $p21^{CIP1}$, p53, $p15^{INK4b}$, $p19^{ARF}$ and $p27^{KIP1}$, inducing permanent cell cycle arrest. Bcl-2 and PI3K/AKT pathways get activated, conferring senescent cell resistance to apoptosis. Urokinase-type plasminogen activator receptor (uPAR) is broadly expressed on the surface of the senescent cells. Senescent cells also undergo changes in size and metabolic changes, like lysosomal and mitochondrial expansion with consequent high ROS and lysosomal SA-β-gal activity. Increasing oxidative stress leads to the generation of protein aggregates and insoluble lipofuscin granules. Senescent cells secrete a range of proactive molecules, which act in an autocrine and paracrine manner. The chromatin undergoes significant changes, with the formation of senescence-associated heterochromatin foci (SAHF) and downregulation of nuclear lamin B1, which leads to leakage of chromatin fragments into the cytosol. Cytosolic chromatin fragments (CCF) are recognized by the cGAS-STING pathway, triggering NFκB activation and expression of the SASP genes. Adapted from De-Carvalho et al., 2021[130].

Although several studies reported that SA-β-gal activity can be detected in non-senescent cells, it is still the most used marker of senescence in the field[131,132]. Additional markers of senescence include DNA damage markers, such as tumour suppressor p53-binding protein 1 (53BP1) and gamma H2A histone family member X (γH2AX), nuclear lamin B1 (Lmnb1) loss, senescence-associated heterochromatic foci (SAHF), enlarged cell size, increased lysosomes and granularity accumulation of lipofuscin and high ROS production, among others[133–136]. Importantly, senescent cells are apoptosis-resistant and can upregulate members of the anti-apoptotic B-cell lymphoma 2 (Bcl-2) family of proteins, including Bcl-2, Bcl-xL, and Bcl-w[137].

2.2 The senescence-associated secretory phenotype

An important aspect of senescent cells is their aberrant metabolism and enhanced secretion of proactive factors, defined as senescence-associated secretory phenotype (SASP) [138–140]. The SASP is critical for many cell-autonomous and non-cell-autonomous biological activities of senescent cells[140]. For instance, secretion of IL-6, IL-8 and their receptors act in an autocrine manner, reinforcing a cell cycle arrest[141,142]. Moreover, SASP can have significant effects on neighbouring cells and even convert them into new senescent cells (so-called secondary senescence or the bystander effect)[140]. The composition of SASP varies between cell types, triggers of senescence and kinetics[127,143,144]. Although the SASP is still not well characterized, it is generally composed of cytokines, growth factors, ECM components and ECM-remodelling proteins. A core SASP factors comprise mainly pro-inflammatory cytokines, such as IL-6, IL-8 and chemokine C-C motif ligand 2 (CCL2), TGFβ and the chemokine C-X-C motif ligand family (CXCL). Among the ECM-modifying enzymes, matrix metalloproteinases (MMPs), serine/cysteine proteinase inhibitors (SERPINs) and tissue inhibitors of metalloproteinases (TIMPs) are mainly present (Table 1)[145]. A recent proteomic study characterized the SASP effectors *in vitro* and identified several candidate biomarkers of senescent cells that overlap with ageing in human plasma, including growth differentiation factor 15 (GDF15), MMP-1 and SERPINs[143]. Different ways of SASP signalling have been proposed: SASP can be released as soluble factors and via extracellular vesicles (EVs), or transmitted through juxtacrine signalling, cytoplasmic bridges and cell-to-cell fusion[146].

Table 1. Distinct SASP components.

Class	Component
Interleukins	IL-6, IL-7, IL-1, IL-1b, IL-13, IL-15
Chemokines	IL-8, CXCL1, CXCL2, CXCL3, CCL8, CCL13, CCL3, CCL20, CCL11, CCL26, CCL25, CXCL5, CCL1, CXCL11
Other inflammatory molecules	TGFβ, GM-CSE, G-CSE, IFNγ, MIF, CXCL13
Growth factors and regulators	Amphiregulin, epiregulin, heregulin, EGF, bFGF, HGF, VEGF, IGFBP-2, -3, -6, -7, GDF15
Proteases and regulators	MMP-1, -3, -10, -12, -13, -14, TIMP-1, TIMP-2, uPA, tPA, PAI-1, -2, cathepsin B
Receptors; ligands	ICAM-1, -3, uPAR, EGF-R
Non-protein molecules	PGE2, nitric oxide, ROS
Insoluble factors	Fibronectin, collagens, laminin

bFGF, basic fibroblast growth factor; EGF, epidermal growth factor; G-CSE, granulocyte colony-stimulating factor; GM-CSE, granulocyte macrophage colony-stimulating factor; MIF, macrophage migration inhibitory factor PAI-1, plasminogen activator inhibitor 1; PGE2, prostaglandin E2; tPA, tissue plasminogen activator; uPA, urokinase-type plasminogen activator. Data from Gorgoulis et al., 2019[135] and Coppé et al., 2010[147].

SASP expression is likely induced in response to persistent DNA damage, by DNA damage response (DDR) proteins ataxia telangiectasia mutated (ATM), checkpoint kinase 2 (CHK2) and Nijmegen breakage syndrome 1 (NBS1). Interestingly, p53 plays the opposite effect to SASP induction, since p53 inhibition further enhances the SASP and pro-inflammatory environment[138]. Several transcription factors and epigenetic regulators are implicated in the regulation of the SASP. Among them, NFκB and transcription factor CCAAT/enhancer-binding protein beta (C/EBPβ) are master regulators of most SASP factors[141,142,148–151]. Inhibition of NFκB signalling via depletion of p65 or v-rel avian reticuloendotheliosis viral oncogene homolog A (RelA), an essential subunit of NFκB, results in reduced expression of the SASP molecules[148,149]. In addition, other inducers of the SASP program include GATA binding protein 4 (GATA4) transcription factor, the mitogen-activated protein kinase p38 (p38MAPK), cyclic GMP–AMP synthase (cGAS)–stimulator of interferon genes (STING) pathway, long-interspersed element 1 (LINE-1) retrotransposon activity, Janus kinase 2/signal transducer and activator of transcription 3 (JAK2-STAT3) signalling and mammalian target of rapamycin (mTOR) pathway[152–161]. Interestingly, the composition of the SASP is temporarily dynamic, with neurogenic locus notch homolog protein 1 (NOTCH1) regulating it. NOTCH1 levels are increased in early senescence, activating TGFβ and its

effectors. Meanwhile, late senescence is characterized by lower NOTCH1 levels and proinflammatory cytokines IL-1, IL-6 and IL-8[144].

Epigenetic regulation of the SASP has also been described. The epigenetic reader bromodomain-containing protein 4 (BRD4) is recruited to the superenhancers close to the SASP genes, binding acetylated histone H3 Lys27 (H3K27) and executing the oncogene senescence program[162]. Re-localization of the high mobility group box 2 (HMGB2) to the SASP genes induces their expression[163]. In the opposite fashion, histone variant MacroH2A1 is removed from the SASP genes in senescent cells, allowing their transcription[164]. Another study suggests that transcription-associated histone methyltransferase mixed-lineage leukaemia 1 (MLL1) is essential for the SASP transcription of DDR-induced SASP genes, as its depletion abrogates it[165]. In addition, increased nuclear pore density during oncogene-induced senescence regulates the SAHF formation and maintenance, affecting the SASP expression[166].

Because the SASP is highly heterogeneous, cellular senescence plays distinct roles in a number of processes in a paracrine manner (Figure 7). Importantly, SASP signalling is highly context-dependent, and understanding it in-depth still requires exhaustive studies.

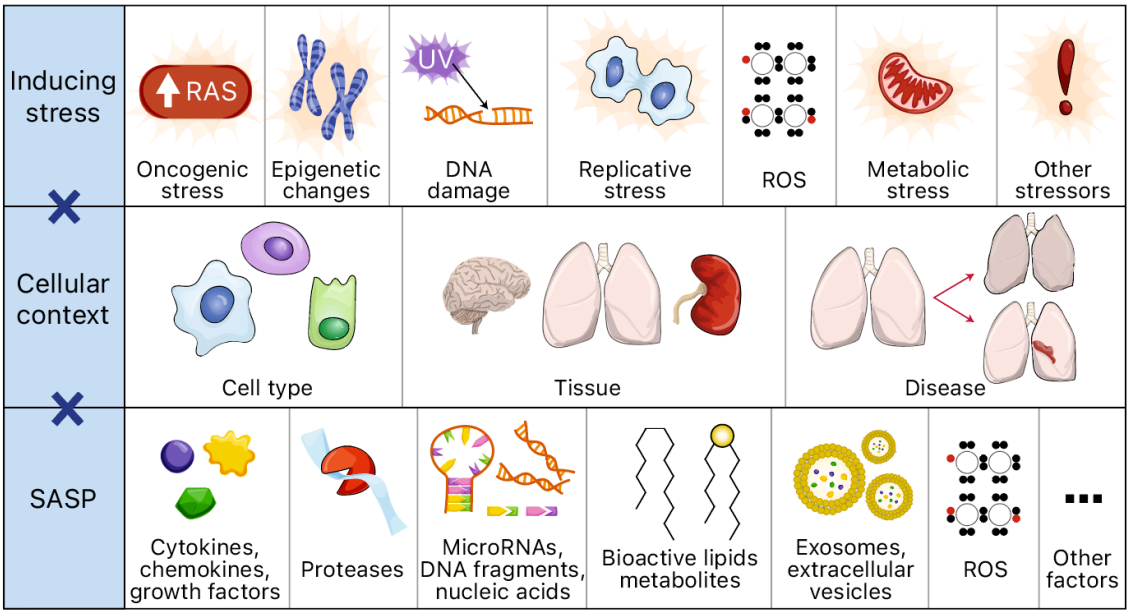

Figure 7. Layers of the complexity of the SASP.
Cellular senescence is highly heterogeneous, with context-dependent phenotypic diversity. Distinct stressors can induce different types of senescence programs, which further depend on the cell population, the state of the tissue and other contexts. Consequently, the resulting SASP spectrum and its role are extremely variable. Adapted from Gasek et al., 2021[167].

It is also worth mentioning that only *in vitro*-generated senescent cells have been used for transcriptome analysis, due to the inexistence of a reliable marker and consequent inability to isolate senescent cells from complex tissues. Thus, the real complexity of *in vivo*-occurring senescent cells is yet to be determined.

2.3 Function of senescent cells

The involvement of senescent cells has been described in many biological contexts, with beneficial or deleterious consequences. Several mouse models emerged to study the role of senescent cells, being p16-3MR and INK-ATTAC models the most used ones. The p16-3MR mouse model contains distinct functional domains under the senescence-sensitive promoter $p16^{INK4a}$, which are synthetic Renilla luciferase, monomeric red-fluorescent protein (mRFP) and truncated herpes simplex virus 1 thymidine kinase (HSV-TK). This model allows the identification of $p16^{INK4a}$-expressing cells by luminescence and mRFP fluorescence, while treatment with ganciclovir (GCV) induces their specific elimination through HSV-TK activity[168]. On the other hand, INK-ATTAC is a model that expresses a death cassette and green fluorescent protein (GFP) under the control of a minimal INK4a/ARF promoter fragment. In this model, $p16^{INK4a}$-positive cells can be visualized by GFP fluorescence and selectively killed upon treatment with synthetic molecule AP20187 and consequent caspase-dependent apoptosis[169]. In addition to genetic approaches, a broad range of molecules with senescence-targeting properties, named senolytics, have been described (Figure 8). These molecules primarily target anti-apoptotic, pro-survival pathways upregulated in the senescent cells, causing senescent cells to enter apoptosis[167]. A combination of dasatinib (D) and quercetin (Q), which target ephrin dependence receptor signalling, phosphatidylinositol 3-kinase (PI3K)– protein kinase B (AKT) pathway and Bcl-2 members, has been used to target distinct senescent populations in mice and even in clinical studies conducted in patients with diabetic kidney disease and idiopathic pulmonary fibrosis[170–172]. Navitoclax (or ABT263) is another widely used senolytic that affects Bcl-2/Bcl-xL signalling in senescent cells[173–175]. Other drugs with senolytic potential include a flavonoid fisetin, a heat shock protein 90 (HSP90) inhibitor 17-dimethylaminoethylamino-17-demethoxygeldanamycin (17-DMAG), and cardiac glycosides[176–178]. Another approach to target the influence of senescent cells is to neutralize their SASP. Senomorphics are compounds that suppress the SASP without inducing apoptosis of the senescent cells. Senomorphics include

inhibitors of NFκB, free radical scavengers and JAK pathway inhibitors[179,180]. For example, rapamycin and metformin work as senomorphics, leading to a decreased SASP expression in distinct contexts[181–183]. It is worth mentioning that none of the senolytic compounds efficiently targets all senescent populations known. Thus, the efficiency of each senolytic should be evaluated, and its effect confirmed by different strategies.

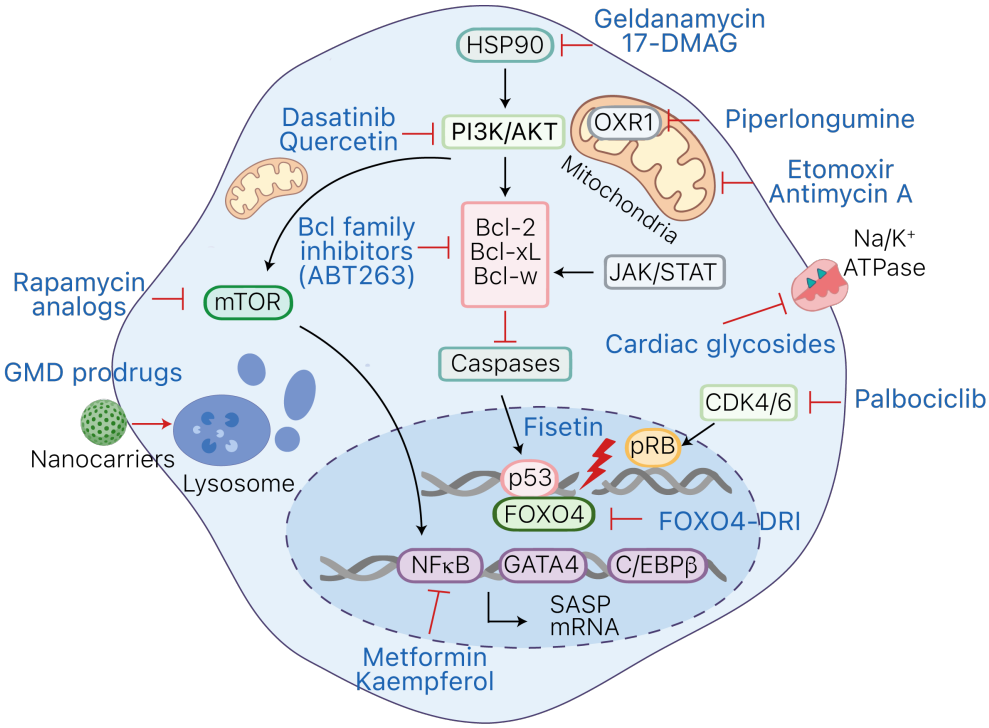

Figure 8. Senolytic and senomorphic therapies.
Distinct senolytics target senescent cell anti-apoptotic pathways, activated in senescent cells to prevent apoptosis entrance. The most common anti-apoptotic signalling is Bcl-2 family, HSP90, p53 and PI3K/AKT/mTOR pathways. Another strategy involves nanoparticles packed with galactose-modified duocarmycin (GMD) through lysosome processing. Senomorphics, such as metformin and rapamycin, blunt the SASP production by targeting NFκB and C/EBPβ transcription factors. OXR1: oxidation-resistant 1. Adapted from Demirci et al., 2021[184].

It is generally believed that cellular senescence is beneficial when it occurs transiently (Figure 9). For example, a distinct form of cellular senescence participates in growth control and patterning during embryonic development in mammals and amphibians[185–187]. In addition, senescent cells promote tissue regeneration in several tissues. In zebrafish, targeting senescent cells prevents fin regeneration following amputation, and in salamanders, senescent cells play an important role in whole limb regeneration[188,189]. In liver fibrosis, senescence limits

the proliferation of ECM-producing hepatic stellate cells and promotes infiltration of natural killer (NK) cells to restore liver homeostasis[190,191]. Similarly, senescent cells limit fibrosis in the pancreas[192]. During wound healing, senescent fibroblasts and ECs promote wound closure by secreting platelet-derived growth factor AA (PDGF-AA) and cellular communication network factor (CCN1)[168,193]. Beneficial effects of cellular senescence are also observed in reprogramming. While cellular senescence acts as a barrier in a cell-autonomous manner, its SASP promotes reprogramming and cellular plasticity in the neighbouring cells[194–198].

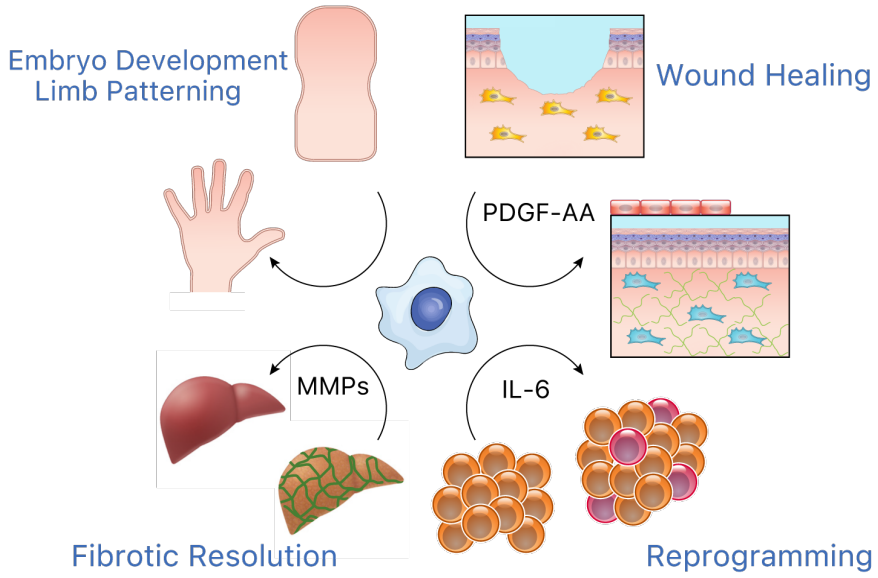

Figure 9. The beneficial role of cellular senescence.
Senescent cells promote wound healing by PDGF-AA secretion, contribute to fibrotic resolution in various tissues by MMPs secretion and promote reprogramming in their niche. Moreover, senescent cells ensure limb patterning during embryogenesis. Adapted from Calcinotto et al, 2019[199].

However, other studies suggest that transient senescence is not always beneficial. For example, the reduction of senescent cells accelerates bone fracture healing[200]. Targeting senescent cells in acute kidney injury prevents fibrosis accumulation and transition to chronic kidney disease[201]. In the liver, downregulation of $p21^{CIP1}$ or inhibition of TGFβ receptor 1 (TGFβR1) reduces the number of senescent cells after injury, increases hepatocellular proliferation, and improves regeneration[202]. Of note, senescent cells can aggravate biliary injuries through the same mechanisms. In this context, inhibition of TGFβ-signalling can also interrupt the deleterious effects of senescent cells and restore liver function[203].

In contrast, chronic exposure to senescent cells has been mostly associated with negative outcomes. Cellular senescence is considered a hallmark of ageing, as a

higher number of senescent cells is observed in different tissues over time[204]. The expression of key cell cycle arrest and senescence regulators $p15^{INK4b}$, $p16^{INK4a}$, and $p19^{ARF}$ (encoded by the *INK4/ARF* gene locus) is considered to be an ageing-related biomarker[205]. Moreover, genome-wide association studies (GWAS) have shown that the INK4/ARF locus is one of the highest disease susceptibility–associated hotspots, correlating with age-related diseases such as cancer, type 2 diabetes, atherosclerosis, and glaucoma, and that it is significantly related to physical dysfunction in elderly[206,207]. Further, key proinflammatory SASP factors (such as IL-6, chemokine CCL4, and TNFα) contribute to age-related inflammation ("inflammageing") and correlate with frailty and multimorbidity in advanced age[143,208,209]. Systemic elimination of senescent cells with genetic and pharmacological strategies in BubR1 mice, which have a shortened lifespan and age-related phenotypes, and naturally-aged mice increases lifespan and prevents kidney dysfunction, cardiomyocyte hypertrophy, lipodystrophy and cataracts among other beneficial effects[169,170,210–212]. Moreover, cellular senescence has been detected in a variety of chronic pathologies (Figure 10).

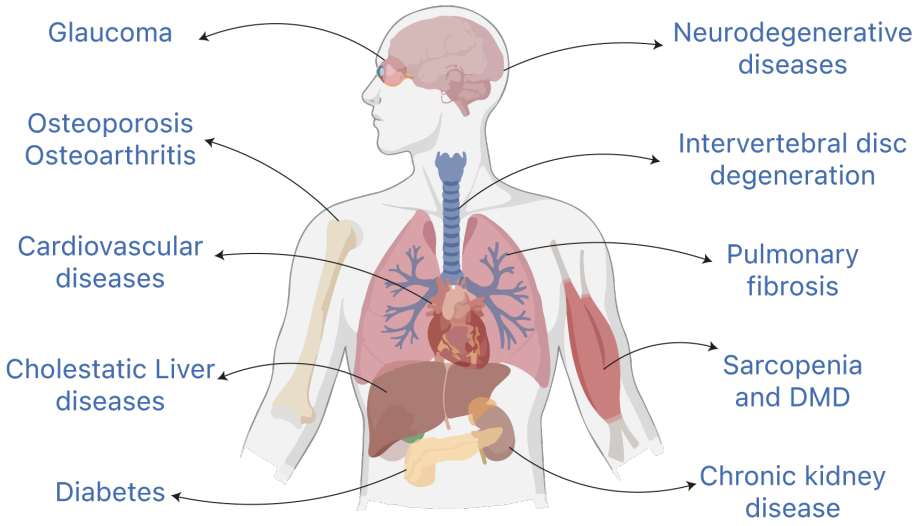

Figure 10. The detrimental role of cellular senescence.
Senescent cells' contribution has been described in the following age-associated pathologies. Figure created with BioRender.

Targeting senescent cells with senolytics, senomorphics and genetic strategies ameliorates the disease progression in idiopathic pulmonary fibrosis, atherosclerosis, chronic kidney disease, neurodegenerative diseases (including Alzheimer's and Parkinson's diseases), diabetes mellitus, intervertebral disc degeneration, osteoporosis, osteoarthritis and others (reviewed in Borghesan et al., 2020[213]). Although the vast majority of studies indicate beneficial effects of

systemic elimination of senescent cells in aged tissues and chronic pathologies, some suggest otherwise[214,215]. For instance, the elimination of $p16^{INK4a}$-expressing cells disrupts blood–tissue barriers and leads to liver fibrosis, due to the elimination of vascular endothelial cells in liver sinusoids, highlighting the nuanced, tissue-dependent roles of senescent cells[215]. Thus, there is not only variation in the molecular and transcriptomic phenotypes as well as the SASPs among the cell populations, triggers and contexts, but also in the role of senescent cells themselves. Therefore, the contributions of senescent cells should be studied in an in-depth way for each context.

2.4 Role of senescence in muscle regeneration, ageing and disease

Markers of senescence accumulate in many tissues with age, including skeletal muscle. Various markers of senescence have been detected in skeletal muscle of aged rats, including increased mRNA expression of *Cdkn2a* ($p16^{INK4a}$) and *Cdkn1a* ($p21^{CIP1}$), coinciding with atrophic fibers[216]. Inactivation of $p16^{INK4a}$ or inducible elimination of $p16^{INK4a}$-expressing cells increases lifespan and delays the onset of sarcopenia (among other ageing-related features) in BubR1 mice, and in INK-ATTAC BubR1 transgenic mouse[169,212]. Treating normally-aged mice with the senolytic compound navitoclax rejuvenates hematopoietic and muscle stem cells[175]. Similarly, treatment with nicotinamide riboside (NR), a precursor of the oxidized form of cellular nicotinamide adenine dinucleotide (NAD^+), rejuvenates SCs by improving mitochondrial function and preventing cellular senescence[217]. Conversely, transplantation of a small number of senescent cells is sufficient to induce physical dysfunction in young mice and to further exacerbate it in old ones, while treatment with the senolytic drugs Q+D abrogates the negative effects of senescent cell transplantation and ameliorates physical dysfunction in naturally-aged (24-month-old) mice[170]. Thus, these studies suggest a role of cellular senescence in promoting ageing and sarcopenia.

Several studies attribute the defective regenerative process observed in ageing to geroconversion, defined as the rapid entry from quiescence into senescence of SCs[218–220]. Physiologically-aged geriatric mice exhibit SCs with increased SA-β-gal activity, high expression of *Cdkn2a*, *Cdkn2b* and *Igfbp5*, and increased p38α/p38β signalling, resulting in a delayed regenerative process upon injury and reduced ability to repopulate, even when transplanted into the young mice[91,221]. Impaired mitophagy, loss of proteostasis and excessive ROS production have been

identified as the cause of senescence entry in the aged SCs[94]. Additionally, excessive upregulation of TGFβ leads to imbalanced pSmad3 and Notch signalling and overexpression of CDK inhibitors, $p15^{INK4b}$, $p16^{INK4a}$, $p21^{CIP1}$ and $p27^{KIP1}$ in aged SCs[102]. Importantly, other cell types undergo senescence in aged skeletal muscle apart from SCs. For example, FAPs express high levels of $p15^{INK4b}$, $p16^{INK4a}$, $p21^{CIP1}$ and other markers of senescence in BubR1 progeroid mice, suggesting their involvement in defective muscle regeneration in these mice[222]. In addition, a recent study on immunosenescence (e.g., age-induced progressive immune system dysfunction) unveiled impaired muscle regeneration in a mouse model with cellular senescence induced exclusively in the hematopoietic populations[223,224]. Interestingly, silencing of $p16^{INK4a}$ in BubR1 mice partially restores the regenerative decline observed, suggesting that senescent cells possibly impair muscle regeneration at advanced age[212]. In a similar fashion, a recent study has shown the beneficial effect of senolytic treatment in naturally-aged mice prior to an injury[225]. Although these studies suggest that the accumulation of senescent cells contributes to impaired muscle regeneration in aged animals, a clear role of senescent cells on muscle regeneration has not been shown. For instance, the beneficial effect of reduction of senescent cells might be due to a systemically rejuvenated organism and not senescent cells *per se*. A deeper understanding of the mechanistic regulation of cellular senescence on muscle regeneration is needed.

In addition to ageing, senescent cells have also been observed in pathological muscle regeneration, such as DMD. Several studies showed the emergence of senescent cells in the mdx mice and human biopsies[226–228]. Senescence of SCs has been reported by several studies performed in different mouse models of DMD and myotonic dystrophy type I, correlating with impaired proliferation rate and myogenic program[217,227,229,230]. In addition, FAPs, endothelial cells and macrophages also present signs of cellular senescence in the rat model of DMD and D2-mdx mice, suggesting that different cell populations undergo senescence in skeletal muscle tissue[228,231]. A recent study with senolytic and genetic interventions has shown improvement of muscular function, regeneration and reduced fibrotic and adipose tissues in skeletal muscle of dystrophic rats and prevented dystrophy-associated loss of weight and muscle strength[228]. On the other hand, some studies suggest a positive role of functional senescent FAPs, induced by exposure to human placental extract or exercise, in the context of chronic inflammatory

myopathy[232,233]. Further studies are needed to establish the role of senescent cells and their nature in chronic muscle disease.

Interestingly, senescent cells have also been detected in the regenerative muscle tissue of young animals[225,227]. Some studies suggest a positive role of injury-induced FAP senescence on myogenesis[233]. On the other hand, senescent cells promote cellular plasticity *in vivo* through IL-6 secretion in skeletal muscle of a reprogrammable mouse model with inducible expression of Yamanaka factors[198]. Thus, the role of cellular senescence is versatile and context-dependent, with many questions still remaining about the contributions of senescent cells to muscle regeneration and disease.

2.5 Role of CD36 in cellular senescence

CD36 is a multi-ligand scavenger receptor, which binds various lipoproteins, lipids, collagen, thrombospondin and other ligands. CD36 is expressed in a variety of tissues and cell populations, including adipose tissue, skeletal and cardiac muscle, small intestine and mammary glands, as well as in monocytes/macrophages, platelets and neurons[234]. CD36 participates in the regulation of energy balance, vascular and adipose homeostasis and generates a strong pro-inflammatory response upon interaction with amyloid-beta (Aβ) or oxidized low-density lipoprotein (oxLDL)[234,235]. Upon Aβ or oxLDL binding, CD36 activates MAPK and NFκB signalling, promoting the expression of pro-inflammatory cytokines and chemokines in immune populations[236]. Recent studies have shown lipid composition to undergo active changes in replicative senescence, as a potential mechanism to prevent lipotoxicity upon increasing oxidative stress in the senescent cells. Apart from compositional changes in various lipid species, senescent cells upregulate CD36, which in turn promotes CD36-mediated fatty acid uptake[237,238]. Further research has shown a regulatory link between CD36 upregulation and cellular senescence establishment. Ectopic expression of CD36 is sufficient to induce a pro-inflammatory program and ultimately senescence entry in proliferating cells *in vitro*[239,240]. Moreover, CD36 is strictly required for the SASP production through NFκB activation in distinct senescent states and cell types. Thus, CD36 acts as a modulator of the SASP program in senescent cells *in vitro*[240]. A study *in vivo* shows that total KO of CD36 results in impaired SCs function and delayed muscle regeneration; however, a more specific approach targeting CD36 in the senescent cells is lacking[241]. Thus, it remains to be confirmed whether CD36:

i) has a role in senescent cells generated *in vivo*, ii) has potential as a senomorphic, and iii) affects muscle regeneration.

OBJECTIVES

1. Defining kinetics of cellular senescence during muscle regeneration

Senescent cells have been previously detected in regenerating muscle. However, the kinetics behind this process are still unknown. The first aim of my thesis is to describe at which time point senescent cells appear and for how long they persist in regenerating tissue. I will also investigate the contribution of ageing to the burden and persistence of senescent cells during muscle regeneration.

2. Characterization of senescent cells in regenerating muscle

Senescent cells have been characterized *in vitro*, which usually underestimates the complexity of what occurs *in vivo*. In my thesis, I will try to establish a protocol for the efficient isolation of senescent cells from complex tissue. I then aim to describe the transcriptomic heterogeneity of senescent populations in regenerating muscle tissue. For a deeper characterization of senescence *in vivo*, I will also look for the differences and commonalities of senescent cells from a kinetic and age-related point of view. Moreover, I will try to unravel the transcriptomic regulation of gene expression and identify the master transcription factor (TF) regulators of senescence-associated functions and their SASP. Based on the transcriptomic data, I will also aim to identify the trigger of senescence entry in regenerating tissue and underline the contribution of ageing to this process and the phenotype of senescent cells.

3. Role of senescent cells in skeletal muscle under different contexts

The role of senescent cells has been described in many conditions and tissues. It is widely accepted that the transient presence of senescent cells is beneficial, while chronic exposure to senescent cells leads to detrimental consequences. Although some research has been done on skeletal muscle, it has not yet been demonstrated how senescent cells influence muscle regeneration and disease. In my thesis, I aim to evaluate the role of senescent cells from different perspectives: in young, very old, and dystrophic mice (mdx mice). Also, I will propose a mechanism by which senescent cells influence the skeletal muscle during muscle regeneration. Finally, I will describe the role of CD36 in SASP production and how it regulates muscle regeneration.

RESULTS

1. KINETICS OF CELLULAR SENESCENCE IN REGENERATING MUSCLE TISSUE

Senescent cells participate in skeletal muscle regeneration[227]. However, the complete kinetics of the process have not been shown, leaving several open questions, such as when they reach their maximum levels and how long they persist during the course of muscle regeneration. Thus, we first decided to characterise the time course of senescent cells in regenerating muscles of young mice. We performed an intramuscular injection of CTX to induce muscle regeneration in p16-3MR mice followed by a luciferase assay to track p16^{INK4a}-expressing cells *in vivo*. Maximum luminescence originating from p16-expressing cells was observed between 3 and 7 DPI, reaching basal levels at 21 DPI (Figure 11).

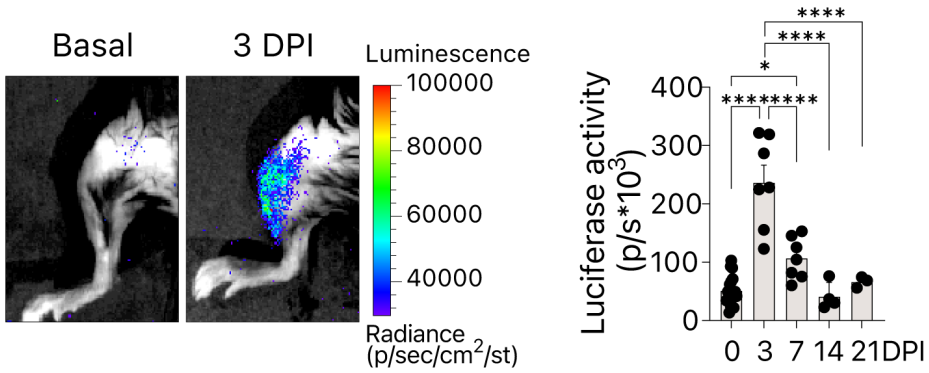

Figure 11. Presence of p16^{INK4a}-expressing cells in skeletal muscle of young mice upon injury.
Representative images and quantification of *in vivo* Renilla luminescence activity in muscles of p16-3MR mice at the indicated DPI with CTX (p/s: photons per second; n=3-18 muscles from 3-12 mice). Results are displayed as mean ± s.e.m.; P-values were calculated by Tukey's test; significance is reported as *p<0.05 and ****p<0.0001.

To corroborate these data, we parallelly performed SA-β-gal staining in regenerating frozen tissue of young animals. Similar to the luciferase assay, SA-β-gal^{+} cells start to appear at 3 DPI, peaking between 3 and 7 days and gradually decreasing until 21 DPI (Figure 12A). Thus, we concluded that senescent cells appear transiently, reaching their maximum levels between 3 and 7 DPI, in the regenerating muscle tissue of young animals.

Muscle regeneration is compromised with ageing, partly due to the entrance of SC into senescence[91,94]. We next questioned whether the kinetics of senescent cells were different during muscle regeneration of very old mice. To address this, we

induced muscle regeneration in geriatric mice (>28 months old) and analysed different markers of senescence.

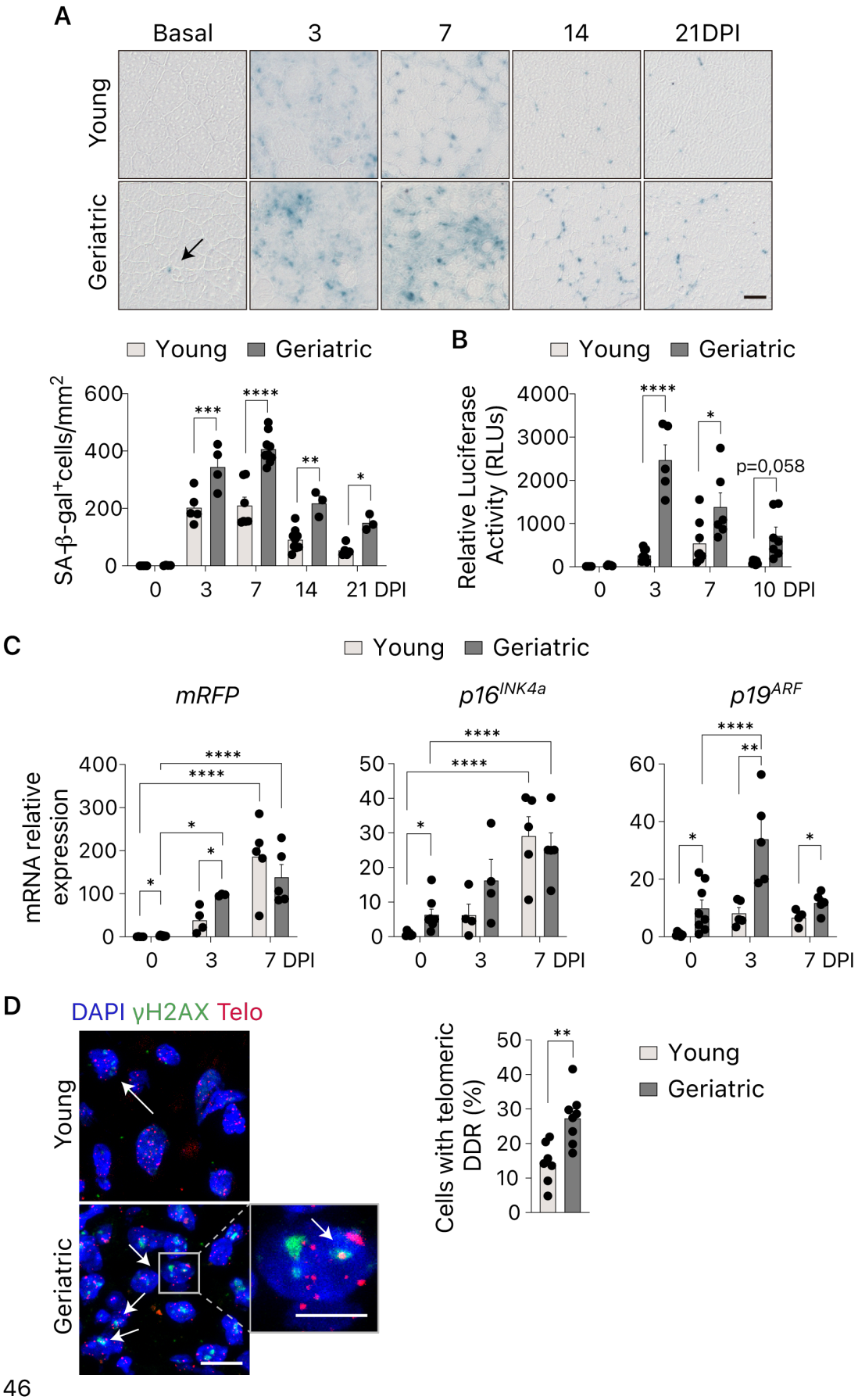

Figure 12. Presence of senescent cells in regenerating muscle of young and geriatric mice.

A) Representative images and quantification of SA-β-gal$^+$ cells in regenerating tibialis anterior (TA) muscles from young (3-6 months) and geriatric (>28 months) mice at the indicated DPI (n=3-9 mice). **B**) Quantification of Renilla luciferase activity in regenerating muscle from young and geriatric animals at the indicated DPI. The luciferase activities are expressed relative to the activity of basal young muscle (n=5-8 TA muscles from 4-7 mice). **C**) RT-qPCR of *p16^{INK4a}*, *p19^{ARF}*, and *mRFP* in young and geriatric muscle tissue from p16-3MR mice at the indicated DPI (n=3-8 TA mice). **D**) Representative images and quantification of cells with telomeric DDR (DDR: DNA damage response) in regenerating TA muscles from young and geriatric mice at 3 DPI (n=7-8 mice). Scale bars: 50 μm in **A**, 10 μm in **D** (low magnification), and 5 μm in **D** (high magnification). Results are displayed as mean ± s.e.m.; P-values were calculated by Sidak's test in **A** and **B**, a two-tailed unpaired t-test in **C** and Mann-Whitney test in **D**; significance is reported as *p<0.05, **p<0.01, ***p<0.001 and ****p<0.0001.

The level of SA-β-gal$^+$ cells was significantly higher in samples of geriatric mice at all time points (Figure 12A). In contrast to young mice, considerable levels of senescent cells were detected even at 21 DPI in samples from geriatric mice, correlating with their less efficient recovery process. Analysis of luminescence activity and RT-qPCR of senescent markers *p16^{INK4a}*, *p19^{ARF,}* and *mRFP* in p16-3MR mice were in line with previous results, confirming higher levels of senescent cells in regenerating muscle at an advanced age (Figure 12B,C). Moreover, cells with telomeric DNA damage, another well-accepted marker of cellular senescence, were more abundant in regenerating muscle tissue from geriatric mice versus the young ones (Figure 12D). Altogether, these results indicate that the burden of senescent cells is higher and more prolonged in geriatric mice, suggesting that senescent cells might be involved in the regenerative decline observed with ageing.

2. TRANSCRIPTOMIC CHARACTERIZATION OF ISOLATED SENESCENT CELLS FROM DAMAGED MUSCLE TISSUE

2.1 Establishment of an isolation protocol for senescent cells

Our next goal was to efficiently isolate senescent cells from a complex tissue *in vivo*. An SA-β-gal-based approach was first proposed for isolating senescent cells; however, it was not clear whether this could be used *in vivo*. A fluorogenic substrate 5-dodecanoylaminofluorescein di-β-d-galactopyranoside (C_{12}FDG), which marks cells with SA-β-gal activity, provided a valuable tool for senescent cell isolation by FACS[242]. However, the use of bafilomycin A1, or of other inhibitors of lysosomal acidification, was needed for the described protocol, but this protocol resulted in high cell death rates when coupled with tissue digestion protocol. To overcome this technical limitation, we obtained a less toxic method with a reagent that mimics the C_{12}FDG mechanism of action, named SPiDER-β-gal[243]. To test this approach, we first induced cellular senescence in myoblasts with etoposide *in vitro* and then evaluated SA-β-gal activity by three strategies: canonical SA-β-gal staining by light microscopy, C_{12}FDG, and SPiDER-β-gal staining by flow cytometry (Figure 13). All three assays showed higher SA-β-gal activity in etoposide-treated cells, thus validating SPiDER-β-gal reagent for detecting senescent cells *in vitro* (Figure 13).

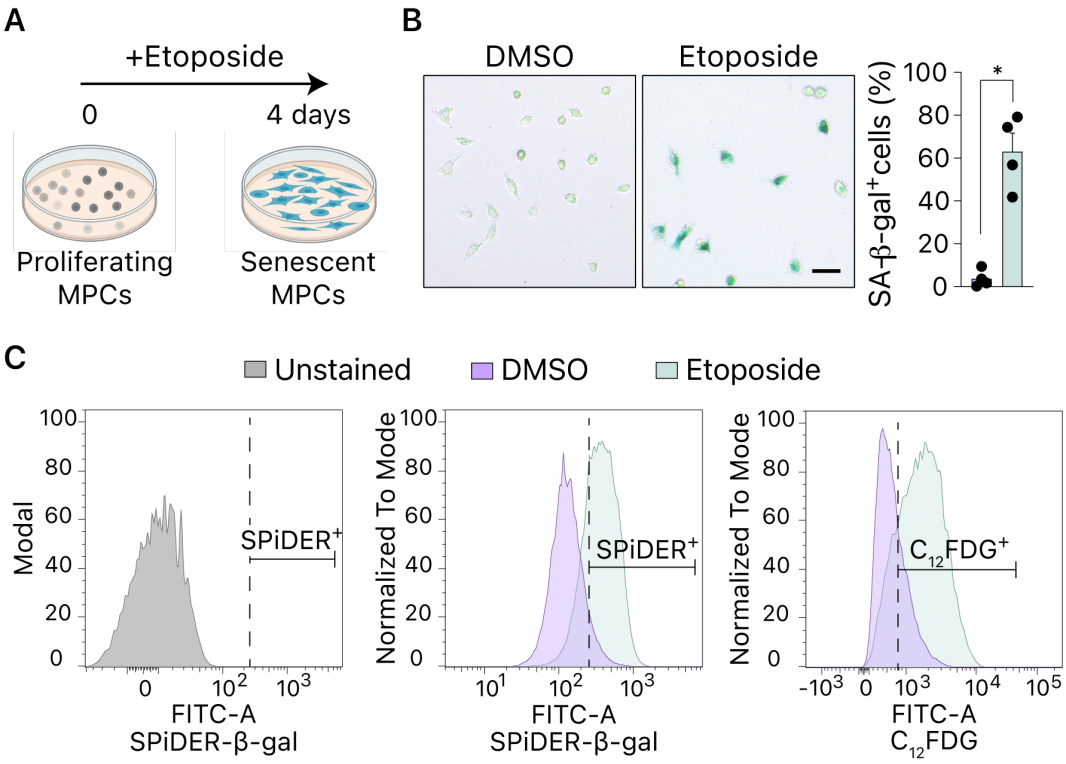

Figure 13. Validation of SPiDER-β-gal in etoposide-treated myoblasts *in vitro*.
A) Schematic representation of senescence induction with etoposide. **B**) Representative images and quantification of SA-β-gal staining in MPCs cultured in the presence of etoposide (1 μM) or dimethyl sulfoxide (DMSO) for 4 days (n=4 mice). **C**) Cells were stained with SPiDER-β-gal and C_{12}FDG in parallel and analysed by flow cytometry to assess their entry into senescence. An unstained control was used for SPiDER-β-gal and C_{12}FDG threshold definition. Histogram representation of SPiDER-β-gal and C_{12}FDG intensity are shown. Scale bar: 10 μm. Results are displayed as mean ± s.e.m.; P-value was calculated by the Mann-Whitney test; significance is reported as *p<0.05.

To translate this strategy to muscle tissue and to isolate senescent cells from regenerating muscle, we collected regenerating muscle tissue at 3 DPI and stained it with SPiDER-β-gal following the first round of digestion and analysed it using a FACS Aria II cell sorter. We identified three populations based on SPiDER-β-gal staining: SPiDER^{Low}, SPiDER^{Medium,} and SPiDER^{High} (Figure 14), which we sorted and analysed for distinct senescence markers.

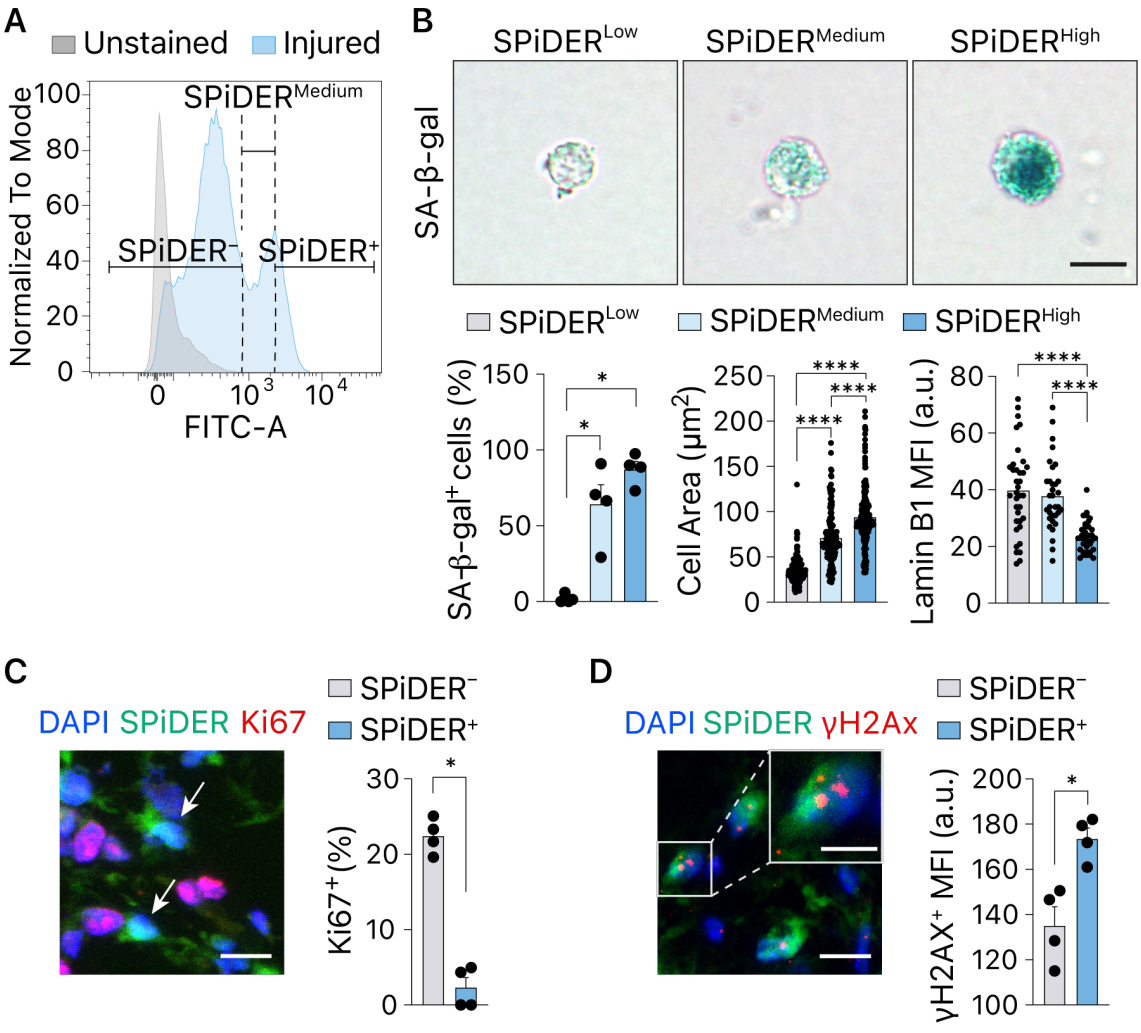

Figure 14. Validation of SPiDER-β-gal in sorted cells from regenerating muscle tissue.

A) Histogram representation of SPiDER-β-gal staining and gating strategy employed for isolation of SPiDER^{Low}, SPiDER^{Medium}, and SPiDER^{High} populations from injured skeletal muscle at 3 DPI. **B**) Representative images and quantification of SA-β-gal staining (n=4 mice), cell area (n=169-220 cells), and lamin B1 expression (n=33-36 cells) in freshly sorted SPiDER^{Low}, SPiDER^{Medium}, and SPiDER^{High} from regenerating muscles at 3 DPI. Representative images and quantification of **C**) Ki67 positivity (n=4 mice) and **D**) γH2Ax intensity (n=4 mice) in SPiDER^{+} and SPiDER^{-} cells in regenerating TA at 4 DPI. Nuclei were stained with 4,6-diaminido-2-phenylindole (DAPI). Arrows indicate SPiDER^{+} cells. Scale bars: 10 μm in **C**, and **D** (low magnification) and 5 μm in **B** and **D** (high magnification). Results are displayed as mean ± s.e.m.; P-values were calculated by a two-tailed unpaired t-test in **B** (middle and right panel) and Mann-Whitney test in **B** (left panel) **C** and **D**; significance is reported as *p<0.05 and ****p<0.0001.

Both SPiDER^{Medium} and SPiDER^{High} presented enrichment in SA-β-gal^{+} cells and enlarged cell area; however, only the SPiDER^{High} population showed downregulation of lamin B1 intensity (Figure 14B). These results suggest that a more restrictive gating strategy leads to a more efficient isolation of senescent cells. To further confirm that SPiDER-β-gal is sufficient to mark senescent cells, we performed simultaneous staining of SPiDER-β-gal with proliferation marker Ki67 or DNA damage marker γH2Ax in regenerating muscle tissue. Notably, SPiDER-β-gal^{+} cells (herein, "SPiDER^{+} cells") presented higher levels of γH2Ax expression compared to SPiDER^{-} cells and very low Ki67 levels, suggesting higher DNA damage and absence of proliferation in SPiDER^{+} cells (Figure 14C,D). Thus, we concluded that SPiDER-β-gal preferentially marks senescent cells, corroborated by several markers of cellular senescence.

2.2 Transcriptomic atlas of senescent cells in regenerating muscle

Once we established an efficient sorting protocol for senescent cell isolation, we asked which cell populations undergo cellular senescence in a muscle regeneration context. For this purpose, we isolated SPiDER^{+} and SPiDER^{-} cells from regenerating muscle and performed single-cell RNA-sequencing (scRNA-seq). We considered some technical limitations and established needed controls before the sequencing. First, we already learned that a more restrictive gating strategy was needed to efficiently sort senescent cells. For that, we used two negative controls to define SPiDER-β-gal threshold, a negatively stained sample (fluorescence minus one, FMO) and a non-injured sample (basal muscle) stained with SPiDER-β-gal (Figure 15). The latter proved highly useful for the background SPiDER-β-gal signal

definition, since we already defined that senescent cells are undetected in resting muscle conditions. Second, due to the high variability of cell populations during muscle regeneration and their autofluorescence, we determined that at least one broad population marker was needed for the correct establishment of SPiDER^{+} gating. Thus, we separated all cell populations that participate during muscle regeneration into hematopoietic and non-hematopoietic, based on high and low autofluorescence, respectively, by labelling with the CD45 surface marker (Figure 15). In addition, this strategy allowed the enrichment of less abundant cellular fractions, enabling us to detect senescent cells even in minor populations.

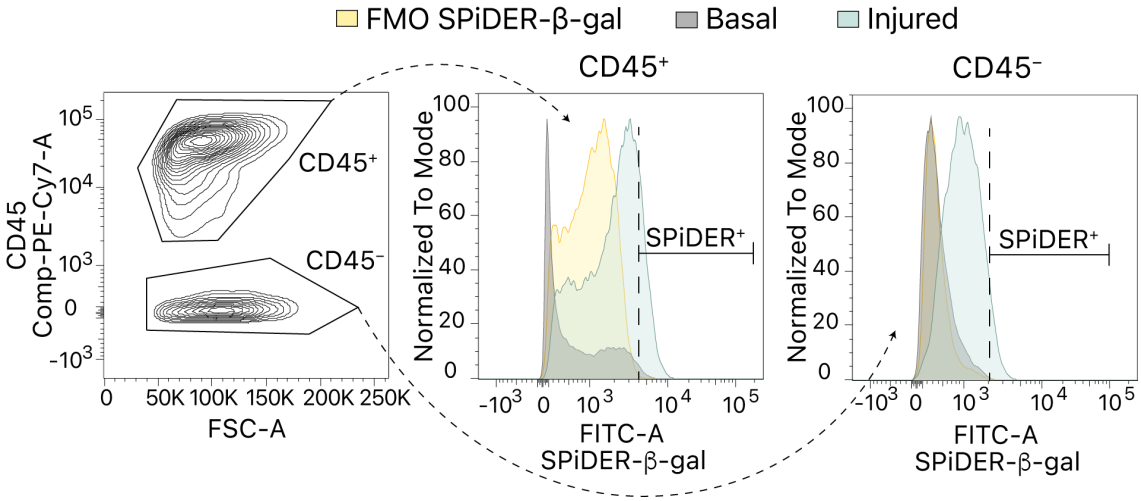

Figure 15. Gating strategy employed for isolation of SPiDER^{+} cells from regenerating muscle tissue of young mice at 3 DPI.
Cells were divided into two major populations with anti-CD45 antibodies to overcome differences in auto-fluorescence of hematopoietic and non-hematopoietic populations. Fluorescence Minus One (FMO) and samples from non-injured muscle tissue were used to set the threshold for SPiDER^{+} staining within each cell population.

We then isolated SPiDER^{+} and SPiDER^{-} populations from regenerating muscle tissue at 3 DPI and sequenced them with a single-cell approach. The clustering analysis showed that the non-senescent SPiDER^{-} populations reproduced recently-published single-cell studies in injured muscle[11–13]. Interestingly, most SPiDER^{+} cells were distributed within 3 major clusters: SCs, FAPs, and MCs (Figure 16A). This suggested that the majority of senescent cells emerged from three major niche-cell constituents after injury. In addition, we also found less abundant SPiDER^{+} populations, including antigen-presenting cells, ECs, B/T/NK cells, and neutrophils (Figure 16A). Differential expression (DE) analysis revealed a core signature of 16 upregulated and 33 downregulated genes in the major senescent

cell populations (Figure 16B), the former included some widely known inflammatory and matrix-remodelling/fibrotic SASP factors (e.g., *Ccl2*, *Ccl8*, *Igfbp4,* and *Timp2*).

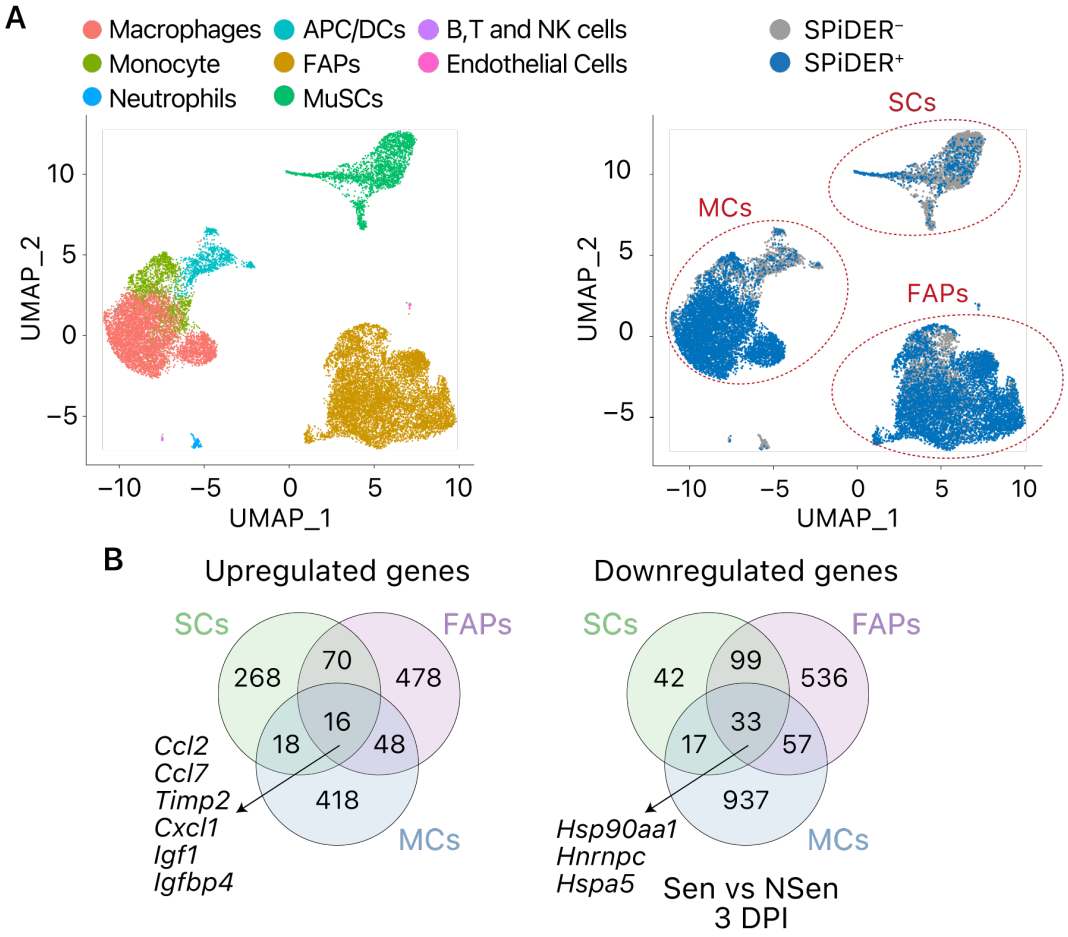

Figure 16. Single-cell atlas of senescent cells from regenerating muscle of young animals.
A) (left) Complete 21449 cell transcriptomic atlas assembled from SPiDER⁺ and SPiDER⁻ samples at 3 DPI from young mice. Data are presented as a uniform manifold approximation and projection (UMAP) to visualize variation in single-cell transcriptomes. Unsupervised clustering resolved at least 8 distinct types of cells (colour-coded in legend). (right) SPiDER⁺ cells were mainly ascribed to the indicated cell populations. **B**) Venn diagram showing the overlap between DE genes in SCs, FAPs, and MCs at 3 DPI from scRNA-seq data (Sen vs NSen were compared, false discovery rate (FDR)<0.05).

We next corroborated the scRNA-seq findings by immunostainings of surface-specific and senescence markers in regenerating muscle tissue. Senescent cells were either identified by $p16^{INK4a}$ or γH2Ax, while Pax7, PDGFRα, or F4/80 served for SC, FAP and MC visualization respectively (Figure 17A,B). Of note, and similar to mouse muscle, SA-β-gal- and $p16^{INK4a}$-positive cells were present in biopsies of damaged adult human muscle but not of intact human muscle (Figure 17C). Moreover, damaged areas of human muscle also contained SCs (NCAM/CD56⁺), FAPs (PDGFRα⁺), and MCs (CD68⁺) that were positive for the DNA-damage

response marker 53BP1 (Figure 17D). Thus, senescent SCs, FAPs, and MCs are specifically induced in damaged muscles of both humans and mice. Together, these results provided 1) the first single-cell cartography of senescent cells *in vivo* to date, and 2) the identity of new senescent niche constituents after tissue injury.

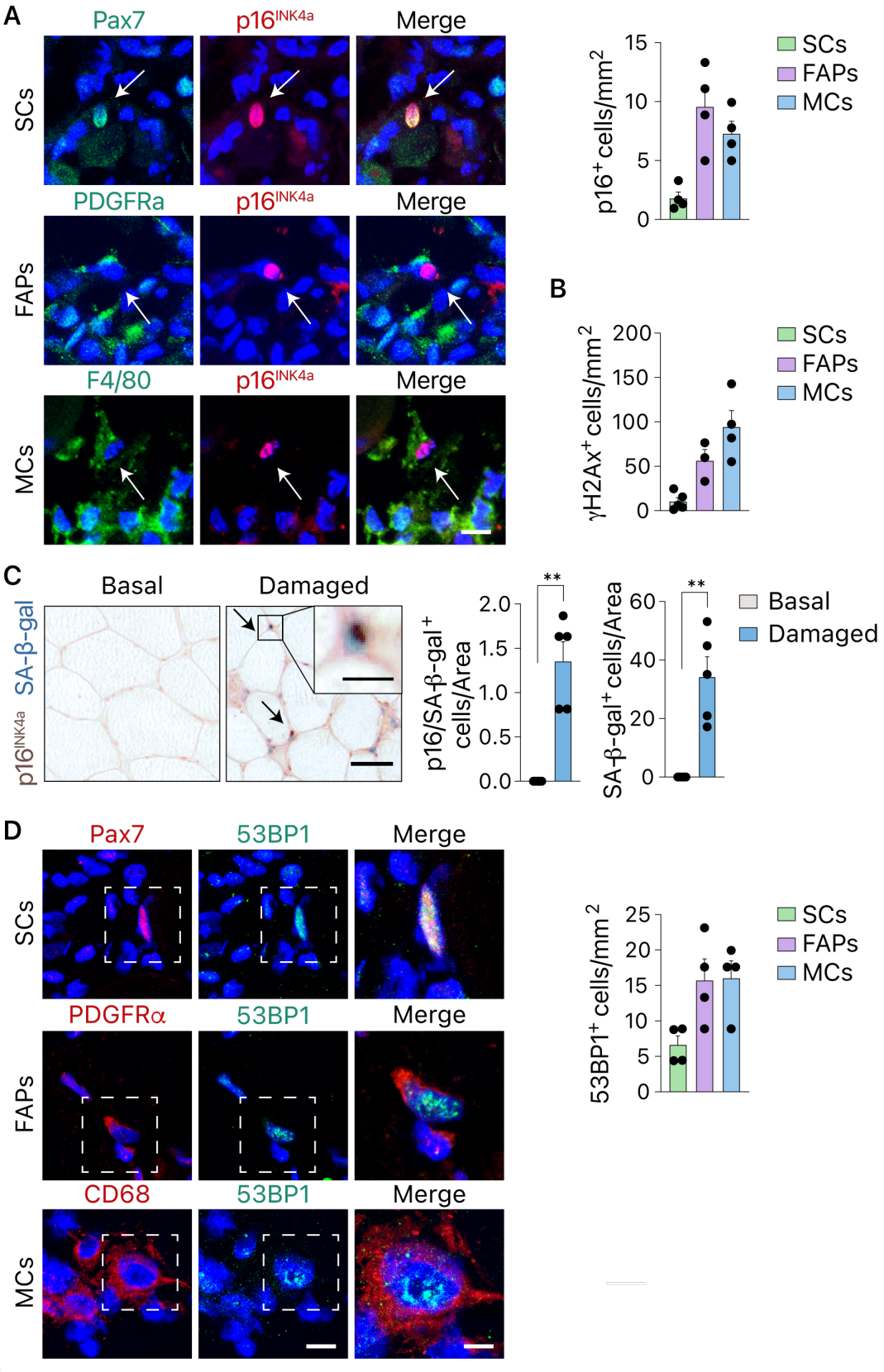

Figure 17. Major niche components undergo cellular senescence in damaged muscles of humans and mice.
A) Representative images and quantification of $p16^{INK4a+}$ cells (n=4 mice) and **B**) $\gamma H2Ax^{+}$ cells (n=3-5 mice) in regenerating muscles from young mice at 4 DPI. Each cell type was labelled with the indicated antibodies and nuclei with DAPI. Arrows indicate $p16^{INK4a+}$ cells. **B**) Quantification of $\gamma H2Ax^{+}$ cells (n=3-5 mice) in regenerating muscles from young mice at 4 DPI. **C**) Representative images and cell quantification of SA-β-gal and $p16^{INK4a+}$ immunohistochemistry staining of uninjured and damaged human muscle samples (n=5 samples/group, age=81±7.5 years old). The arrow shows a double-positive cell. **D**) Representative images and quantification of $53BP1^{+}$ cells in regenerating human muscle. Each cell type was labelled with indicated antibodies, and nuclei with DAPI (n=4 samples/group, age=81±7.5 years old). Scale bars: 50 μm in **C** (low magnification) 10 μm in **A** and **D** (low magnification) and 5 μm in **C** (high magnification) and **D** (high magnification). Results are displayed as mean ± s.e.m.; P-values were calculated by the Mann-Whitney test; significance is reported as **p<0.01.

2.3 A novel method for separating distinct types of senescent cells *in vivo*

We also aimed to obtain an in-depth characterization of senescent cells in regenerating muscle, including ageing and kinetics perspective. Although single-cell techniques provide valuable information on cellular heterogeneity, they also present limitations in sequencing depth and complicated downstream analysis. It might be challenging to define a pattern of gene expression in such complex data, especially when different variables are combined (e.g. age, time point, three populations). Further, single-cell technology is expensive and therefore not practical for studies with a vast number of conditions. Thus, we decided to use low-input RNA-seq technology to generate deep transcriptomic data of the three main populations of senescent cells, given their scarce numbers in regenerating muscle.

For that, we generated a complex sorting panel for simultaneous isolation of senescent and non-senescent SCs, FAPs, and MCs. Briefly, cells were selected using forward (FSC) and side (SSC) scatter detectors, and live cells were chosen by $DAPI^{-}$ staining. From live cell population, MCs were identified as $CD45^{+}$ and $F4/80^{+}$. SCs were gated from $CD45^{-}$ $F4/80^{-}$ population as $\alpha7\text{-integrin}^{+}$ meanwhile, FAPs were identified by $Sca1^{+}$ staining from $\alpha7\text{-integrin}^{-}$ $CD31^{-}$ cell population. Finally, we stained with SPiDER-β-gal to isolate $SPiDER^{+}$ and $SPiDER^{-}$ cells within each population of interest (Figure 18).

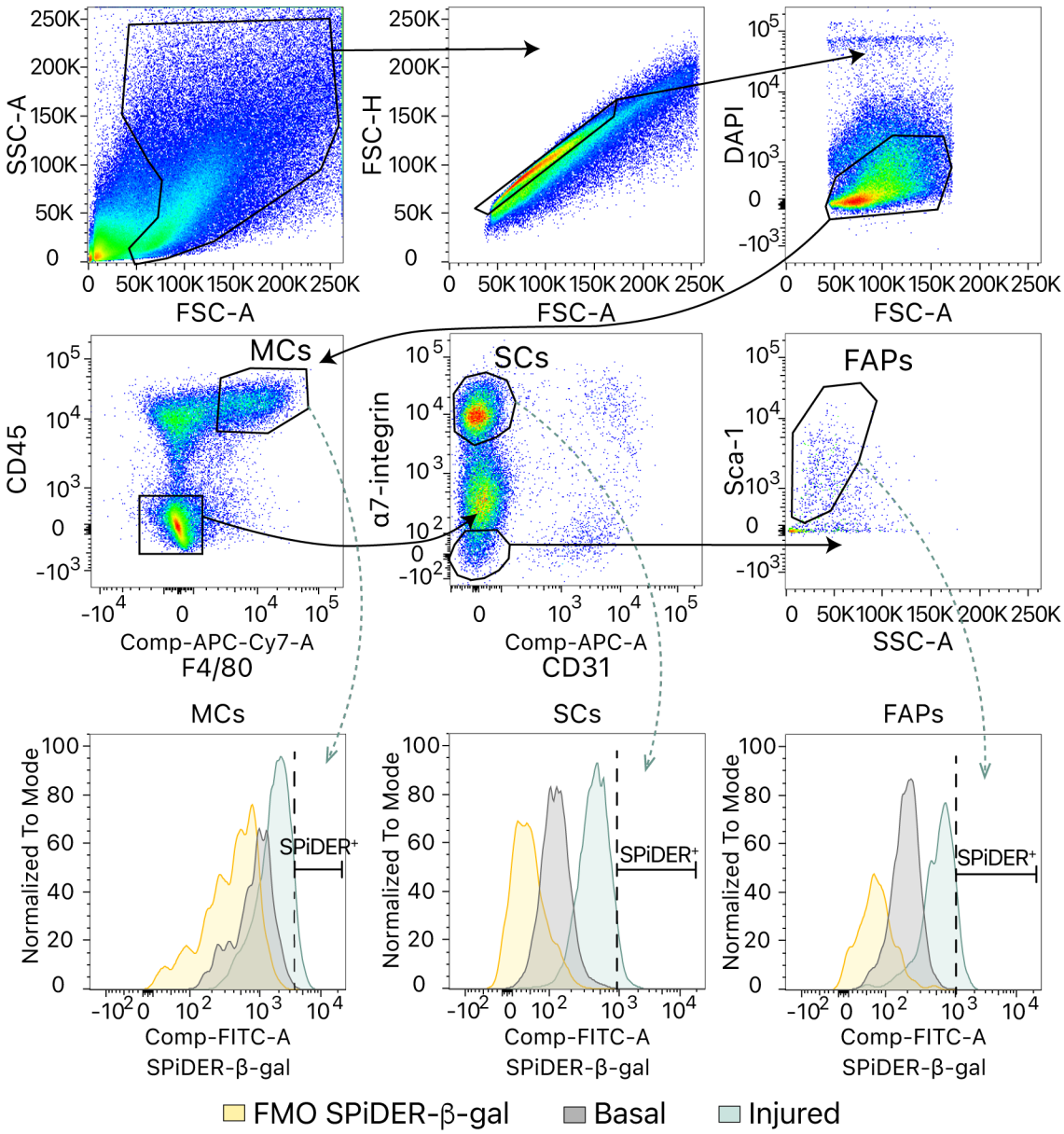

Figure 18. Gating strategy used to simultaneously isolate SCs, FAPs, and MCs from wild-type (WT) mice.
Representative histogram plots from cytofluorimetric analysis employed to assess SPiDER levels in the cell populations are shown. FMO controls and non-injured samples were used to determine the threshold for SPiDER within each cell population.

We next confirmed the nature of sorted cells by immunostaining of cell-type-specific markers, by using Pax7 for SCs, TCF4 for FAPs, and CD11b for MCs (Figure 19A). Additionally, we double-checked the correct isolation of the three cell populations in posterior gene expression analysis (Figure 19B). Indeed, all sorted SCs populations (Basal, NSen, and Sen) expressed *Pax7* and *Itga7* (gene codifying for α7-integrin), while FAPs expressed *Pdgfra* and *Ly6a* (codifying for PDGFRα and Sca-1), and MCs presented *Itgam* and *Adgre1* (CD11b and F4/80) (Figure 19B).

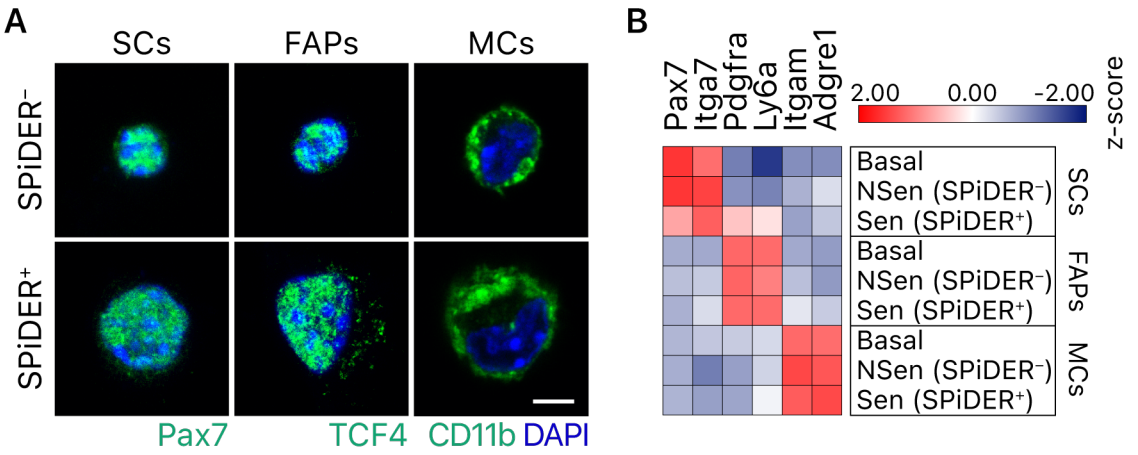

Figure 19. Validation of simultaneous isolation protocol for SCs, FAPs, and MCs from WT mice.

A) Representative pictures of Pax7, TCF4, and CD11b expression in sorted SCs, FAPs, and MCs respectively. **B**) Heatmap of gene expression levels of the indicated genes in basal, NSen, and Sen SCs, FAPs, and MCs. Scale bar: 1 μm.

Subsequently, we checked markers of senescence in the SPiDER^{+} fractions of SCs, FAPs, and MCs. The sorted SPiDER^{+} fractions presented lower proliferation rates in SCs and FAPs and higher levels of SA-β-gal activity, increased cell area, decreased lamin B1 expression, absence of apoptotic programmed death (terminal deoxynucleotidyl transferase biotin-dUTP nick end labelling [TUNEL] assay), and higher expression of p16^{INK4a} in all three populations, providing a thorough validation of our sorting strategy (Figure 20A-F). Thus, we established a protocol for simultaneous isolation of different senescent populations from regenerating muscle tissue, combining antibodies of cell surface markers and SPiDER-β-gal staining.

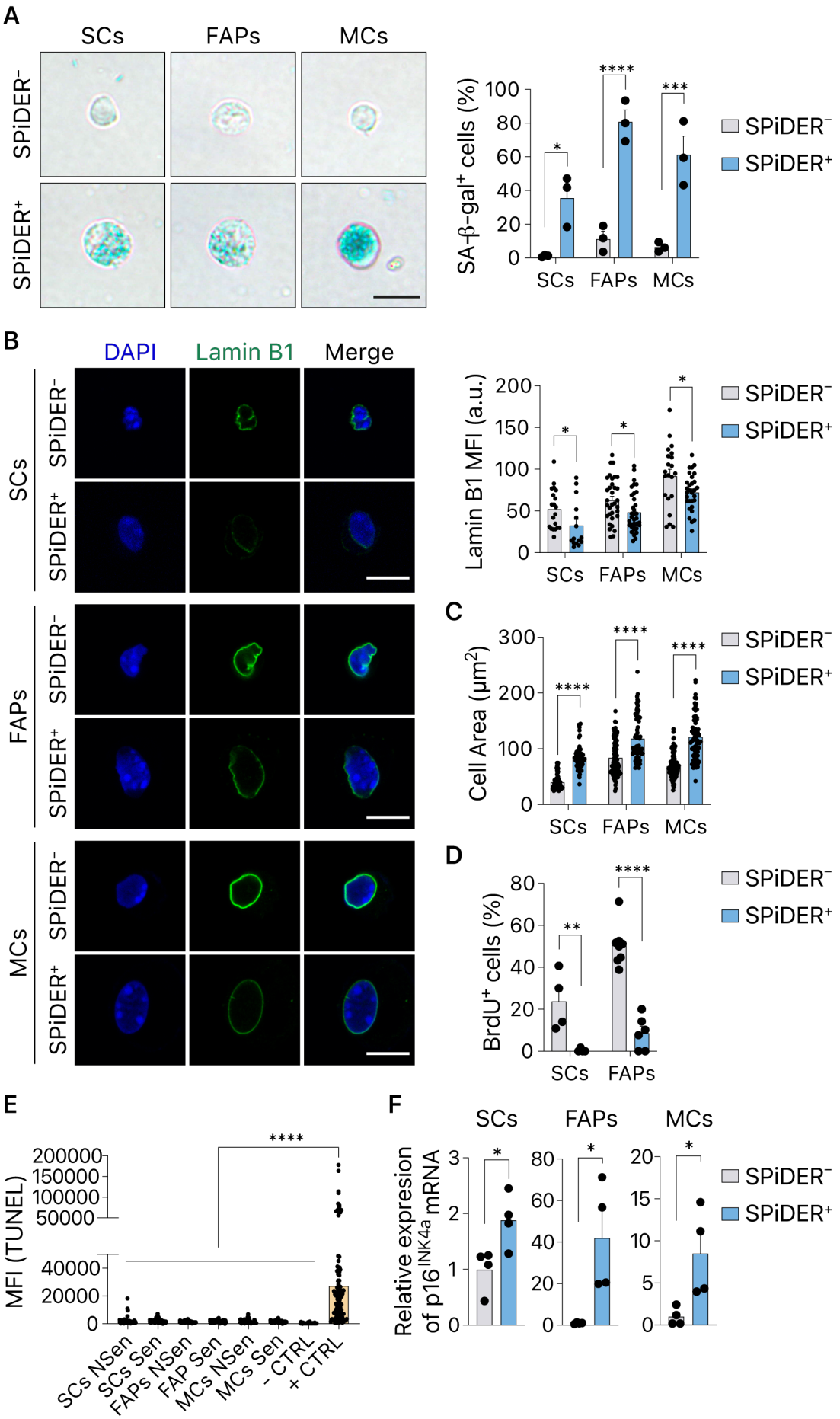
A
SCs
FAPs
MCs
SPiDER⁻
SPiDER⁺
SA-β-gal⁺ cells (%)
SPiDER⁻
SPiDER⁺
B
DAPI
Lamin B1
Merge
SCs
FAPs
MCs
Lamin B1 MFI (a.u.)
C
Cell Area (μm²)
D
BrdU⁺ cells (%)
E
MFI (TUNEL)
SCs NSen
SCs Sen
FAPs NSen
FAP Sen
MCs NSen
MCs Sen
- CTRL
+ CTRL
F
Relative expresion of p16INK4a mRNA

Figure 20. Validation of senescent SCs, FAPs, and MCs simultaneous isolation with SPiDER-β-gal-based protocol from WT mice.
Analysis of freshly sorted SPiDER^{+} and SPiDER^{-} SCs, FAPs, and MCs from regenerating muscles at 3 DPI. **A**) Representative images and quantification of SA-β-gal staining (n=3 mice). **B**) Representative images and quantification of lamin B1 expression (n=15-35 cells; arbitrary units: a.u.). **C**) Quantification of cell area (n=55-106 cells). **D**) Freshly isolated SPiDER^{+} and SPiDER^{-} SCs and FAPs were obtained at 7 DPI, cultured for 3 days, and BrdU incorporation quantified (n=4-8 mice). **E**) Quantification of TUNEL assay in freshly sorted SPiDER^{+} and SPiDER^{-} SCs, FAPs, and MCs. Cells treated with DNase were used as a positive control (n=32-101 cells). **F**) RT-qPCR of p16^{INK4a} in freshly sorted SPiDER^{+} and SPiDER^{-} SCs, FAPs, and MCs from regenerating muscles at 3 DPI (n=4 mice). Scale bars: 10 μm in **B** and 5 μm in **A**. Results are displayed as mean ± s.e.m.; P-values were calculated by Sidak's test in **A**, **D**, and **E**, two-tailed t-test in **B** and **C**, and Mann-Whitney test in **F**; significance is reported as *p<0.05, **p<0.01, ***p<0.001 and ****p<0.0001.

2.4 Senescent cells retain their homeostatic identity while gaining lineage-inappropriate traits in old age

Cellular senescence has been described as a highly heterogeneous state, with distinct transcriptomic profiles of senescent cells depending on the trigger, cellular type, and kinetics[127]. Nevertheless, previous studies on senescent cells have been exclusively performed *in vitro,* and it is unknown whether the same trends occur *in vivo*. Thus, we opted to describe how senescent cells resemble or differ among different cell populations, ages, and time points. For that, we isolated senescent (Sen) and non-senescent (NSen) SCs, FAPs, and MCs from resting (with only NSen populations) or regenerating muscle at 3 and 7 DPI from young and geriatric mice, using our newly established approach based on SPiDER-β-gal. Altogether, we generated a blueprint comprised of 36 different conditions to define the behaviour of senescent cells in regenerating muscle. Principal component analysis (PCA) showed that the different conditions primarily clustered according to their cell type, rather than their state, age, or time point; however, some populations of senescent cells (e.g. Y-SC^{Sen7d} and G-SC^{Sen3d}) did not follow this trend (Figure 21A). When the clustering was performed within a particular cell type, we could observe clear segregation according to the cell state, with a strong influence of senescence (Figure 21B).

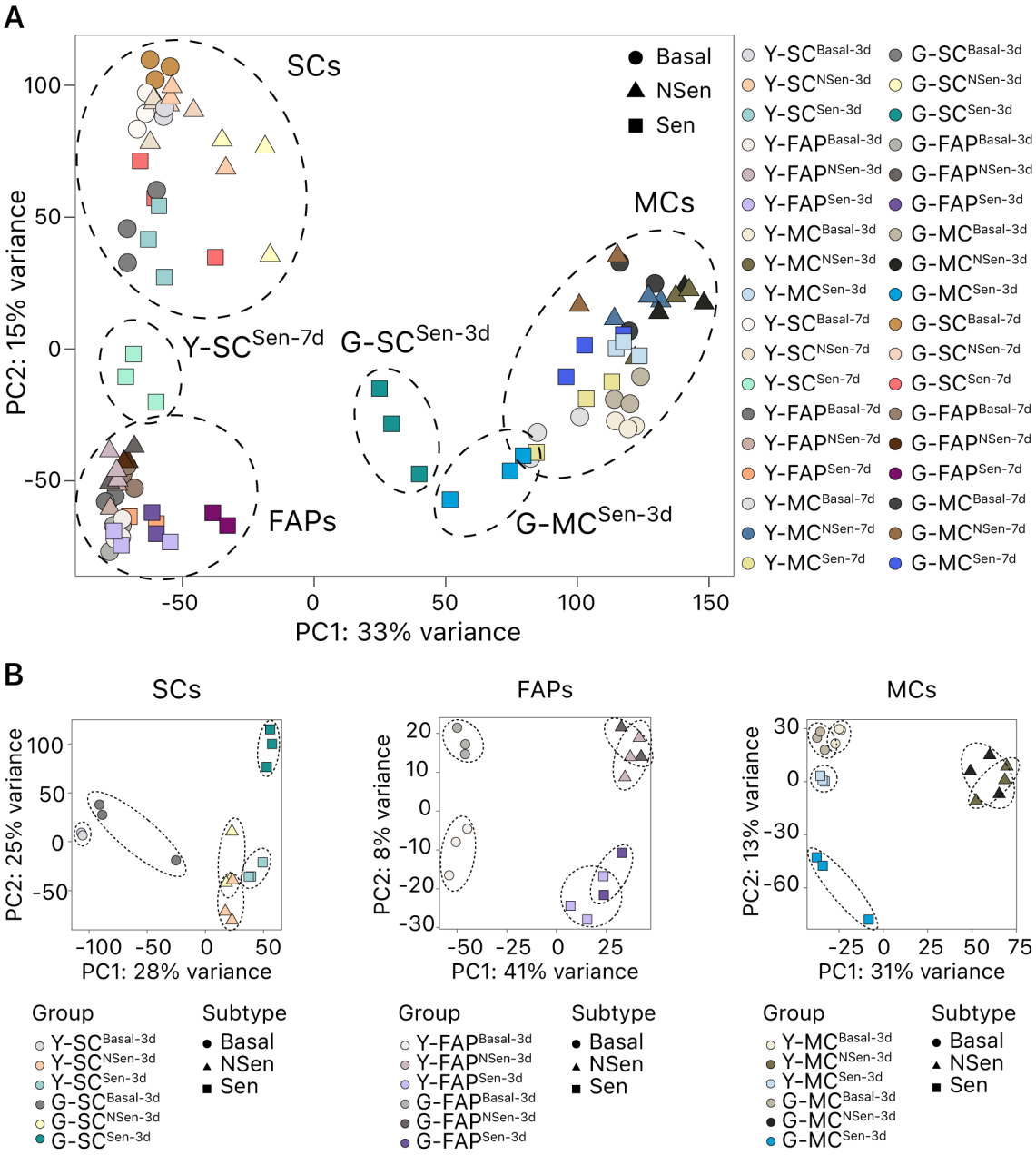

Figure 21. Senescent cells majorly cluster according to their cell identity.

A) Principal component analysis (PCA) of the full transcriptome of senescent (Sen), non-senescent (NSen), SCs, FAPs, and MCs isolated from resting (basal) and regenerating muscles of young and geriatric mice at 3 and 7 DPI. **B**) PCA of SCs (Sen, NSen, or basal), FAPs, and MCs from basal and regenerating muscles at 3 DPI of young or geriatric mice.

Differential expression analyses between Sen and NSen subpopulations at 3 DPI in young mice revealed 4958 differentially expressed (DE) genes in Sen MCs, 2251 in Sen SCs, and 1805 in Sen FAPs (Figure 22A), indicating high transcriptional heterogeneity of senescent cells even within the same niche.

A

		Early Senescence (3 DPI)		Late Senescence (7 DPI)	
		Genes ↑	Genes ↓	Genes ↑	Genes ↓
Young	SCs	1473	778	1723	838
	FAPs	998	807	359	354
	MCs	2667	2291	506	194
Geriatric	SCs	2682	2080	598	153
	FAPs	226	30	803	397
	MCs	1922	565	582	511

B

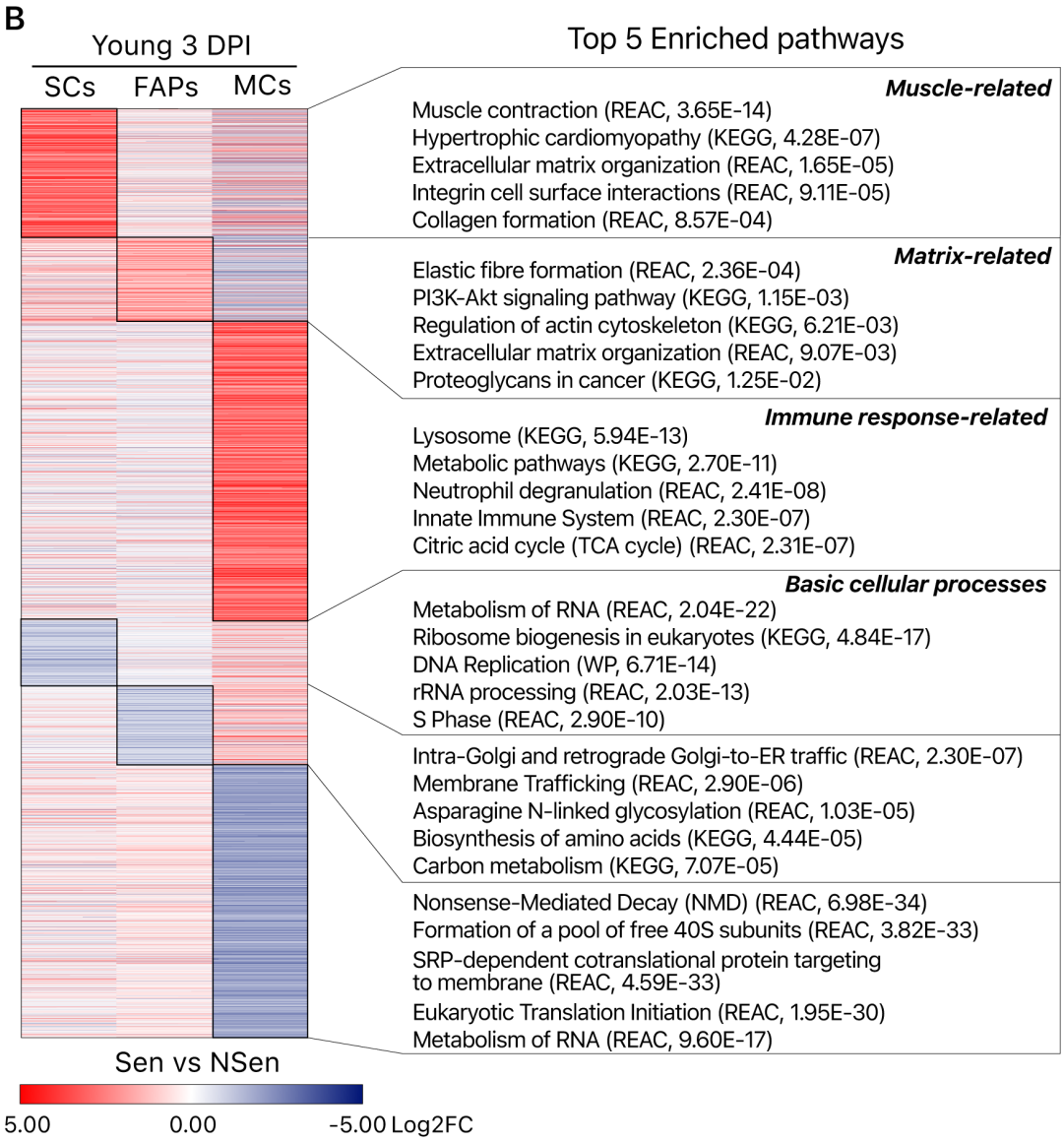

Figure 22. Senescent cells maintain the expression of cell-type-specific genes.
A) Table with DE genes in Sen vs NSen SCs, FAPs, and MCs from young and geriatric mice at 3 and 7 DPI (FDR <0.05). **B**) Heatmap of genes that were differentially expressed (DE) uniquely by one population of interest and the corresponding canonical pathways enrichment (CP) analysis (g:Profiler webserver). The heatmap shows base 2 logarithm fold change (log2FC) for Sen versus (vs) their NSen counterparts isolated from regenerating muscles of young mice at 3 DPI.

Basic cell processes, such as transcription, RNA metabolism, and translation, were downregulated in all three Sen subpopulations (Figure 22B). Nevertheless, many DE genes and associated enriched pathways were specific to each Sen cell type and revealed the cell of origin: muscle contraction and integrin/cell-surface interactions in Sen SCs, actin cytoskeleton and elastic fiber regulation in Sen FAPs, and innate immune functions and high lysosomal content in MCs (Figure 22B). This cell-of-origin memory accounted in part for the heterogeneity of senescent cells within the regenerative niche. With ageing, however, all geriatric Sen cells seemed to gain additional cell plasticity traits and had exacerbated pro-inflammatory traits (Figure 23). Thus, in addition to having a higher number of senescent cells with age (Figure 12), aged Sen cells also have exacerbated inflammatory features, which altogether may contribute to the regenerative failure of muscle tissue in extreme old age (Figure 23).

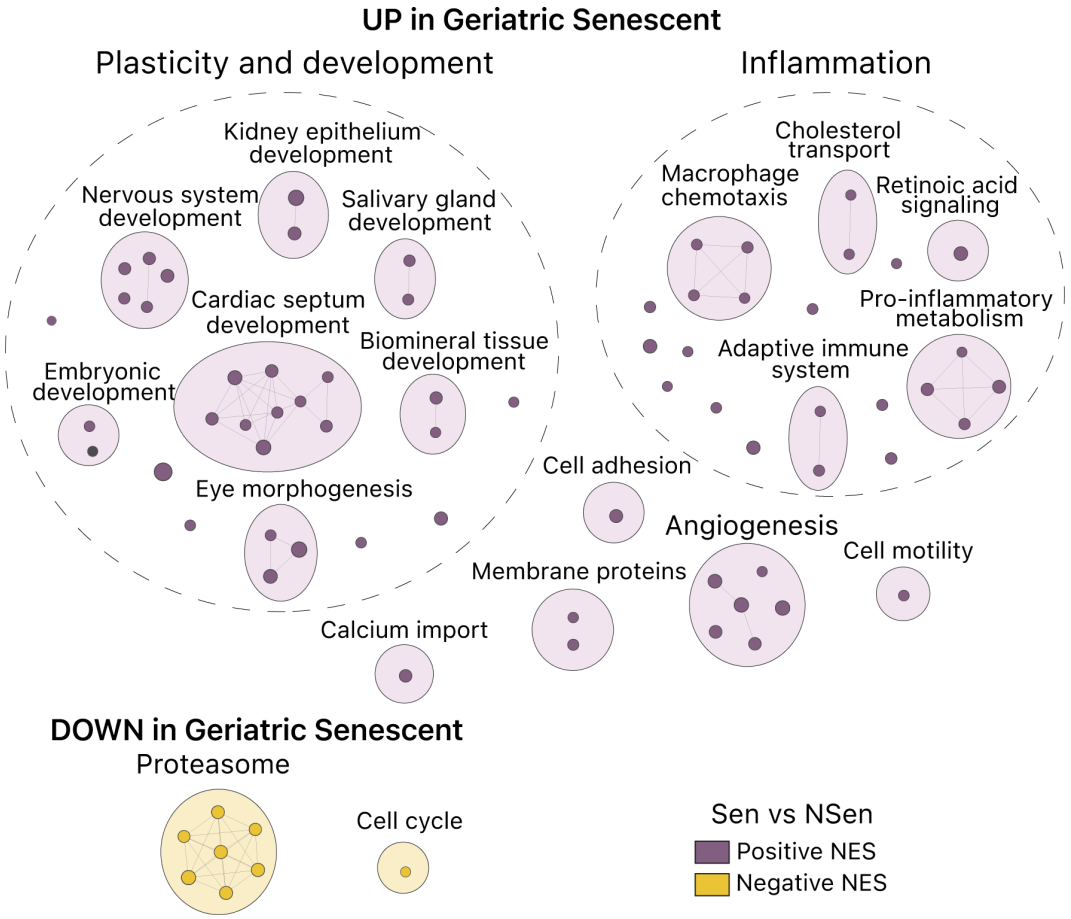

Figure 23. Senescent cells gain expression of lineage-inappropriate genes with ageing. Clusters of gene sets (GSEA) differentially enriched at 3 DPI in geriatric Sen populations, but not in young Sen populations. Gene sets were considered common with FDR<0.25 for all three geriatric Sen populations with the exclusion of gene sets common for at least two young Sen populations. Node size is proportional to the number of genes identified in each gene set. Grey edges indicate gene overlap.

2.5 Tissue injury drives senescence by inducing severe oxidative stress and DNA damage in a subset of niche cells

To understand how senescence is induced in the regenerative niche, we searched for pathways enriched in Sen cells early after muscle injury (e.g, at 3 DPI). Interestingly, Sen cells were enriched in pathways implicated in cellular stress, such as oxidative and metabolic stress (including ROS and OXPHOS production and lipid transport and metabolism), with concomitant downregulation of pathways implicated in DNA damage repair responses and mitochondrial functions as compared to NSen cells (Figure 24).

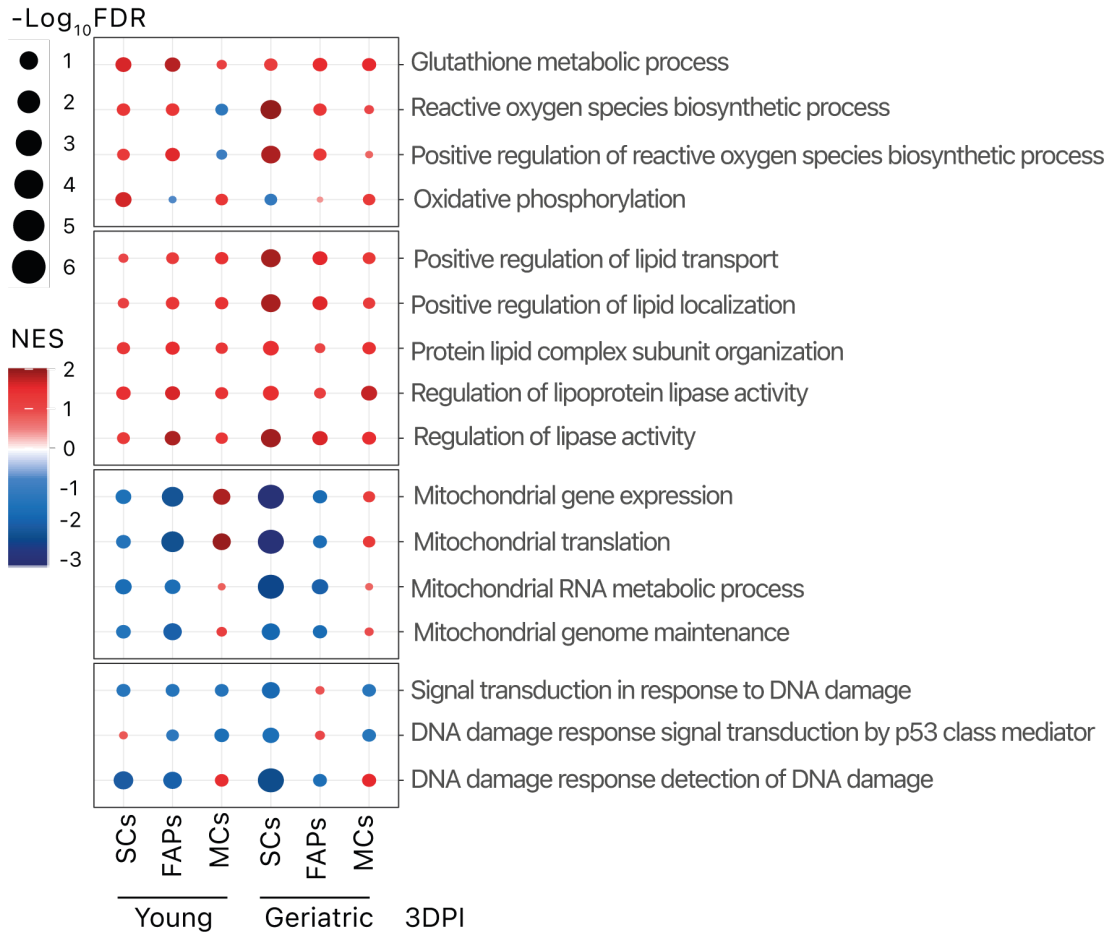

Figure 24. Senescent cells differentially express pathways implicated in stress and DNA damage response.
Dot plot of common up- and downregulated GO processes (GSEA, FDR<0.25) related to indicated functions in Sen vs NSen SCs, FAPs, and MCs from young and geriatric mice at 3 DPI.

We thus hypothesized that the high levels of DNA damage and high oxidative stress caused by injury are not efficiently repaired in a fraction of niche cells, triggering the cells to enter senescence rather than continue with their normal proliferative fate. Supporting this idea, all Sen cell types (SCs, FAPs, and MCs) had more DNA

damaged foci than NSen or basal cells (as shown by γH2Ax immunostaining) (Figure 25A).

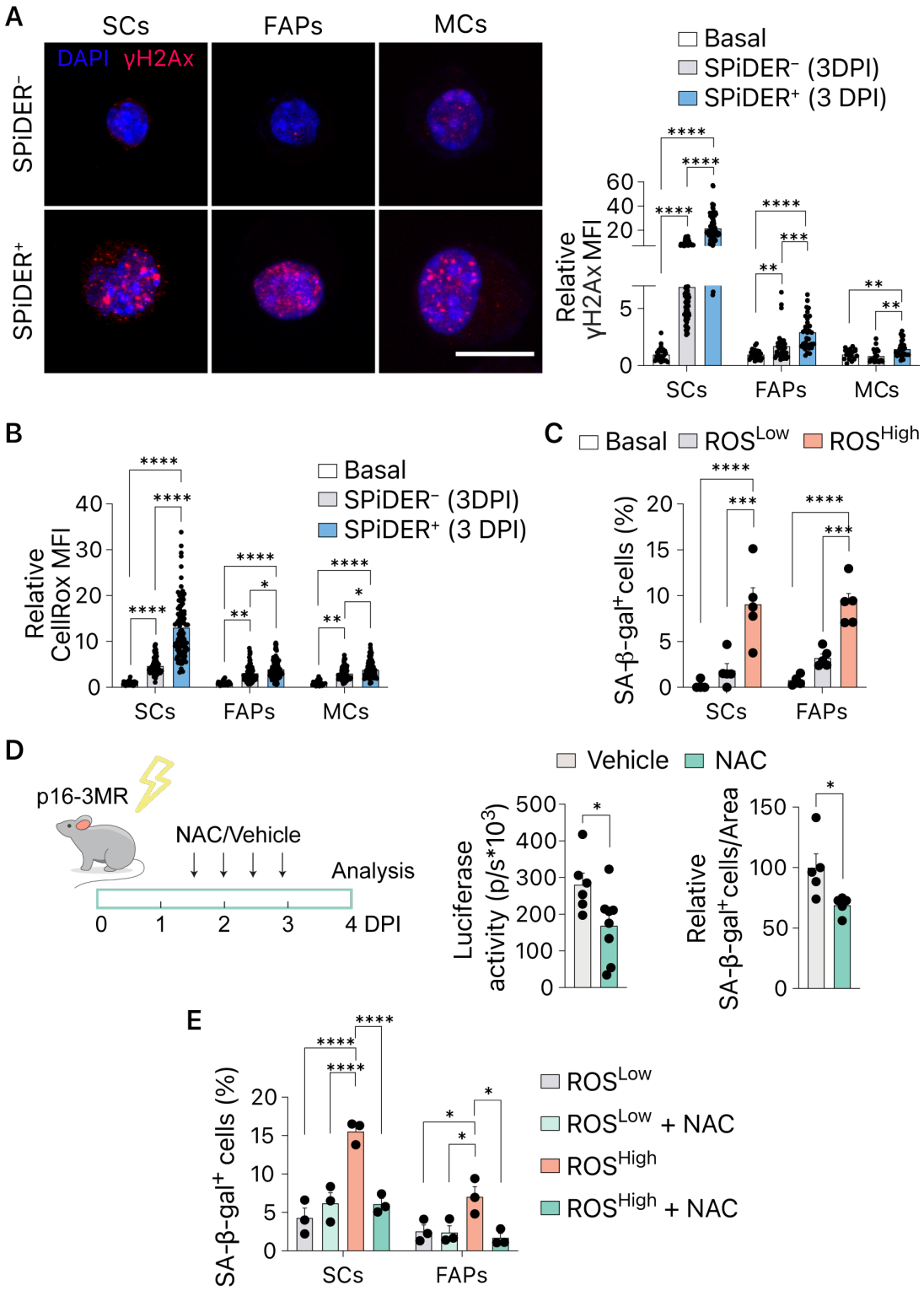

Figure 25. Tissue injury triggers niche cells to undergo senescence by inducing intolerable levels of oxidative stress and DNA damage.

A) Representative images of γH2Ax and quantification of γH2Ax (n=20-91 cells) and **B**) CellRox levels (n=20-104 cells) in freshly sorted SCs, FAPs, and MCs populations from Basal and regenerating muscles at 3 DPI. **C**) ROS^{High} and ROS^{Low} SCs and FAPs were isolated

from regenerating muscle at 1 DPI and cultured *in vitro* for 3 days. Quantification of SA-β-gal$^+$ cells in each population compared to basal cells (n=4-5 mice). **D**) Young p16-3MR mice were injured with CTX and treated with N-acetylcysteine (NAC) in drinking water during regeneration. (Left) Renilla luciferase activity in TA muscles at 4 DPI (n=6-8 TA from 4-6 mice), (Right) quantification of SA-β-gal$^+$ cells (n=5-6 TA from 4 mice). **E**) As in **C**, cells were sorted from regenerating muscles at 1 DPI and cultured for 3 days with or without NAC *in vitro* (n=3 mice). Scale bar: 10 μm. Results are displayed as mean ± s.e.m.; P-values were calculated by two-tailed t-test in **A** and **B**, Tukey's test in **C** and E, and Mann-Whitney test in **D**; significance is reported as *p<0.05, **p<0.01, ***p<0.001 and ****p<0.0001.

Further, Sen SCs, FAPs, and MCs at 3 DPI had more intense CellRox (ROS) staining than their NSen (or basal) counterparts (Figure 25B), which may be related to mitochondrial dysfunction in Sen cells (Figure 24). These results further validate the SPiDER-based FACS detection of distinct senescent cell types *in vivo*. To assess the causality of high ROS levels in driving injury-induced senescence, we sorted ROS^{High} and ROS^{Low} SCs and FAPs at 1 DPI (before the appearance of senescent cells at 3 DPI). Freshly sorted ROS^{High} cells, but not ROS^{Low} cells, became senescent in culture (shown by SA-β-gal staining) (Figure 25C). Conversely, inhibiting ROS with the antioxidant drug N-acetylcysteine (NAC) led to reduced senescence burden during muscle regeneration, as shown by luciferase activity *in vivo* and SA-β-gal staining in tissue (Figure 25D). Similar results were obtained *in vitro*, with NAC blocking senescence entry of ROS^{High} SCs and FAPs (Figure 25E).

2.6 Ageing primes niche cells for exacerbated injury-induced senescence

Senescent cells are more abundant in regenerating muscles of geriatric mice, and geriatric senescent cells displayed an increased pro-inflammatory profile. Thus, we hypothesised that ageing primes niche cells for increased senescence entry with a stronger phenotype. We first analysed the effect of ageing on SCs, FAPs, and MCs in resting conditions. Differential expression and pathway enrichment analysis revealed upregulation of immune-inflammatory response, DNA damage and cell-cycle arrest, lipid metabolism, matrix remodelling, insulin signalling, and downregulation of mitochondrial maintenance and function traits (Figure 26A). Accordingly, geriatric basal cells contained more DNA damage foci in telomeric regions than young Basal cells, as shown by telomere immunostaining of γH2Ax (Figure 26B). This coincided with previously reported increased ROS levels in geriatric cells, suggesting that the intrinsic accumulation of damage primes aged cells for senescence entry upon injury[94]. We also confirmed increased matrix deposition (Figure 26C) and expression of cell cycle inhibitors and inflammatory

factors in resting geriatric muscles (Figure 26D), which is consistent with the concept of basal inflammageing[244].

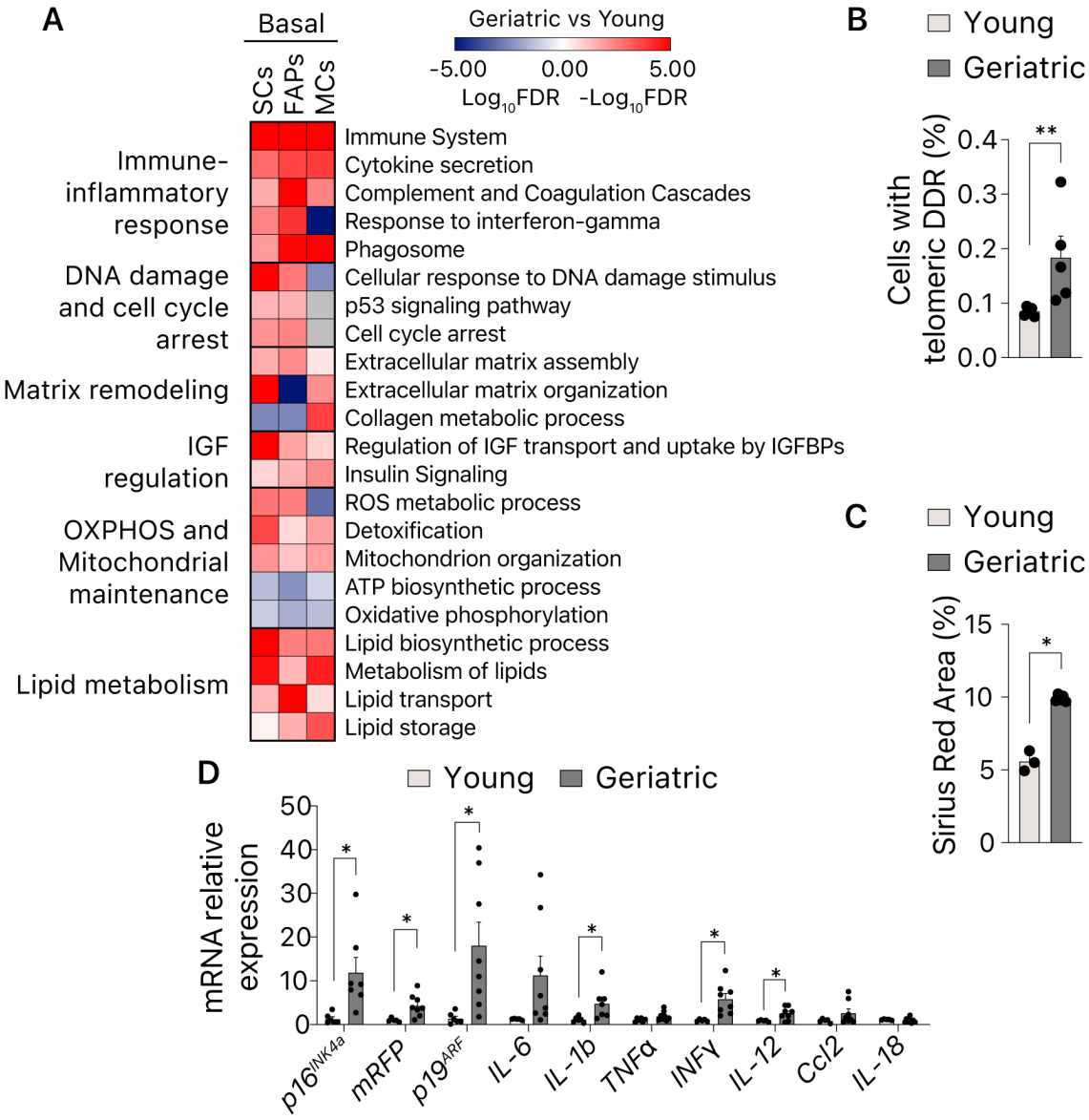

Figure 26. Ageing primes niche cells for exacerbated injury-induced senescence.
A) Heatmap of gene sets enriched in DE genes from Geriatric vs Young SCs, FAPs, and MCs (g:Profiler web server, FDR<0.05) isolated from non-injured muscle tissue. **B**) Quantification of cells with telomeric DDR and **C**) Sirius Red in TA muscles from young and geriatric mice (n=3-5 mice). **D**) RT-qPCR of indicated genes in TA muscles from young and geriatric mice (n=5-8 mice). Results are displayed as mean ± s.e.m.; P-values were calculated by Mann-Whitney test in **B** and **C**, and two-tailed t-test in **D**; significance is reported as *p<0.05 and **p<0.01.

Together, our results show that injury and ageing induce the accumulation of high levels of oxidative stress and DNA damage in subsets of cells within the muscle regenerative niche, driving senescence entry. Ageing by itself also leads to the accumulation of intracellular stressors and activation of inflammatory-response

pathways, thus priming aged niche cells for senescence, which in turn results in a deeper senescent state upon injury.

2.7 Two major shared hallmarks define senescent cells across cell types, stages of regeneration, and lifespan

The definition of cellular senescence has been changing over time, due to the high heterogeneity of senescent cells. Currently, one of the major questions regarding the core senescence signature, which would specifically recognize senescent cells, remains unanswered. We next aimed to identify a common gene expression signature that would unequivocally define senescent cells despite their nature, time, and age. For that, we analysed DE genes between Sen and NSen populations across all the conditions. Although we did not detect any gene that would be significantly up- or downregulated among all 12 comparisons, we identified 47 largely conserved genes, including pro-inflammatory cytokines (e.g., *Ccl2*, *Ccl7*, *Ccl8*), matrix components, and remodelling enzymes (e.g., *Col1a2*, *Col3a1*, *Timp2*) and IGF regulators (e.g., *Igfbp4*, *Igfbp6*, *Igfbp7*), previously linked to senescence. On the other hand, the cell cycle progression gene *Cenpa* was downregulated, in agreement with previous observations in senescent cells[245,246]. Notably, expression of the pro-inflammatory/pro-fibrotic genes *Ccl2*, *Ccl7*, *Igf1*, *Igfbp4*, and *Timp2* was also detected in the scRNA-seq mapping (Figure 16B). To confirm these findings, we validated key genes of each category by RT-qPCR in the three cell populations at young and geriatric ages (Figure 27A).

We hypothesized that, despite limited coincidence at the gene-expression level, senescent cells retain common traits at a functional level. To address this, we performed a simultaneous comparison of Sen cells with their NSen and Basal counterparts to exclude the changes related to the cell growth arrest (i.e. quiescence) state *per se*. Pathway enrichment analysis showed upregulation of two major global functions: inflammation and matrix remodelling/fibrosis (Figure 27B). Minor shared conserved traits were related to stress responses and IGF regulation (Figure 27B). Conversely, the basic cellular machinery (including gene expression to protein translation, cell cycle, and DNA repair) was strongly downregulated across all conditions (Figure 27B). In conclusion, our data indicate that *in vivo* senescent cells have a common profile of cellular pathways, rather than having closely aligned changes in the expression of a fixed set of genes.

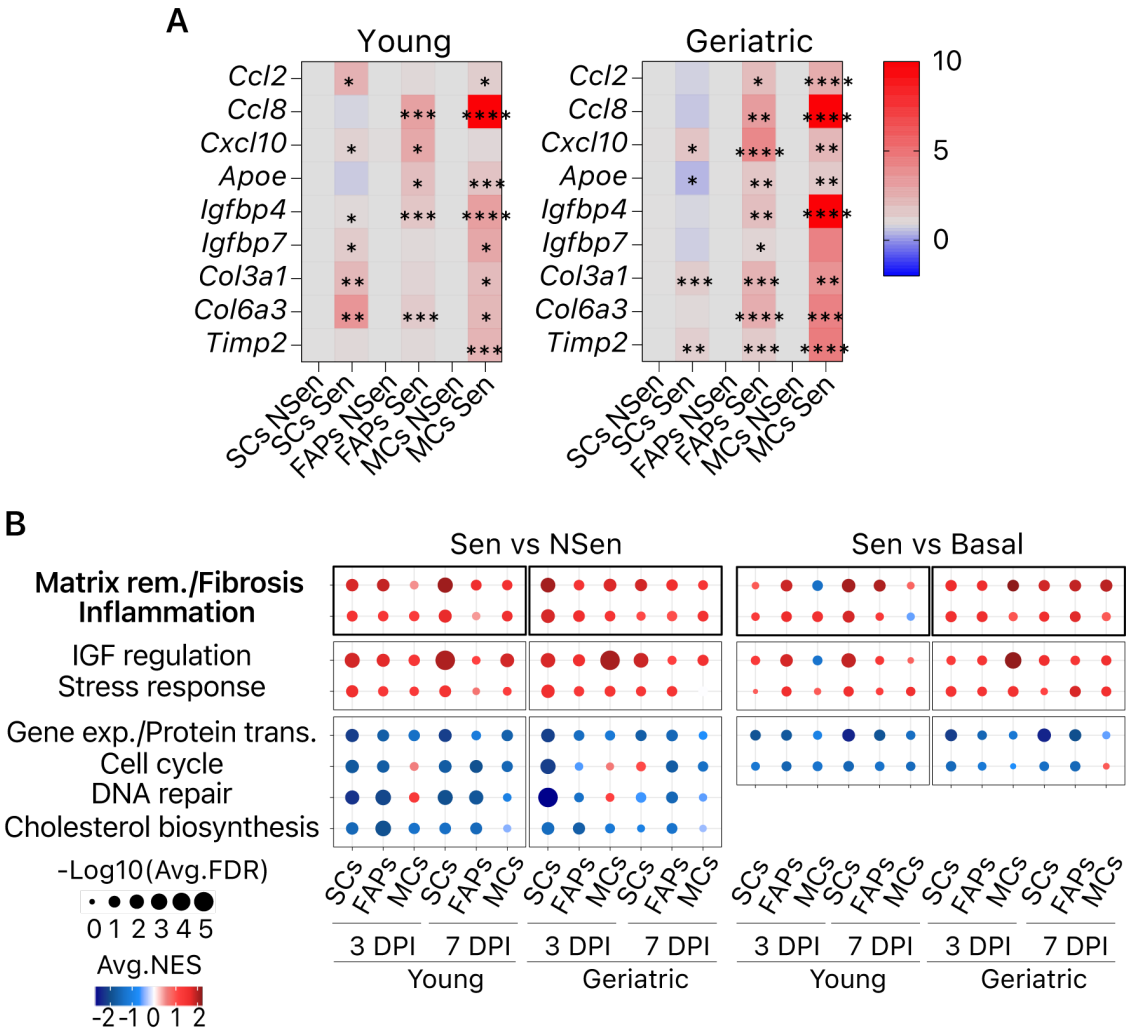

Figure 27. Two major shared hallmarks define senescent cells across cell types, stages of regeneration, and lifespan.

A) mRNA quantification by RT-qPCR of indicated genes in SPiDER^{+} and SPIDER^{-} SCs, FAPs, and MCs isolated from regenerating muscles of young and geriatric mice at 3 DPI (n=4-7 mice). **B**) Dot plot representing common clusters of gene sets (GSEA) from Sen vs NSen and Sen vs Basal SCs, FAPs, and MCs from young and geriatric mice at 3 and 7 DPI. Gene sets were considered common with FDR<0.25 in at least 8/12 comparisons for Sen vs NSen and Sen vs Basal. P-values were calculated by two-tailed t-test in **A**; significance is reported as *p<0.05, **p<0.01, ***p<0.001 and ****p<0.0001.

To elucidate how the senescence program is regulated in senescent cells, we performed transcriptional factor (TF) enrichment analysis and pathway enrichment analysis of TF targets, which allowed us to map common TFs to the main pathway hallmarks enriched in Sen cells in all conditions. The analysis revealed enrichment occupancy of known transcriptional regulators of inflammation and the SASP, NFκB[179], C/EBPβ[142], and STAT1/3[247], as well as the regulators of matrix remodelling and fibrosis, Smad3/4 (and inhibition of Smad7)[248] (Figure 28).

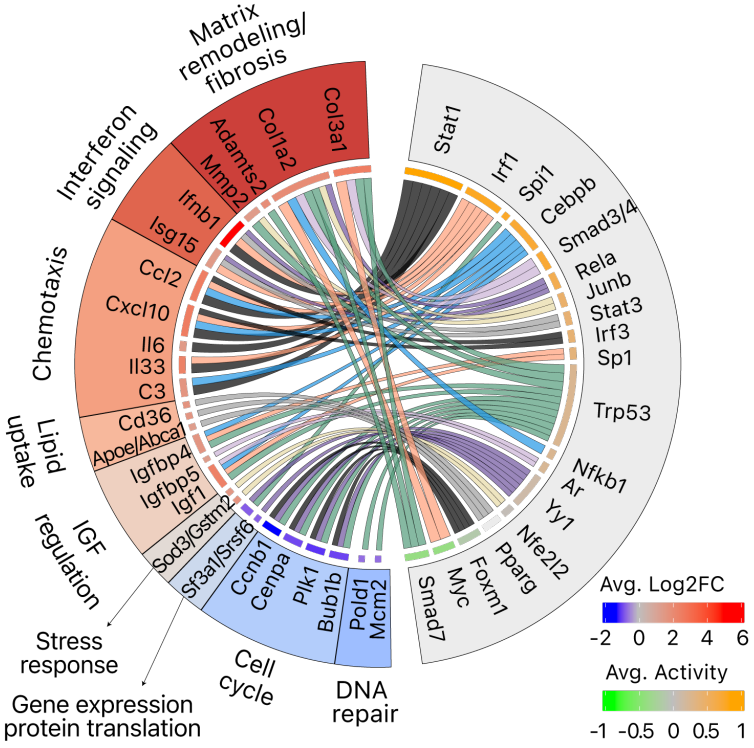

Figure 28. Transcription factor occupancy reflects the activation of major inflammatory and fibrotic senescence hallmarks.
Chord diagram showing TFs regulating the DE genes in Sen vs NSen and their respective categories. Chord width is proportional to the -log10 of the average minimum FDR for CP and GO:BP enrichment (gprofiler2) within a given functional category. The green-to-orange scale indicates the average predicted TF activity.

In conclusion, we established a protocol for senescent cell isolation and characterized the nature of senescent cells in a single-cell fashion. Following this, we generated deep transcriptomic data of the major populations constituting the senescent population (SCs, FAPs, and MCs) for the investigation of kinetic and ageing components in these cells. We identified DNA damage and excessive ROS as a trigger of cellular senescence in regenerating muscle. Also, we underlined the role of ageing on exacerbated senescence entry and its phenotype. Not only did we observe the transcriptional heterogeneity in the senescent populations, as established by previous research, but we also proposed their definition by the conserved functional core, primarily constituted by pro-inflammatory and pro-fibrotic traits. Finally, we described how TFs regulate gene expression and functions in senescent populations based on the generated transcriptomic data.

3. ROLE OF SENESCENT CELLS IN MUSCLE REGENERATION

3.1 Role of senescent cells in muscle regeneration at young and geriatric age

The role of senescent cells has been described in a variety of conditions, such as development, cancer, wound healing, and ageing among others. Although several studies suggested both, beneficial and deleterious roles of senescent cells in acute muscle regeneration, they did not provide clear evidence on the contribution of the senescent cell during muscle regeneration and the mechanism behind it. Hence, the role of senescent cells is yet unclear and needs further insights. To study the role of newly emerging senescent cells during muscle regeneration, we first ablated senescent cells in young and geriatric p16-3MR mice by daily administration of GCV. GCV reduced the presence of senescent cells in injured muscles, indexed by lower luciferase activity *in vivo*, and reduced SA-β-gal$^+$ cells on muscle sections (Figure 29A,B).

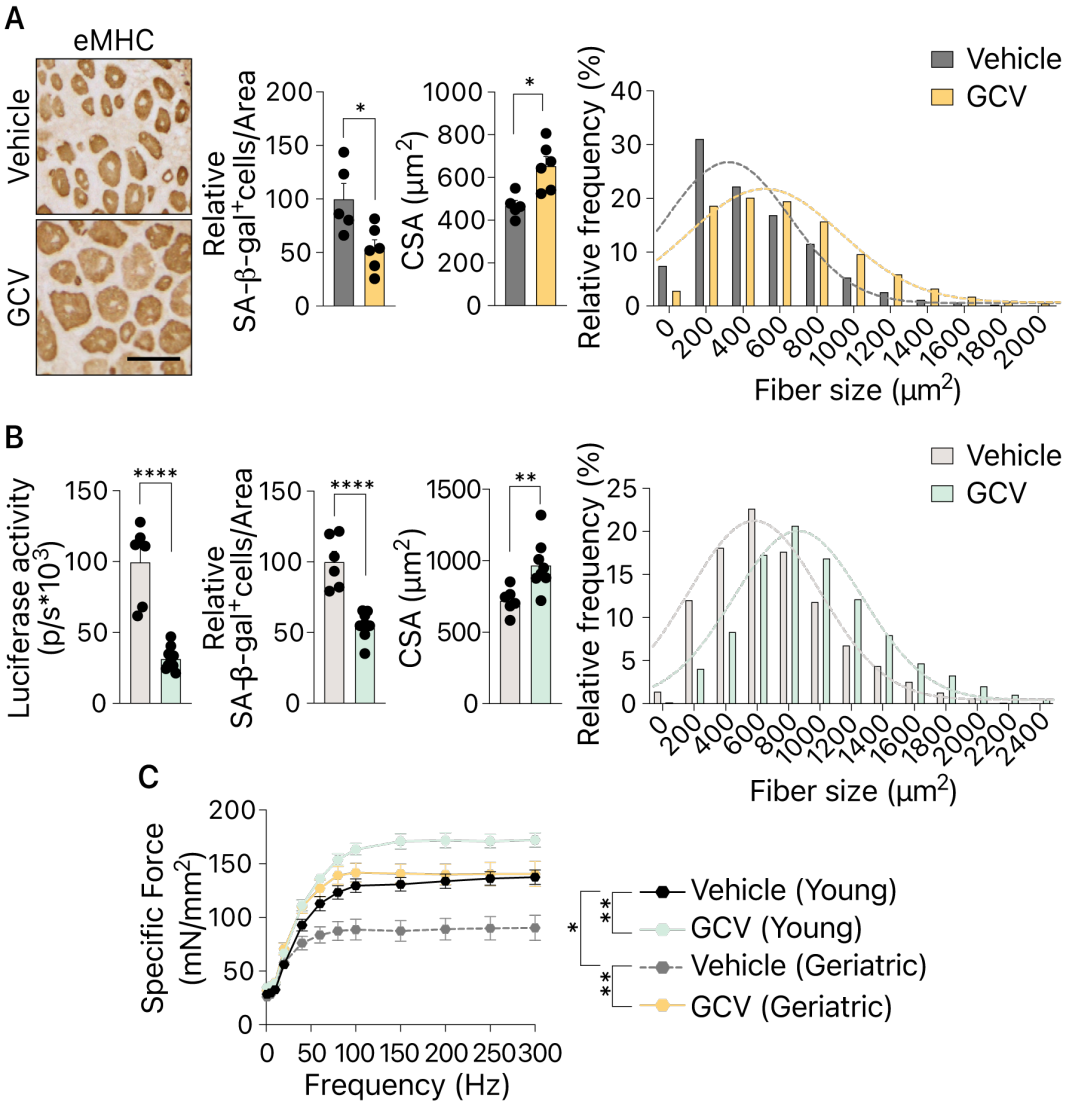

Figure 29. Reduction of senescent cells leads to accelerated muscle regeneration in young and geriatric animals.
Young and geriatric p16-3MR mice were subjected to CTX injury, treated with vehicle or GCV during the course of regeneration, and analysed at 7 DPI. **A**) Representative images and quantification of SA-β-gal$^+$ cells, cross-sectional area (CSA), and frequency distribution of eMHC$^+$ fibers in regenerating TA muscles from vehicle- and GCV-treated geriatric mice (n=5-6 TA from 3 mice). **B**) Quantification of *in vivo* Renilla luminescence activity (n=6-10 muscles from 3-5 mice), SA-β-gal$^+$ cells, CSA, and frequency distribution analysis of eMHC$^+$ fibers (n=6-8 TA muscles from 4 mice) in cryosections from young p16-3MR mice. **C**) Force-frequency curves of extensor digitorum longus (EDL) muscles of vehicle- and GCV-treated young and geriatric p16-3MR mice at 10 DPI (n=5-11 EDL from 4-7 mice). Scale bar: 50 μm. Results are displayed as mean ± s.e.m.; P-values were calculated by Mann-Whitney test in **A** and **B**, and two-way ANOVA in **C**; significance is reported as *p<0.05, **p<0.01, and ****p<0.0001.

In geriatric p16-3MR mice, GCV not only rescued the defective tissue regeneration but also enhanced muscle force generation (Figure 29A,C). Unexpectedly, these beneficial effects were also evident in GCV-treated young mice (Figure 29B,C). Moreover, advanced fiber regeneration was accompanied by reduced fibrosis and inflammation in both young and geriatric mice, as monitored by reduced expression of pro-inflammatory cytokines *IL-6*, *Ccl-2*, *IL-18*, and *INFγ*, (Figure 30).

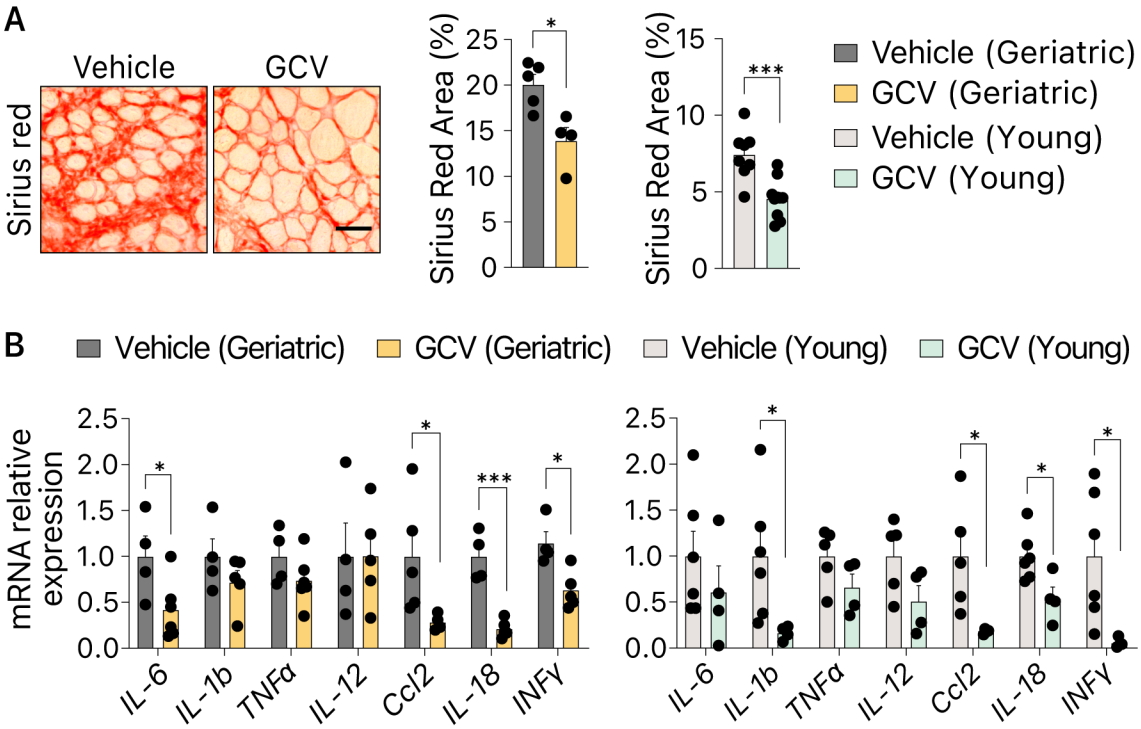

Figure 30. Targeting senescent cells leads to reduced inflammation and fibrosis in young and geriatric p16-3MR animals.
Young and geriatric p16-3MR mice were subjected to CTX injury, treated with vehicle or GCV during the course of regeneration, and analysed at 7 DPI. **A**) Representative images and quantification of Sirius Red staining in regenerating TA muscles from vehicle- and GCV-

treated geriatric (n=5-6 TA from 3 mice) and young (n=6-8 TA muscles from 4 mice) mice. **B**) RT-qPCR of *IL-6, IL-1b*, *TNFα*, *IL-12*, *Ccl2*, *IL-18*, and *INFγ*, in muscle tissue from young (n=4-6 TA muscles from 3-4 mice) and geriatric (n=4-6 TA muscles from 3-4 mice) p16-3MR mice. Scale bar: 50 μm. Results are displayed as mean ± s.e.m.; P-values were calculated by Mann-Whitney test in **A** two-tailed t-test in **B**; significance is reported as *p<0.05 and ***p<0.001.

We then tested an alternative that has potential use in humans, using daily treatment with the senolytic compounds quercetin and dasatinib (Q+D). Senolytics reduced SA-β-gal$^+$ cell numbers, accelerated regeneration, increased force, and reduced matrix deposition, in both young and geriatric WT mice (Figure 31). Thus, the reduction of senescent cells decreased the inflammatory and fibrotic load in the regenerative niche, accelerated regeneration in young mice, and rejuvenated muscles of extremely old mice that are usually refractory to any improvement.

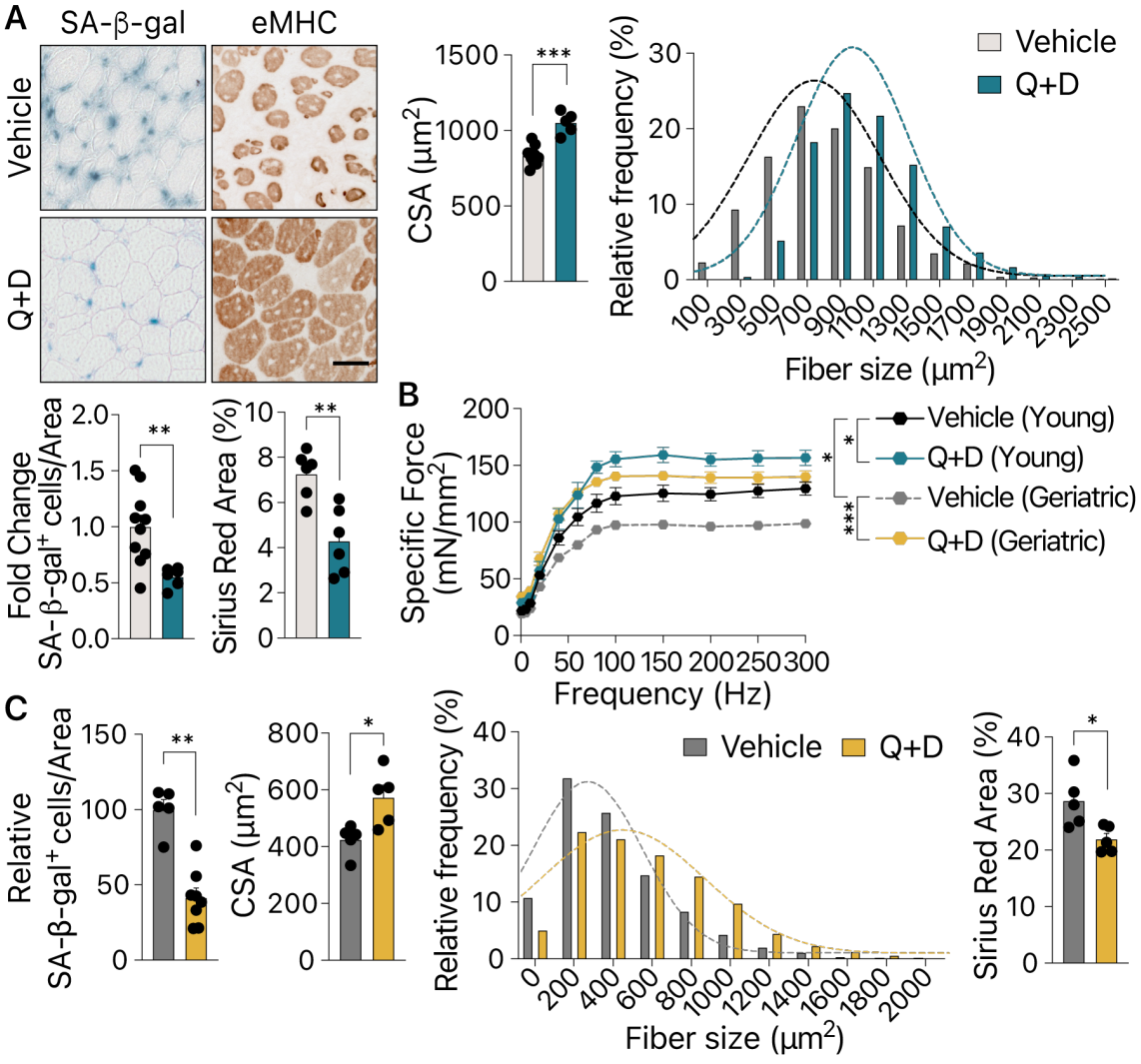

Figure 31. Targeting senescent cells with senolytics leads to accelerated muscle regeneration in young and geriatric WT animals.
Young and geriatric WT mice were subjected to CTX injury, treated with vehicle or Q+D during the course of regeneration, and analysed at 7 DPI. **A**) Representative images and quantification of SA-β-gal$^+$ cells, Sirius Red staining, CSA, and frequency distribution analysis of eMHC$^+$ fibers in cryosections from young mice (n=6-10 muscles from 3-5 mice). **B**) Force-frequency curves of EDL muscles of vehicle- and Q+D-treated young and geriatric mice at 10 DPI (n=5-8 EDL from 3-5 mice). **C**) Quantification of SA-β-gal$^+$ cells, Sirius Red staining, CSA, and frequency distribution analysis of eMHC$^+$ fibers in cryosections from geriatric mice (n=5 mice). Scale bar: 50 µm. Results are displayed as mean ± s.e.m.; P-values were calculated by Mann-Whitney test in **A** and **C**, and two-way ANOVA in **B**; significance is reported as *p<0.05, **p<0.01, and ***p<0.001.

Consistently, transplantation of DiI-labelled sorted SPiDER$^+$ or SPiDER$^-$ cells into pre-injured muscles of young mice revealed that only senescent cells delayed the regeneration of host muscles (Figure 32), mimicking the defective regeneration in geriatric muscles. Thus, senescent cells were detrimental to muscle regeneration in both young and aged mice, challenging the prevalent view that senescent cells are beneficial when transiently present after acute injury, particularly in young tissues (revised in Rhinn et al., 2019[249] and Prieto et al., 2020[250]).

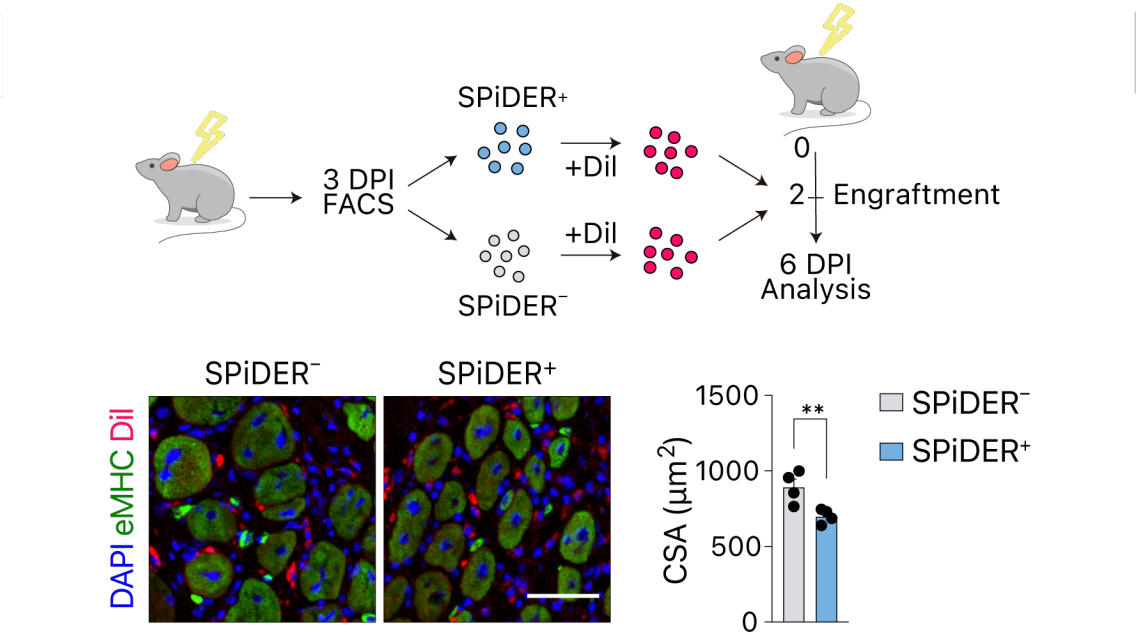

Figure 32. Engraftment of senescent cells delays muscle regeneration in young mice.
An equal amount of SPiDER$^+$ or SPiDER$^-$ cells isolated from young regenerating muscles at 3 DPI were stained with DiI and transplanted into pre-injured TA muscles of young recipient mice for 4 days (n=4 mice). The strategy scheme, representative images, and quantification of eMHC$^+$ fibers are shown. Scale bar: 50 µm. Results are displayed as mean ± s.e.m.; P-values were calculated by the Mann-Whitney test; significance is reported as **p<0.01.

3.2 Role of senescent cells in chronic muscle disease

It has been suggested that the contribution of senescent cells can be majorly defined depending on the persistence of senescent cells in the process. Thus, transient senescence has been majorly classified as beneficial, for example in wound healing, and prolonged, chronic presence of senescent cells has been believed to lead to detrimental outcomes. As we described in the previous section, it is not the case for muscle regeneration, as even the transient presence of senescent cells resulted in delayed muscle regeneration. Thus, we next addressed how senescent cells impact muscle structure and function in a chronic context. For that, we brought p16-3MR mice to the mdx dystrophic background, characterized by chronic muscle degeneration/regeneration cycles. Monitoring of luciferase activity and additional senescence markers showed a higher number of senescent cells in the muscles of mdx/p16-3MR mice than in age-matched, non-dystrophic p16-3MR mice (Figure 33A,B). Mdx mice also presented higher numbers of SA-β-gal$^+$ cells in muscle sections (Figure 33C). In addition, we identified the presence of senescent SCs, FAPs, and MCs in the dystrophic mice by FACS analysis with SPiDER-β-gal (Figure 33D).

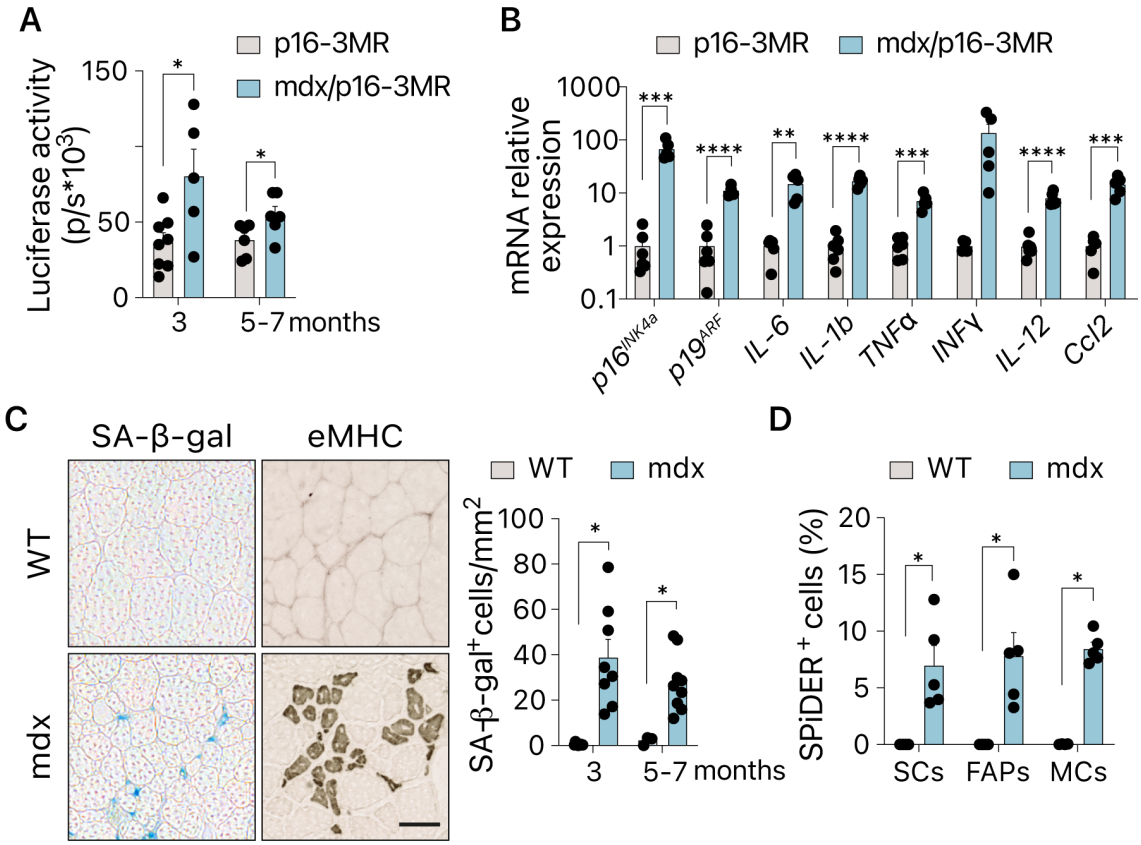

Figure 33. Senescent cells persist in the muscle tissue of mdx mice throughout life.
A) *In vivo* quantification of Renilla luminescence activity in basal muscles of p16-3MR and mdx/p16-3MR mice at the indicated age (n=5-8 muscles from 3 mice). **B**) mRNA quantification of the indicated genes by RT-qPCR in TA muscles from young WT and mdx/p16-3MR mice of 5 months of age (n=4-6 mice). **C**) Representative images of SA-β-gal and eMHC staining and quantification of SA-β-gal$^+$ cells in uninjured TA muscles from WT and mdx mice at indicated age (n=3-9 mice per group). **D**) FACS analysis of SPiDER$^+$ fraction within the SCs, FAPs, and MCs populations in WT and mdx mice (n=4-5 mice). Scale bar: 50 μm. Results are displayed as mean ± s.e.m.; P-values were calculated by Mann Whitney test in **A**, **C**, and **D**, and two-tailed t-test in **B**; significance is reported as *p<0.05, **p<0.01, ***p<0.001 and ****p<0.0001.

Longer-term treatment (twice weekly for 2 months) of mdx/p16-3MR mice with GCV reduced the senescent cell burden and alleviated the regenerative impairment of dystrophic muscles, as shown by larger fibers, reduced fibrosis, and enhanced muscle force (Figure 34A,B). We further corroborated these results in mdx mice treated with senolytics Q+D in a similar fashion. We confirmed the reduction of senescent cells by total SA-β-gal activity quantification in frozen tissue and particularly in the SCs, FAPs, and MCs populations by FACS (Figure 34C,D). Targeting senescent cells with Q+D notably improved muscle force and structure, monitored by strength assay, fiber size measurement, and fibrotic deposition (Figure 34E,F). Importantly, a recent study showed that the reduction of senescent cells with ABT263, another broadly used senolytic, ameliorated disease progression in DMD rats[228]. Thus, our results, together with other research, demonstrated that senescent cells have a negative impact on chronic muscle disease, suggesting a novel potential therapeutic target for DMD treatment.
We concluded that senescent cells play a detrimental role in muscle regeneration, irrespectively of any condition that we investigated. The irruption of senescent cells in the regenerative muscle niche, either transiently (in acute injury) or persistently (in chronic injury), is always deleterious for regeneration, irrespective of age.

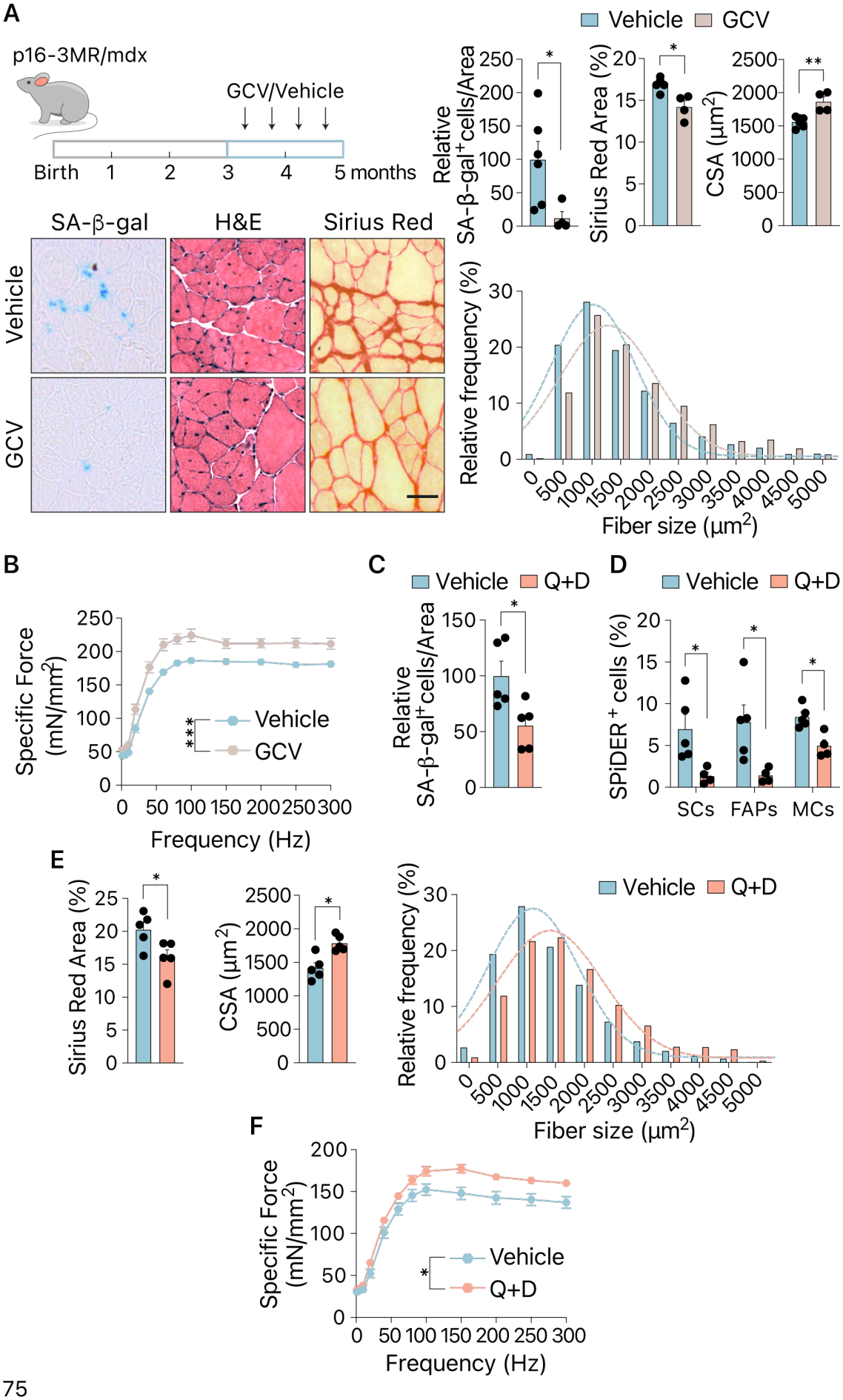
A
p16-3MR/mdx
GCV/Vehicle
Birth
1
2
3
4
5 months
SA-β-gal
H&E
Sirius Red
Vehicle
GCV
Vehicle
GCV
Relative SA-β-gal+ cells/Area
Sirius Red Area (%)
CSA (μm2)
Relative frequency (%)
Fiber size (μm2)
B
Specific Force (mN/mm2)
Frequency (Hz)
Vehicle
GCV
***
C
Vehicle
Q+D
Relative SA-β-gal+ cells/Area
D
Vehicle
Q+D
SPiDER+ cells (%)
SCs
FAPs
MCs
E
Sirius Red Area (%)
CSA (μm2)
Vehicle
Q+D
Relative frequency (%)
Fiber size (μm2)
F
Specific Force (mN/mm2)
Frequency (Hz)
Vehicle
Q+D
*

Figure 34. Senescent cells persist in the muscle tissue of mdx animals throughout life. **A**) Young mdx/p16-3MR mice received GCV twice a week for 2 months and were collected at 5 months of age. Representative images of SA-β-gal, H&E, and Sirius Red staining in TA muscles of vehicle- and GCV-treated mice. SA-β-gal$^+$ cells Sirius Red staining, CSA, and frequency distribution of regenerating fibers (n=4-6 mice). **B**) Force measurements in EDL muscles of vehicle- and GCV-treated mdx/p16-3MR mice after 2 months of treatment are represented (n=5-9 EDL from 3-6). **C**) Young mdx mice received Q+D twice a week for 2 months and muscle samples were collected at 5 months of age. Quantification of SA-β-gal$^+$ cells in muscle cryosections is shown (n=5 mice). **D**) FACS analysis of senescent fraction in SCs, FAPs, and MCs by SPiDER-β-gal staining (n=4-5 mice). **E**) Quantification of CSA and frequency distribution of regenerating fibers and Sirius Red staining in muscle cryosections of vehicle- and Q+D-treated mdx animals (n=5 mice). **F**) Force measurements in EDL muscles of vehicle- and Q+D-treated mdx mice after 2 months of treatment are represented (n=7-8 EDL muscles from 5-6 mice). Scale bar: 50 μm. Results are displayed as mean ± s.e.m.; P-values were calculated by Mann Whitney test in **A**, **C**, **D,** and **E**, and two-way ANOVA in **B** and **F**; significance is reported as *p<0.05, **p<0.01, and ***p<0.001.

3.3 Senescent cells impact their microenvironment by secreting their SASP

One of the most important features of senescent cells is their high metabolic profile and secretion of proactive molecules. We next hypothesized that the detrimental role of senescent cells observed in the previous sections might be attributed to the SASP of these cells. To understand how senescent cells impair regeneration, we studied their SASP *in vivo*, in regenerating muscles, and during ageing. We first studied the transcriptomics of the genes related to the SASP. For that, we selected DE genes with extracellular or secreted protein products and compared them between injury-induced Sen versus NSen cells. Depending on cell type and conditions, the number of SASP components ranged from 78 to 365, highlighting the diversity in SASP production (Figure 35A), in line with the gene expression heterogeneity of senescent cells. Pathway enrichment identified two major functions: 1) inflammation, including complement and coagulation, innate immune system, lipoprotein remodelling, and cytokines and TNFα/NFκB signalling (e.g., *Ccl2*, *Ccl7*, *Ccl8*, *Isg15*); and 2) fibrosis, including matrix organization and collagen metabolism, matrix metalloproteinases and TGFβ signalling (e.g., *Col3a1*, *Col6a2*, *Timp2*). Other features, such as IGF regulation by IGFBPs (e.g., *Igfbp4*, *Igfbp6*, *Igfbp7*, *Igf1*), were also present (Figure 35B).

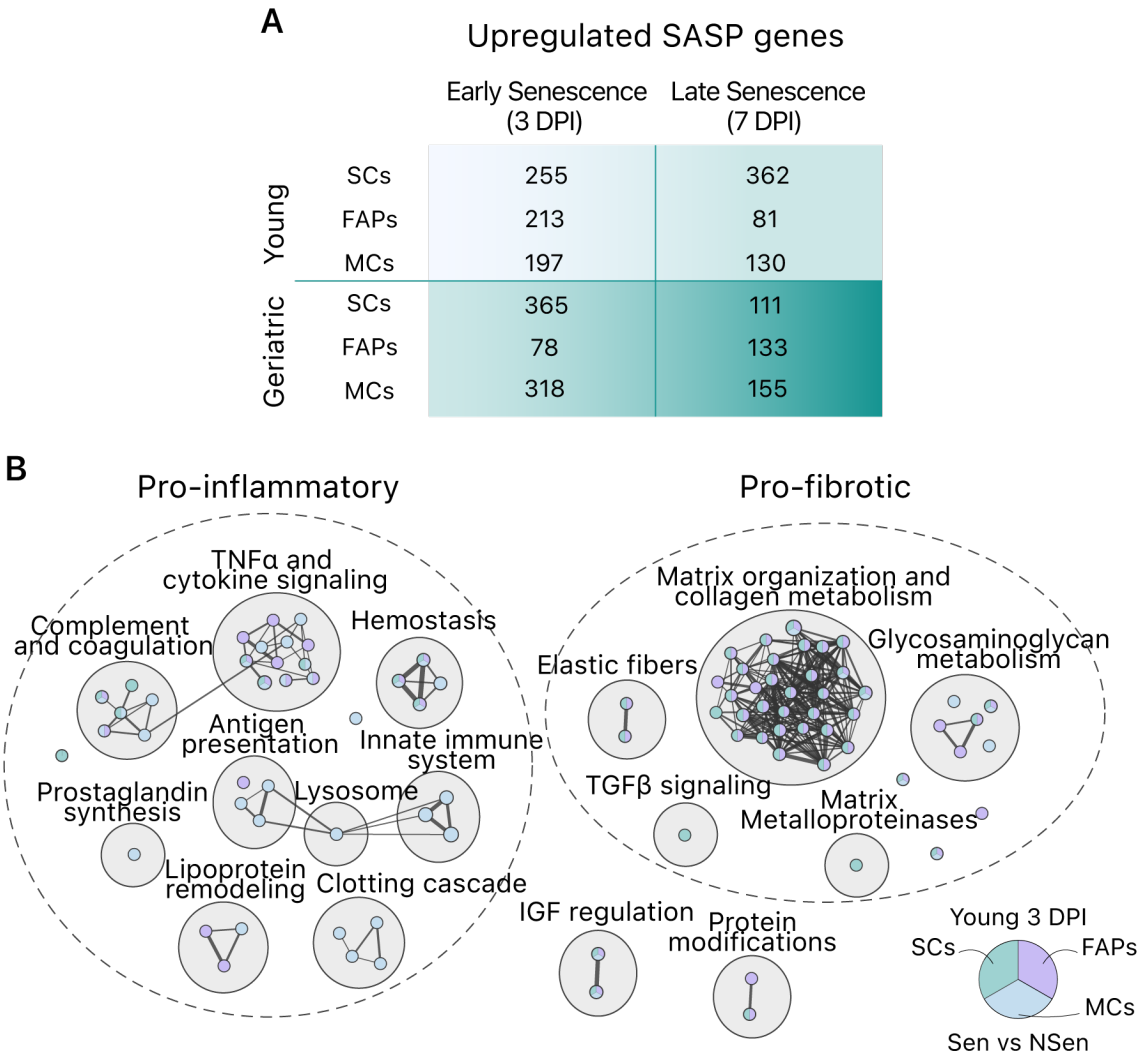

Figure 35. Transcriptomic characterization of SASP in the senescent cells *in vivo*. **A**) Table of upregulated SASP genes in SCs, FAPs, and MCs from young and geriatric mice at 3 and 7 DPI (FDR <0.05). **B**) Clusters of gene sets enriched in SASP-related genes from Sen SCs, FAPs, and MCs from young mice at 3 DPI (g:Profiler web server, FDR <0.05). Node size is proportional to the number of genes identified in each gene set. Grey edges indicate gene overlap. SASP genes were identified using different published databases (see methods). Differentially upregulated genes (FDR<0.05) were considered as "SASP genes" when overexpressed in Sen populations vs their NSen counterparts.

Moreover, functional profiling of the transcriptional regulation of SASP confirmed the association of NFκB, STAT1/3, and Smad3/4 with the identified groups of inflammatory and matrix-related SASP genes (Figure 36), reinforcing the transcriptional control of the inflammatory and fibrotic SASP. Overall, these results indicated that major SASP features correspond tightly with the previously identified universal hallmarks of senescent cells *in vivo* (Figure 27B).

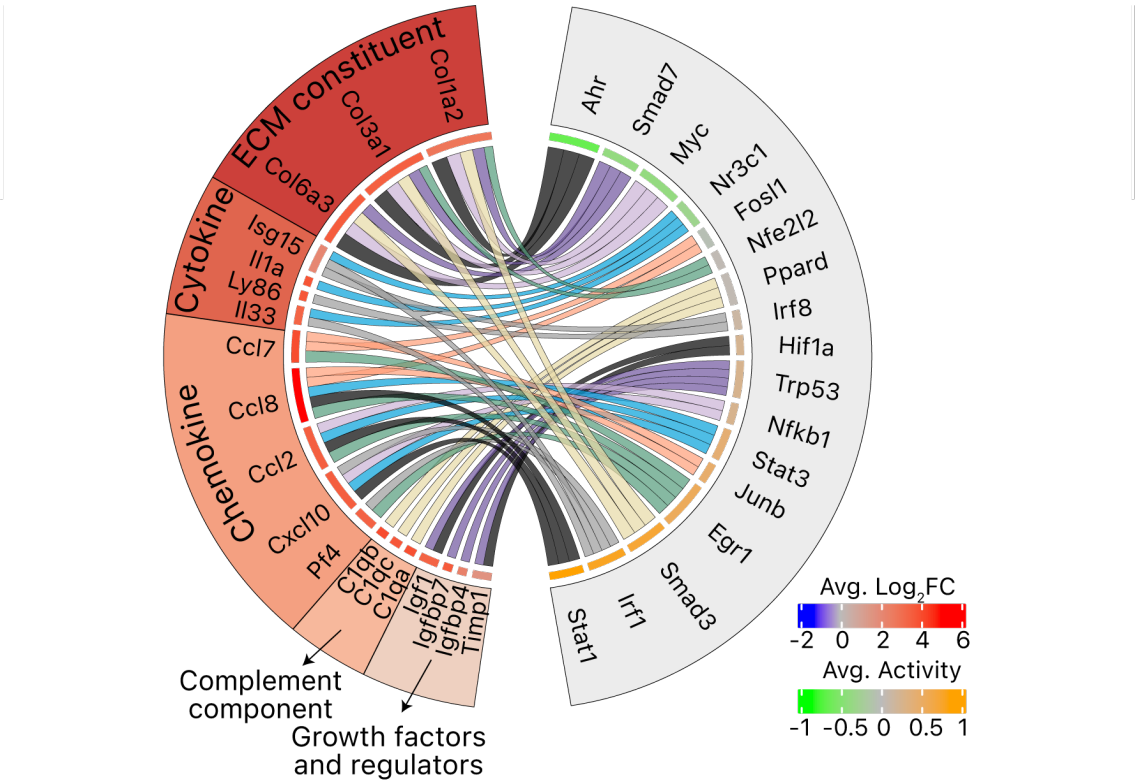

Figure 36. Transcription factor occupancy of SASP-related genes in senescent cells from regenerating muscle.
Chord diagram showing TFs regulating the SASP genes and their respective categories in Sen vs NSen. Chord width is proportional to the -log10 of the average p-value for GO:MF cluster enrichment.

The SASP profile strongly reminded us of those in inflammageing. Therefore, we compared the transcriptomes of ageing tissues from various species with those of the distinct Sen cells in injured young muscles and found an increase in inflammatory pathways, including interferon, complement, and cytokine signalling, or TNFα via NFκB signalling (Figure 37A), consistent with multiple previously published transcriptional datasets of ageing in human, rodent, and killifish[251–253]. Supporting these data, a secreted-protein array-based assay confirmed the secretion of inflammatory (and matrix-remodelling) proteins in freshly sorted Sen cells from young and geriatric muscles (e.g., CCL2, IGFBP6, CD40, IL13, CXCL1, IL1A, CXCL11, MMP2, among others) (Figure 37B). Furthermore, at the whole tissue level, we found that many of these secreted SASP proteins were commonly upregulated in injured muscles of young mice and in non-injured muscles of geriatric mice (as compared to non-injured young muscles) (Figure 37C), indicating a shared upregulated inflammatory secretome after young-tissue injury and ageing conditions.

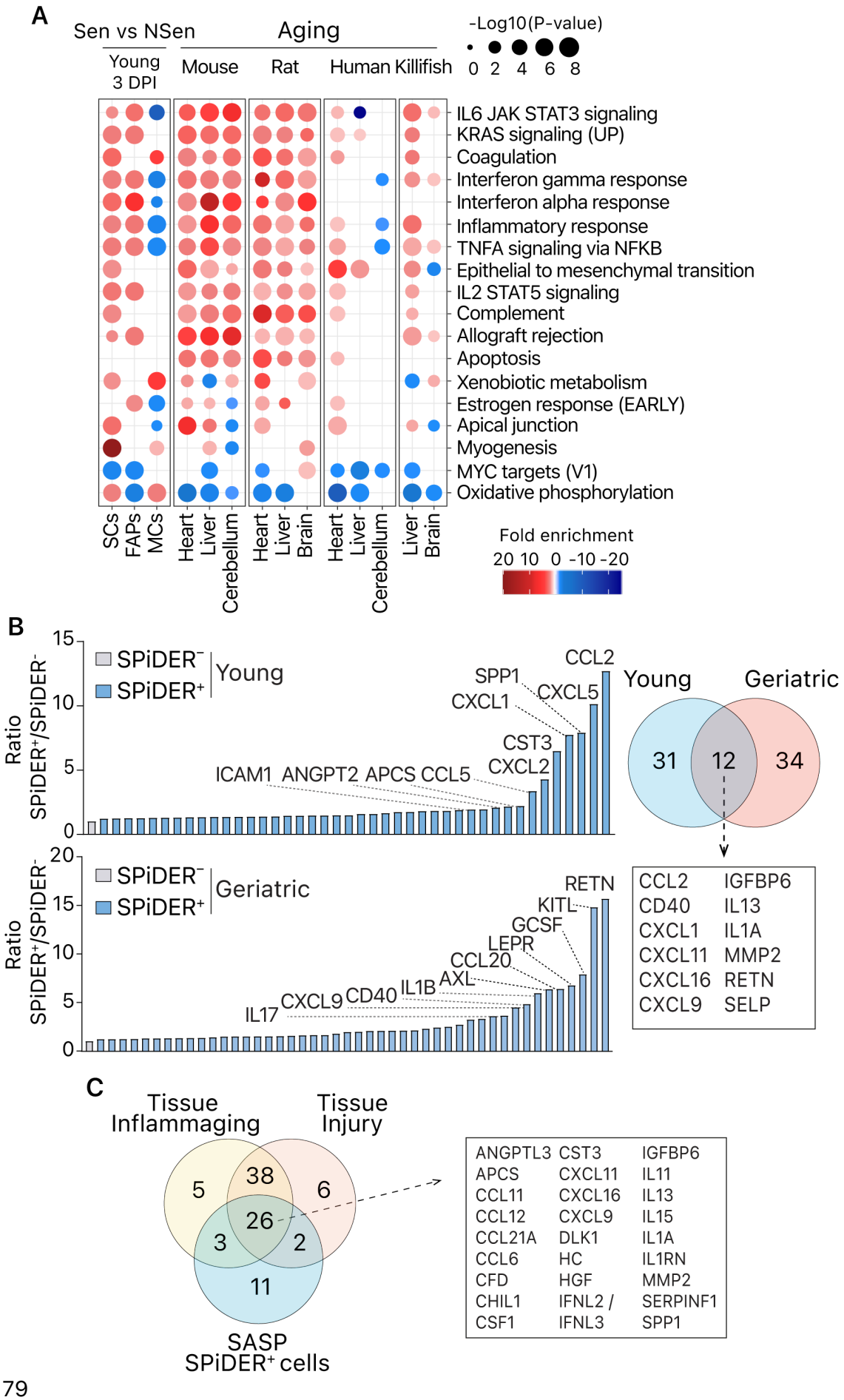
A
Sen vs NSen
Aging
Young 3 DPI
Mouse
Rat
Human
Killifish
-Log10(P-value)
0 2 4 6 8
IL6 JAK STAT3 signaling
KRAS signaling (UP)
Coagulation
Interferon gamma response
Interferon alpha response
Inflammatory response
TNFA signaling via NFKB
Epithelial to mesenchymal transition
IL2 STAT5 signaling
Complement
Allograft rejection
Apoptosis
Xenobiotic metabolism
Estrogen response (EARLY)
Apical junction
Myogenesis
MYC targets (V1)
Oxidative phosphorylation
SCs
FAPs
MCs
Heart
Liver
Cerebellum
Heart
Liver
Brain
Heart
Liver
Cerebellum
Liver
Brain
Fold enrichment
20 10 0 -10 -20
B
Ratio SPiDER+/SPiDER-
SPiDER-
SPiDER+
Young
ICAM1
ANGPT2
APCS
CCL5
CXCL2
CST3
CXCL1
SPP1
CXCL5
CCL2
Young
Geriatric
31
12
34
Geriatric
IL17
CXCL9
CD40
IL1B
AXL
CCL20
LEPR
GCSF
KITL
RETN
CCL2 IGFBP6
CD40 IL13
CXCL1 IL1A
CXCL11 MMP2
CXCL16 RETN
CXCL9 SELP
C
Tissue Inflammaging
Tissue Injury
5
38
6
26
3
2
11
SASP SPiDER+ cells
ANGPTL3 CST3 IGFBP6
APCS CXCL11 IL11
CCL11 CXCL16 IL13
CCL12 CXCL9 IL15
CCL21A DLK1 IL1A
CCL6 HC IL1RN
CFD HGF MMP2
CHIL1 IFNL2 / SERPINF1
CSF1 IFNL3 SPP1

Figure 37. Transcription factor occupancy of SASP-related genes in senescent cells from regenerating muscle.
A) Dot plot comparing functional enrichments of MSigDB 5.1 hallmarks obtained by using the minimum hypergeometric test for differential RNA expression in different tissues from aged mice, rats, humans, killifish[253] and muscle senescent populations from young mice at 3 DPI. **B**) Cytokine array of freshly sorted SPiDER^{+} or SPiDER^{-} cells from regenerating muscle at 3 DPI from young (top) or geriatric (middle) mice. Cells were cultured for 24 hours in serum-deprived media, then the conditioned media were collected, and the levels of the indicated protein were assessed. Graphs represent the top 10 proteins whose levels were increased in the comparison. Venn diagram indicating the overlap between secreted proteins in young and geriatric cells is shown. **C**) Venn diagram showing the overlap between secreted proteins during ageing, injury-induced regeneration, and secreted proteins by isolated young SPiDER^{+} cells in **B**. Common secreted proteins are indicated.

Thus, we concluded that the SASP of Sen cells transiently present in injured young muscles mimics an aged-like inflammageing[244,251–253]. In contrast, in geriatric muscle, the exacerbated inflammation observed during regeneration is a result of combining senescent secretome with existing inflammageing prior to the injury.

3.4 Senescent cells block muscle stem cell expansion through the SASP paracrine actions

Once we characterized the SASP of senescent cells *in vivo*, we next aimed to describe how exactly the SASP affects muscle regeneration. We performed a ligand-receptor (L-R) analysis in collaboration with specialists in computational biology[254]. With this analysis, we predicted L-R interactions between senescent populations and non-senescent SCs (which are in charge of the formation of the new fibers) and the downstream response induced in the receptor cells. The ligands of the senescent cells (the SASP) underlined mostly pro-inflammatory and pro-fibrotic interactions among senescent cells and muscle stem cells (Figure 38A). Signalling pathway impact analysis (SPIA) of TFs acting downstream of these interactions revealed common downstream responses induced by SASP ligands on non-senescent SCs (Figure 38B). The downstream responses resulting from the SASP signalling included activation of pathways such as “cellular senescence”, “apoptosis”, and inflammatory responses, including “TNFα and TGFβ signalling”, in the receptor non-senescent SCs. On the other hand, SPIA predicted inhibition of pathways such as “cell cycle” and proliferative pathways (such as the “MAPK and AKT signalling cascades”) in the muscle stem cells by the SASP signalling. Thus, we hypothesized that the SASP produced by senescent cells during muscle

regeneration negatively impacts muscle stem cell expansion, by either promoting proliferative arrest or paracrine senescence (through a bystander effect).

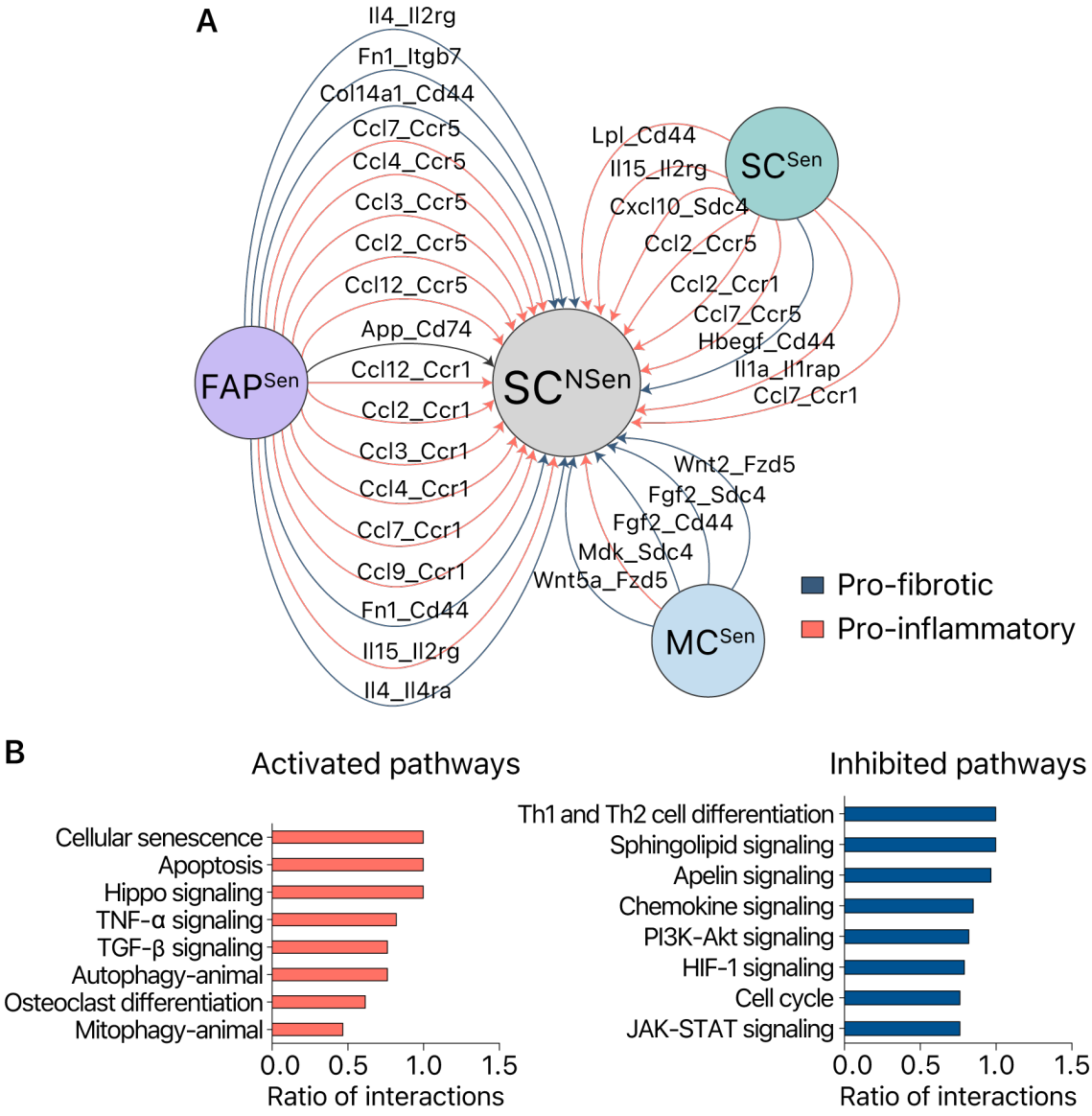

Figure 38. Ligand-receptor analysis between senescent and non-senescent SCs. **A**) Cytoscape network showing ligand-receptor (L-R) interactions between Sen populations and NSen SCs from geriatric mice at 3 DPI predicted by a modified version of FunRes. **B**) Major activated and inhibited KEGG pathways predicted by SPIA in NSen SCs downstream the predicted interactions showed in **A**. Ratio of interactions represents the proportion of L-R that induce the pathway of interest.

To test these predictions, we transplanted sorted SPiDER^{+} and SPiDER^{-} fractions containing SCs, FAPs, and MCs, labelled with the lipophilic vital dye DiI, into pre-injured muscles of recipient mice. In contrast to DiI-labelled SPiDER^{-} cells, DiI-labelled SPiDER^{+} cells increased the number of senescent cells in the host tissue, induced recruitment of inflammatory cells to the damaged area, increased fibrosis,

and delayed the regeneration of host muscles (Figure 39A), simulating the exacerbated regeneration defect of geriatric muscles. Moreover, paracrine senescence induction was confirmed by transplantation of *ex vivo*-induced senescent (or non-senescent) cells into pre-injured muscles of p16-3MR reporter mice, evidenced by enhanced luciferase activity in muscles transplanted with senescent cells (Figure 39B), which may explain the delayed regeneration of host muscles.

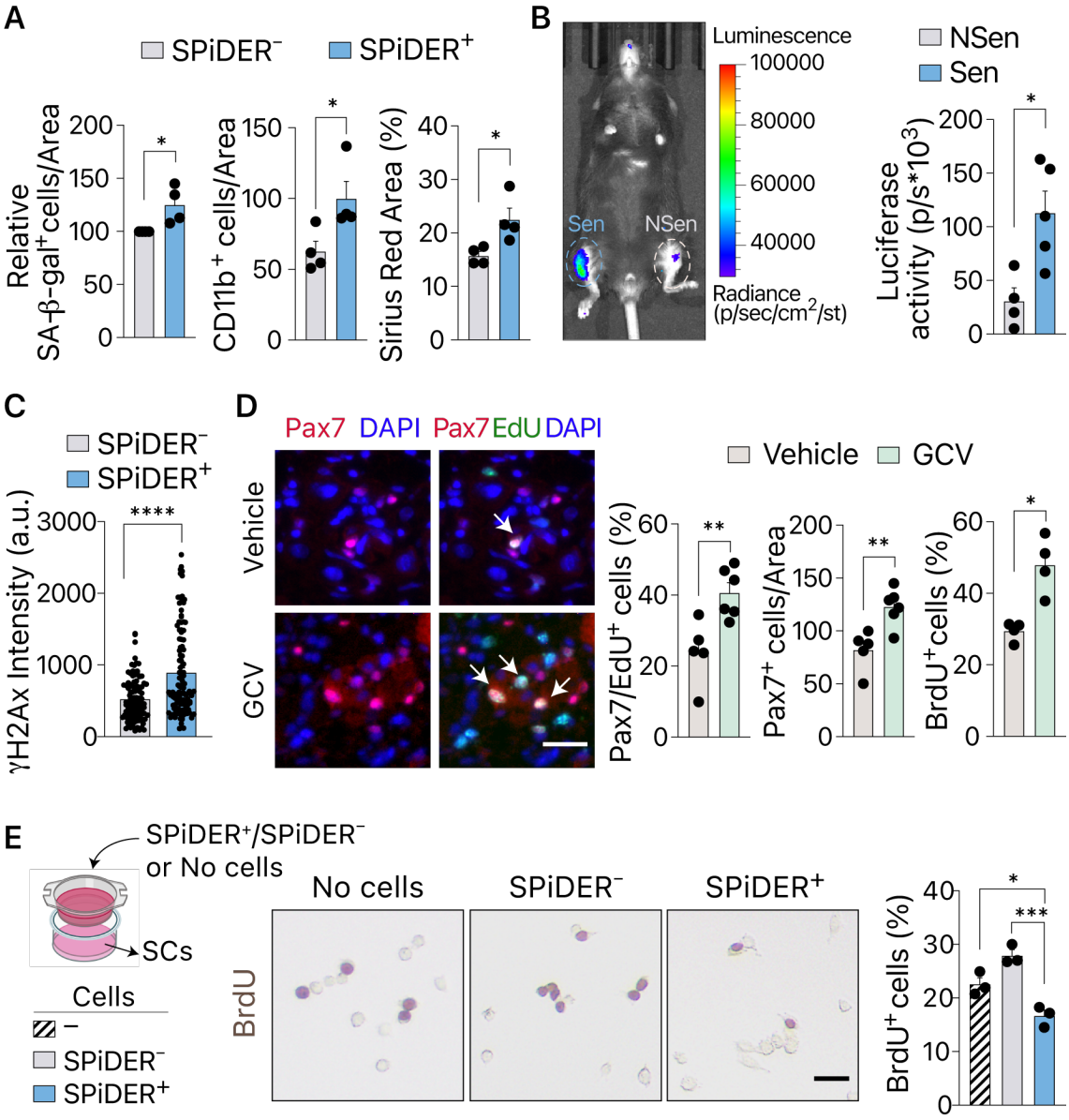

Figure 39. Senescent cells restrain muscle stem cells expansion through the SASP secretion.

A) SPiDER⁺ or SPiDER⁻ cells isolated from young regenerating muscle at 3 DPI were stained with Dil and transplanted into pre-injured TA muscle of the recipient young mice for 4 days (n=4 mice). Quantification of SA-β-gal⁺ cells, CD11b⁺ cells, and Sirius Red staining are shown. **B**) Senescent and non-senescent C2C12 cells were stained with Dil and transplanted into pre-injured TA muscle of the recipient young p16-3MR mice for 5 days.

Representative images and quantification of *in vivo* Renilla luminescence activity in muscles of p16-3MR mice (n=4-5 mice). **C**) SPiDER^{+} or SPiDER^{-} cells isolated from young regenerating muscle at 3 DPI were stained with DiI and transplanted into resting TA muscle of the recipient young mice for 4 days. Quantification of γH2Ax expression in resident Pax7^{+} cells is shown (n=100-110 cells). **D**) p16-3MR mice were injured with CTX and daily treated with vehicle or GCV from the day of injury to 4 DPI (n=5-6 TA from 3-4 mice). (Left) Representative images of EdU or Pax7 staining and quantification of EdU incorporation in SCs and the total number of SCs in the regenerating area. (Right) quantification of BrdU incorporation in SCs *in vitro*. At 3 DPI, in mice treated as before, SCs were FACS-sorted and cultured for 3 days (n=4 mice). **E**) SPiDER^{-} SCs were isolated at 3 DPI from regenerating muscles of young/geriatric mice, then cultured for 3 days in transwells with total SPiDER^{+}, SPiDER^{-} cells, or medium. After 3 days of culture, SCs proliferation was assessed by BrdU incorporation. Representative images and quantification of BrdU^{+} cells (n=3 replicates). Scale bars: 20 μm in D and 10 μm in **E**. Results are displayed as mean ± s.e.m.; P-values were calculated by Mann Whitney test in **A**, **B**, **C**, and **D**, and Sidak's test in **E**; significance is reported as *p<0.05, **p<0.01, and ***p<0.001.

Strikingly, transplantation of sorted Sen (SPiDER^{+}) and NSen (SPiDER^{-}) from donor mice into non-injured muscles of recipient mice sufficed to induce DNA damage in the endogenous SCs (Figure 39C). Conversely, the reduction of senescent cells in GCV-treated p16-3MR mice increased the number of proliferating and total SCs within the regenerative muscle niche (Figure 39D), in agreement with the accelerated muscle regeneration. Consistent with these *in vivo* results, SCs sorted from GCV-treated p16-3MR mice had a higher proliferation capacity *ex vivo* than SCs from vehicle-treated mice (Figure 39D). We also performed a transwell assay, which physically separates seeded populations but allows the interchange of secreted molecules. We observed a reduced proliferation rate of NSen SCs when seeded in the presence of Sen secretome (Figure 39E). Together, these findings demonstrate that senescent cells restrain muscle regeneration through paracrine pro-inflammatory and pro-fibrotic SASP functions that blunt SCs proliferation.

To examine the relative contribution to muscle regeneration of the senescent cells that either reside within the tissue or that are blood-derived, we first used a model of whole-muscle grafting, in which the extensor digitorum longus (EDL) muscle from one mouse is grafted onto the tibialis anterior (TA) muscle of a recipient mouse[91]. In this model, the transplanted EDL muscle undergoes *de novo* myogenesis at the expense of its own SCs, while recruited bone marrow-derived cells come from the host. EDL-grafting combined with GCV-mediated senescent cell depletion revealed that p16-3MR-EDL grafts in WT host mice, or WT-EDL grafts in p16-3MR hosts, had larger regenerating myofibers than WT-EDL grafts in WT mice (Figure 40A). These results confirmed that EDL-resident senescent SCs

and FAPs, as well as blood-derived inflammatory senescent cells, blocked muscle regeneration. Similar detrimental effects on muscle regeneration were seen upon transplantation of equal numbers of Sen (SPiDER^{+}) SCs, FAPs, or MCs, either separately or combined, independently of the Sen cell type (Figure 40B). These results strongly suggest that conserved secretory inflammatory and fibrotic hallmarks across the three Sen cell types account for their similar negative effects on tissue regeneration. Consistent with this idea, improved muscle regeneration after senescent cell depletion was always accompanied by reduced inflammation and fibrosis in both young and aged muscles, whereas the reduced muscle regeneration rate caused by the paracrine action of transplanted Sen cells was associated with increased muscle inflammation and fibrosis. These findings further challenge the prevalent view that the SASP of senescent cells is beneficial when acting transiently after injury.

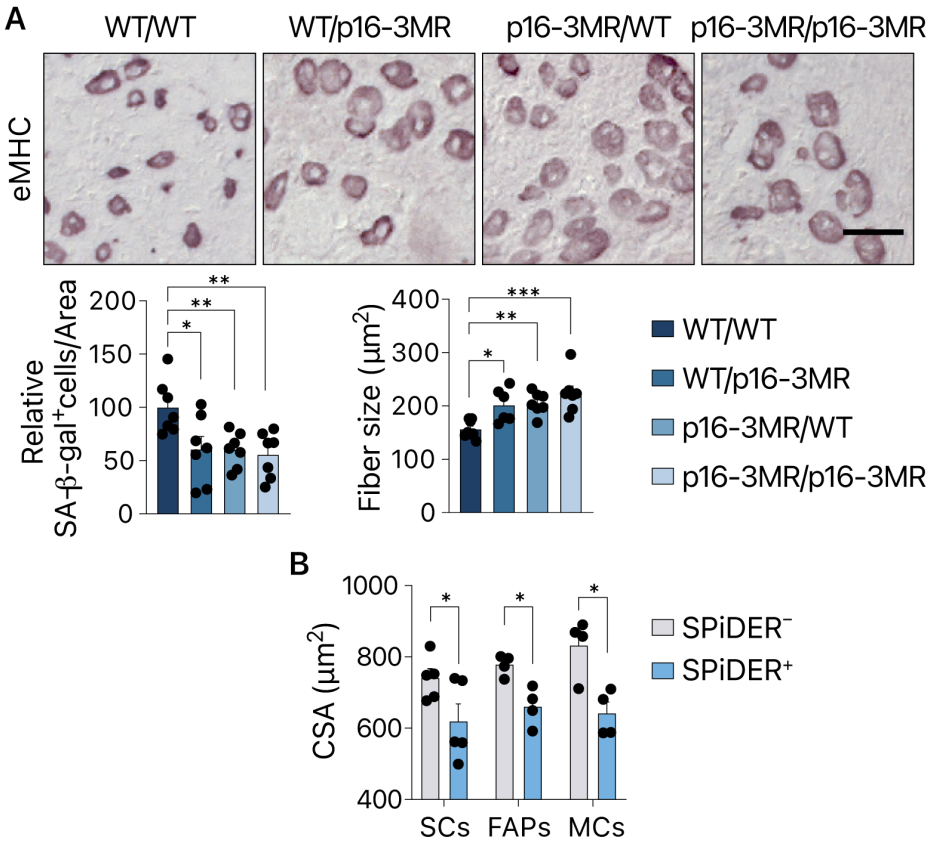

Figure 40. Distinct senescent populations play a similar role during muscle regeneration.

A) EDL from either WT or p16-3MR donor mice were transplanted into WT or p16-3MR recipient mice or *vice versa*. Recipient mice were treated with GCV and regeneration was assessed 7 days later. Representative images, and quantification of fiber size and SA-β-gal^{+} cells (n=6-8 mice). **B**) SPiDER^{+} or SPiDER^{-} SCs, FAPs, or MCs isolated from young regenerating muscle at 3 DPI were stained with DiI and transplanted into pre-injured TA muscle of the recipient young mice for 4 days (n=4-5 mice). Quantification of CSA of

eMHC⁺ fibers is shown. Scale bar: 20 µm. Results are displayed as mean ± s.e.m.; P-values were calculated by Mann Whitney test; significance is reported as *p<0.05, **p<0.01, and ***p<0.001.

3.4 Role of the CD36 in the regulation of the SASP and muscle regeneration.

To further explore the beneficial effects of senescent cell targeting, we aimed to specifically neutralize the SASP. Given the observed heterogeneity of SASPs *in vivo*, we searched for a broad SASP-targeting approach rather than targeting a particular molecule. Lipid transport, which is tightly associated with inflammatory responses[255,256], was consistently included in the inflammatory hallmark of Sen cells (Figure 27B) and of the SASP (Figure 35B) in all conditions. Notably, we found that Sen cells had more lipid droplets than NSen cells (Figure 41A). Analysis of lipid metabolism genes identified upregulation in all Sen cells of numerous lipid-transport genes, including *Fabp3*, *Apoe*, *Star*, *Pltp*, *Lpl*, *Cd68*, and *Cd36* (Figure 41B).

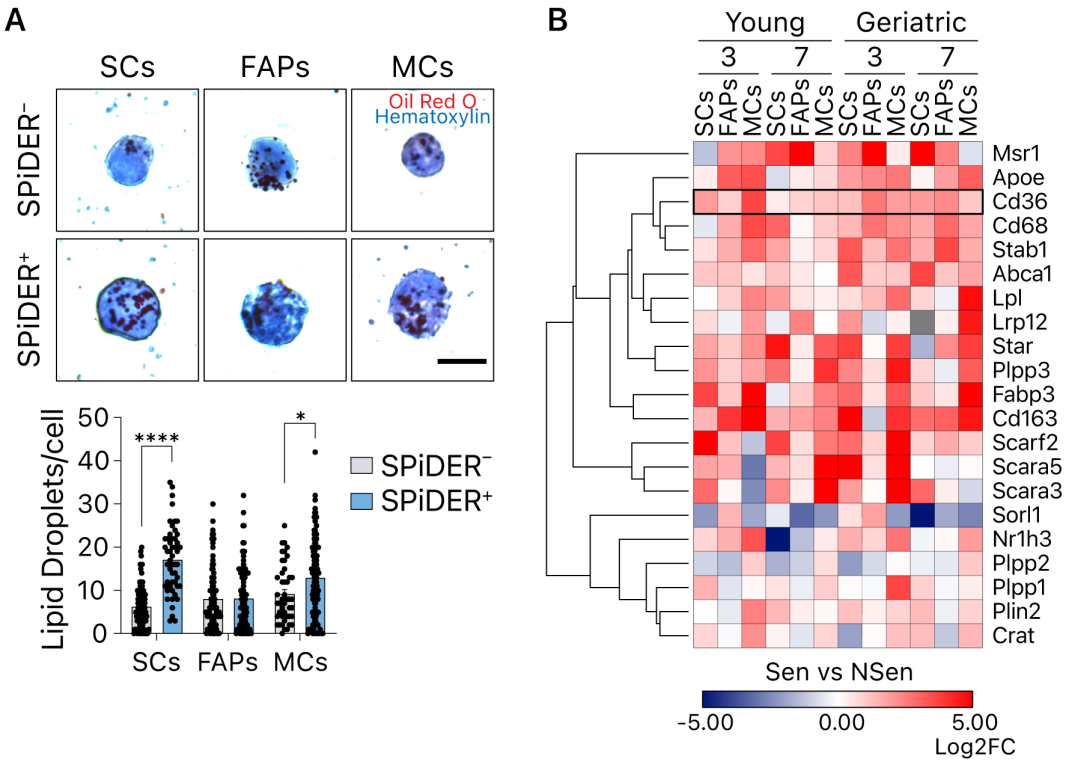

Figure 41. Senescent populations display lipid accumulation and related genes *in vivo*. **A**) SPiDER⁺ and SPiDER⁻ populations from regenerating muscle at 3 DPI were stained with Oil Red O and haematoxylin. Representative images and quantification of lipid droplets are shown (n=45-94 cells). **B**) Heatmap showing lipid-transport related genes that were DE in at least 3/12 comparisons between Sen and their NSen counterparts. The colour indicates log2FC of gene expression. Scale bar: 10 µm. Results are displayed as mean ± s.e.m.; P-values were calculated by a two-tailed unpaired t-test; significance is reported as *p<0.05 and ****p<0.0001.

As lipid uptake and CD36 are related to SASP *in vitro*[239,240], CD36 might also be related to the SASP produced by senescent cells *in vivo*. By applying a modified version of the predictive computational method FunRes[254] to our RNA-seq expression data sets of Sen and NSen cells, we obtained a CD36 signalling network that predicted downstream activation of NFκB and other inflammation/stress-related pathways (including MAPK signalling and interferon responsive factors (IRF)), as well as enhanced induction of several downstream SASP components, such as *Il6*, *Tgfb1*, *Mmp3*, *Igfbp5*, *Ccl2*, *Cxcl10*, among others (Supplementary Figure 1). Based on these transcriptomic-coupled computation premises and given that *Cd36* was consistently upregulated in all the Sen cell conditions, we hypothesized that CD36 might regulate the *in vivo* senescence secretory program, impairing regeneration.

All three Sen cell types had higher CD36 protein expression in injured muscles (Figure 42A). *Cd36* expression was also induced in cells rendered senescent in response to etoposide treatment *in vitro* (Figure 42B), confirming that distinct senescence triggers induce *Cd36* expression *in vivo* and *in vitro*.

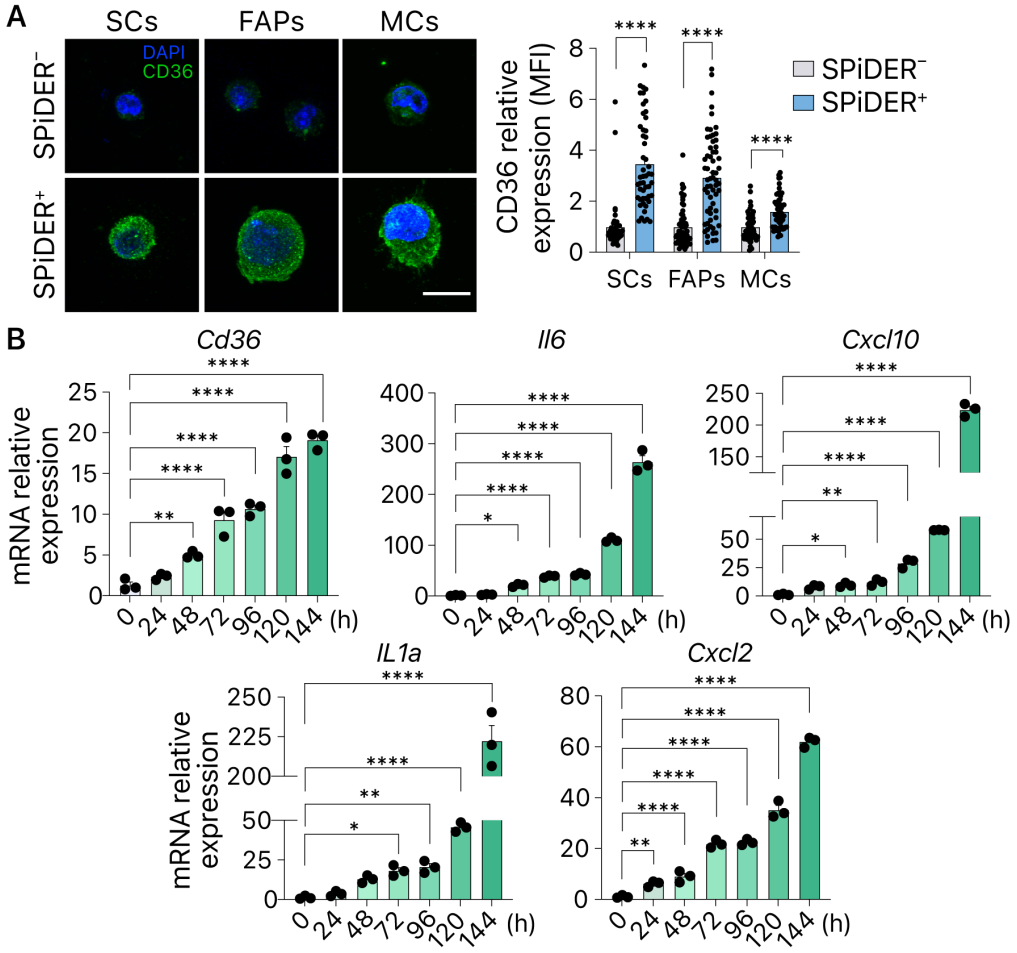

Figure 42. Senescent populations display lipid accumulation and related genes *in vivo*. **A**) Representative images and quantification of CD36 levels in freshly sorted SPiDER^{+} and SPiDER^{-} populations from regenerating muscles at 3 DPI (n= 46-62 cells). **B**) C2C12 cells were treated with etoposide to induce cellular senescence and harvested at the indicated time points. Graphs show relative mRNA expression levels of *Cd36* and SASP-related genes normalized to untreated C2C12 cells at different times after etoposide treatment (n=3 replicates). Scale bar: 10 μm. Results are displayed as mean ± s.e.m.; P-values were calculated by a two-tailed unpaired t-test in **A** and two-way ANOVA in **B**; significance is reported as *p<0.05, **p<0.01 and ****p<0.0001.

We next analysed muscles from young or old mice that had been treated for 4 days (starting at 3 DPI) with an anti-CD36 neutralizing antibody (at two distinct doses), or a control IgA antibody. CD36 blockade did not trigger a reduction in senescent cell number -unlike senolytic treatment- (Figure 43A,B) but did induce a reduction in several SASP components, revealed by an analysis of proteins secreted by Sen cells (Figure 43C).

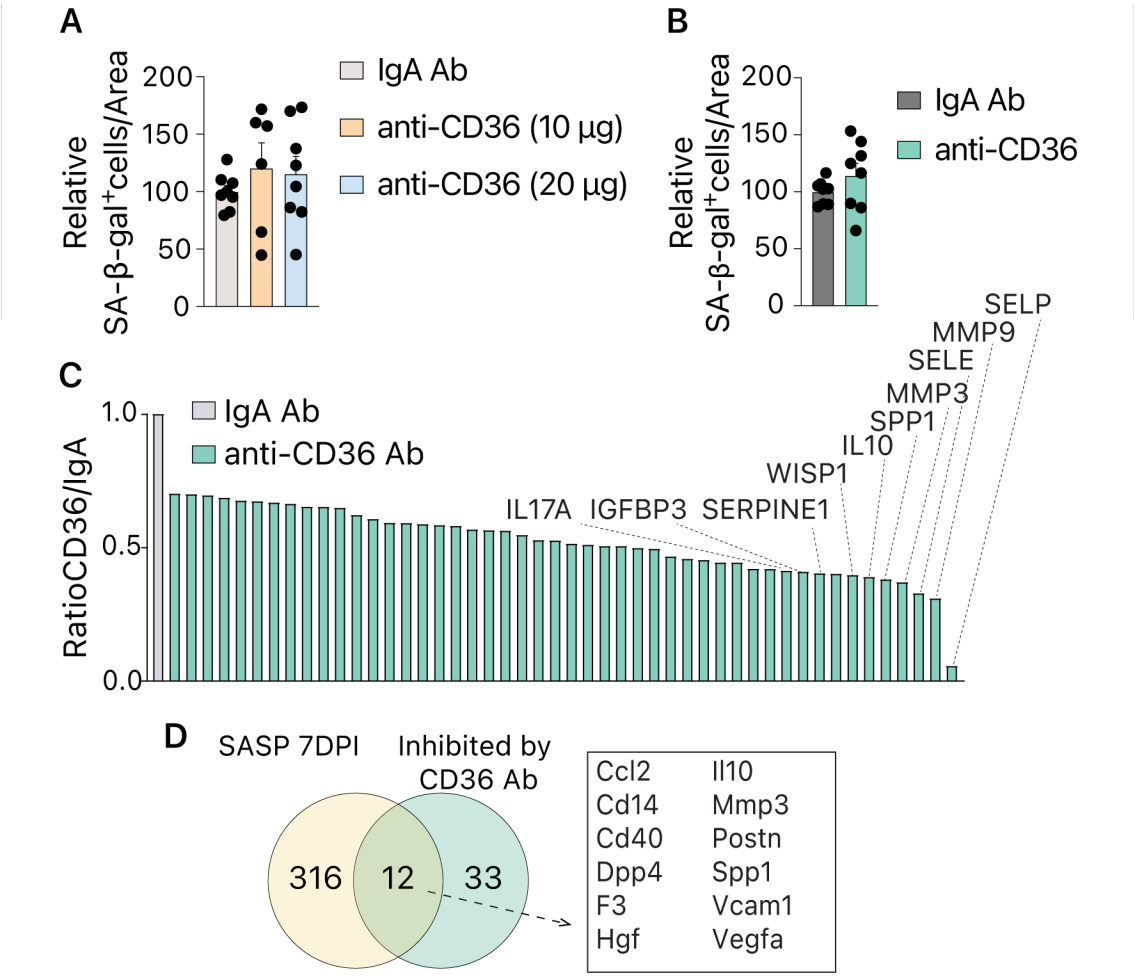

Figure 43. CD36 blockade leads to reduced SASP secretion in senescent cells *in vivo*. Mice were injured with CTX and treated with control anti-IgA or anti-CD36 antibody from 3 to 7 DPI once per day. Quantification of SA-β-gal^{+} cells in the damaged area of TA muscles from **A**) young (n=6-8 muscles from 3-7 mice) and **B**) aged mice (20-month-old) (n=8 TA

from 4 mice). **C**) Freshly sorted SPiDER^{+} cells from IgA- or anti-CD36 antibody-treated old mice at 7 DPI were cultured for 24 hours in serum-deprived media, conditioned media was collected, and protein levels were assessed by cytokine array. Quantification showing the proteins which levels were reduced by 30% in the presence of anti-CD36 antibody. **D**) Venn diagram showing the overlap between SASP-related upregulated genes in senescent populations isolated from geriatric mice at 7 DPI and genes codifying for protein reduced by anti-CD36 antibody treatment in **C**. Results are displayed as mean ± s.e.m.

Remarkably, many of the CD36-regulated secreted proteins coincided with upregulated SASP genes in Sen SCs, FAPs, and MCs, such as those encoding chemokines, cytokines, and complement factors, including *Ccl2*, *Il10*, *Mmp3*, *Hgf*, and *Postn* (Figure 43D). Together, these results indicated that CD36 blockade acts as a senomorphic rather than a senolytic, principally affecting the inflammatory SASPs. Of interest, several Sen cell-secreted inflammatory SASPs (e.g., *Ccl2*, *Ccl4*, *Cxcl10*, among others) that induced downstream signalling in NSen SCs in the L-R interactive network analysis were predicted to negatively impact SC functions and muscle regeneration, and some of them appeared as CD36-regulated SASP components (Supplementary Figure 1). More importantly, CD36 blockade not only improved muscle regeneration in both young and old mice (Figure 44A,B) but also reduced inflammation (Figure 44C) and fibrosis (Figure 44A,B). Furthermore, regenerating muscles from anti-CD36 antibody-treated old mice showed increased force (Figure 44D). Improved muscle regeneration after CD36 neutralization was comparable to the improvement observed after senescent cell elimination (either pharmacological or genetic) in mice. These results reinforced the predicted CD36 network and L-R interactions analysis and indicate that CD36 inactivation unleashes repressive inflammatory downstream effects in SCs within the regenerative niche. We next silenced *Cd36* in freshly sorted Sen cells using specific siRNA (*si-Cd36*); scrambled siRNA (*si-Scramble*) was used as a control. Upon transplantation to injured muscle, *si-Scramble*-Sen cells delayed its regeneration, whereas engraftment of *Cd36*-silenced Sen cells had no negative effects (Figure 44E). Consistent with this result, the SASPs produced by freshly sorted Sen cells reduced SC proliferation in *ex vivo* transwell assays (Figure 44F), but this effect was not observed when *Cd36* was silenced in senescent cells before co-culturing with SCs (Figure 44F). Overall, these results demonstrate that CD36 is crucial for the paracrine effects of Sen cells on muscle regeneration by regulating the production of the SASP (principally via pro-inflammatory factors) *in vivo*. These SASPs create an inflamed “aged-like” niche that blunts the SC proliferation and regeneration.

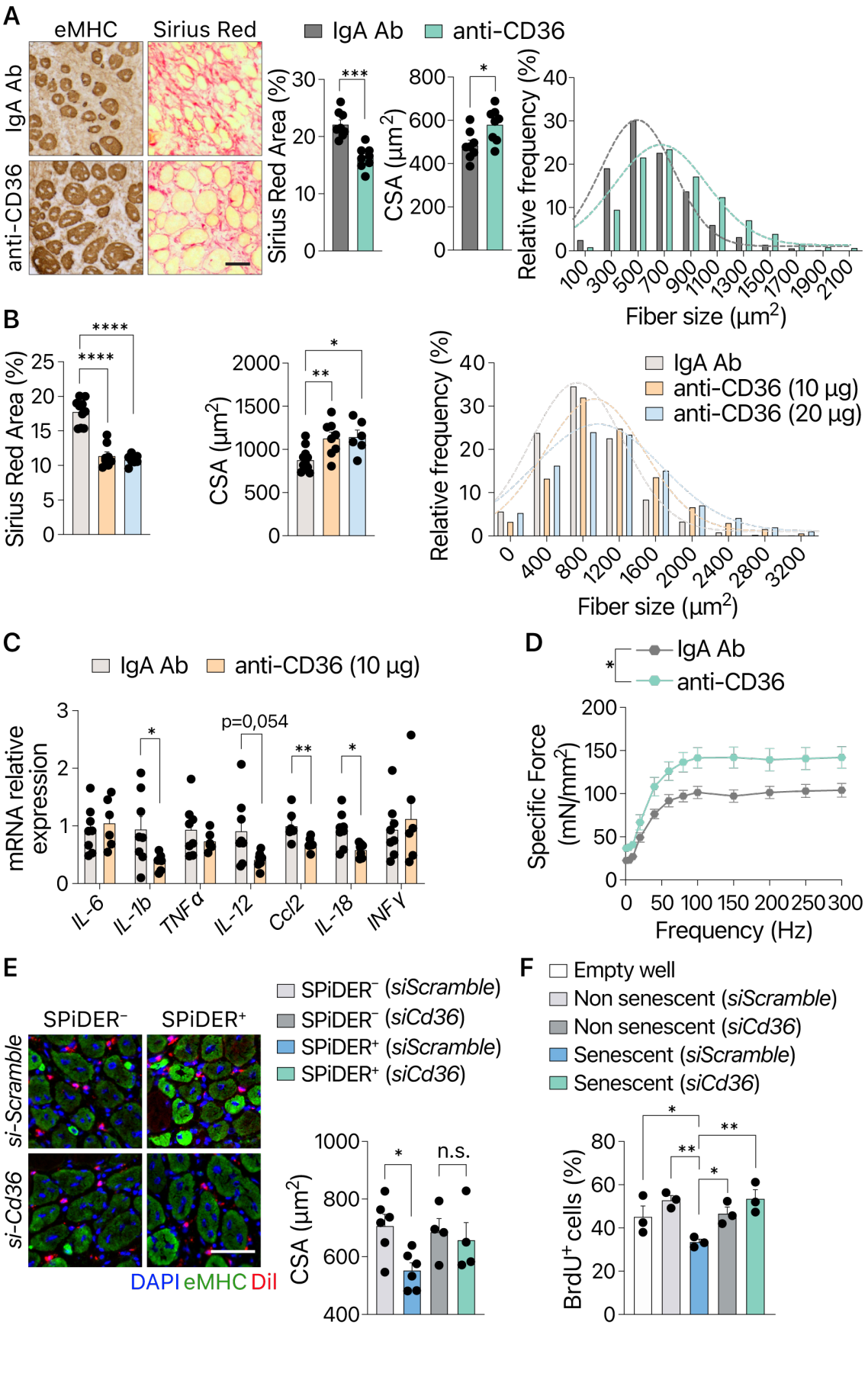
A
eMHC
Sirius Red
IgA Ab
anti-CD36
Sirius Red Area (%)
CSA (µm²)
Relative frequency (%)
Fiber size (µm²)
B
IgA Ab
anti-CD36 (10 µg)
anti-CD36 (20 µg)
C
mRNA relative expression
p=0,054
IL-6
IL-1b
TNFα
IL-12
Ccl2
IL-18
INFγ
D
Specific Force (mN/mm²)
Frequency (Hz)
E
SPiDER⁻
SPiDER⁺
si-Scramble
si-Cd36
DAPI eMHC DiI
SPiDER⁻ (siScramble)
SPiDER⁻ (siCd36)
SPiDER⁺ (siScramble)
SPiDER⁺ (siCd36)
n.s.
F
Empty well
Non senescent (siScramble)
Non senescent (siCd36)
Senescent (siScramble)
Senescent (siCd36)
BrdU⁺ cells (%)

Figure 44. CD36 blockade improves muscle regeneration in young and old mice.
Mice were injured with CTX and treated with control anti-IgA or anti-CD36 antibody from 3 to 7 DPI once per day. **A**) Representative images, quantification of CSA, and frequency distribution analysis of eMHC$^+$ fiber size and Sirius Red staining of regenerating TA muscles are shown (n=7-8 TA from 4 mice). **B**) TA muscles of young mice were subjected to CTX injury and animals were treated with control IgA or anti-CD36 antibody from 3 to 7 DPI once per day. Quantification of mean CSA and frequency distribution analysis of eMHC$^+$ fibers and Sirius Red staining in muscle cryosections are shown (n=6-11 muscles from 3-7 mice). **C**) As in **B**, mRNA expression levels of the indicated genes by RT-qPCR (n=6-8 muscles from 3-4 mice). **D**) EDL muscles of old mice were injured with CTX, and mice were treated with anti-IgA or anti-CD36 antibodies from 3 to 10 DPI (n=5 EDL from 3 mice). Force-frequency curves are shown. **E**) SPiDER$^+$ or SPiDER$^-$ cells isolated from young regenerating muscles at 3 DPI were transfected with *si-Scramble* or *si-Cd36*, stained with DiI, and transplanted into pre-injured TA muscle of the recipient young mice. Samples were collected 4 days after transplantation. Representative images and quantification of CSA of eMHC$^+$ fibers in damaged areas (n=4-6 mice). **F**) SCs were isolated at 3 DPI from regenerating muscles of young mice, then cultured for 3 days in transwells with senescent or non-senescent C2C12 cells, previously treated with *si-Cd36* or *si-Scramble*, or without adding cells. After 3 days of culture, SCs proliferation was assessed by BrdU incorporation. quantification of BrdU+ cells is shown (n=3 mice). Scale bars: 50 μm. Results are displayed as mean ± s.e.m.; P-values were calculated by Mann Whitney test in **A**, **B**, **C**, and **E**, two-way ANOVA in **D**, and Fisher's LSD in **F**; significance is reported as *p<0.05, **p<0.01, ***p<0.001, and ****p<0.0001.

DISCUSSION

Cellular senescence is transiently present during muscle regeneration

Cellular senescence is a multifaceted process involved in a variety of physiological and pathological contexts. Although cellular senescence has been detected in skeletal muscle during ageing, regeneration, and disease, its purpose has not been fully investigated in these processes. Our first aim was centred on the description of cellular senescence from a kinetic point of view. Based on the SA-β-gal staining, we established that senescent cells appear at 3 DPI, peak around 3-7 DPI, and decrease until reaching almost basal levels at 21 DPI. These data indicate that cellular senescence is a transient phenomenon, which mostly coincides with the second/third pro-inflammatory wave and expansive/differentiating phases of niche-residing cells in the muscle regeneration process. Interestingly, we observed that the generation of senescent cells was higher in regenerating tissue of geriatric animals, coinciding with its delayed regenerative capacity. Thus, exacerbated levels of senescent cells might also partially explain the regenerative delay in geriatric mice, as previously suggested[91,94]. Moreover, senescent cells persisted longer in aged muscles and still presented considerable levels even at 21 DPI. These results made us realize that certain "chronification" of cellular senescence occurs at an advanced age, perturbing the normal regeneration course. Whether this occurs due to a higher predisposition of aged cells to enter senescence upon injury (similar to the geroconversion observed in SCs[94]) or to a lower capacity of the aged immune system in clearing senescent cells during muscle regeneration remains to be answered. Indeed, we and others have shown that muscle-residing cells accumulate DNA damage, dysfunctional mitochondria, increased ROS levels, misfolded proteins, and other abnormalities, with age (reviewed in Sousa-Victor et al., 2022[17]). All of these are potential causes of senescence entry, present in aged muscle prior to an injury. On the other hand, it is known that dysregulated immune response, and particularly a compromised pro-inflammatory to pro-fibrotic switch in macrophages, leads to delayed muscle regeneration in aged mice[109,111]. Similarly, mdx mice display an impaired pro-inflammatory to pro-fibrotic switch of macrophages[257], as well as an accumulation of senescent cells. Of note, senescence of the immune system (or immunosenescence) also occurs with age, greatly affecting immune cell functions and fuelling pro-inflammatory response (inflammageing) and cellular senescence in peripheral tissues[223,258]. Thus, the senescent immune system can also contribute to the exacerbated and prolonged presence of senescent cells in aged muscle tissue. Nevertheless,

immunosenescence, age-related accumulation of senescent cells, inflammageing and other components are tightly connected to each other, making it complicated to dissect their precise role in muscle regeneration and other contexts (Figure 45). Future studies are needed to unravel the exact contribution of these components to the generation of senescent cells in old tissues.

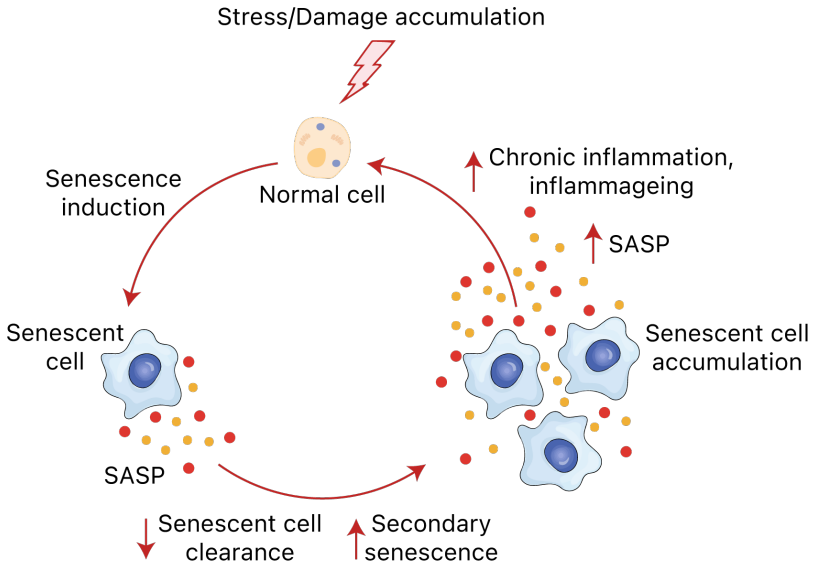

Figure 45. Feedback loop of senescent cell accumulation.
Senescent cells can be generated in response to stress and accumulation of cellular damage due to the ageing process. If the senescent cell is not efficiently eliminated (due to an aged immune system), its SASP can potentiate secondary senescence induction, accumulation of senescent cells and chronic inflammation. Adapted from Gasek et al., 2021[167].

A novel strategy allows the isolation of senescent cells from complex tissue

Our next step towards understanding cellular senescence in muscle regeneration relied on the isolation and characterization of senescent cells. For that to occur, we first had to generate a protocol for senescent cells isolation from a complex tissue, a major challenge in the field of senescence. Senescent cells have been exclusively studied *in vitro* due to the inability to separate them from other non-senescent cells. Why is it so difficult to isolate senescent cells from other populations? A major reason is because the senescent state lacks a universal marker that would unequivocally identify it. Even the mouse models based on $p16^{INK4a}$ and $p21^{CIP1}$ expression are limited, as not all $p16^{INK4a}$- and $p21^{CIP1}$-expressing cells are senescent and *vice versa*. Although none of the known markers of cellular senescence is exclusive, it is widely accepted that a combination of several markers is useful for senescent cells' identification. While our strategy relied on a

single marker of senescence, SPiDER-β-gal (or SA-β-gal activity), other markers validated it afterwards. For instance, subsequent analysis of sorted populations demonstrated enrichment in many other parameters: DNA damage, high ROS, reduced lamin B1 and proliferation levels, lack of apoptosis, increased cell size, and $p16^{INK4a}$ expression. Noticeably, these parameters were checked in distinct populations, suggesting that this protocol can be applied to different cell types and tissues. Of course, it is worth mentioning that this method does not provide a 100% pure senescent population. Nevertheless, it represents a big step towards the characterization of senescent cells *in vivo*, much needed in the field.

Three major cell populations undergo senescence in skeletal muscle upon injury

A scRNA-seq approach, together with the SPiDER-β-gal-based sorting, allowed the identification of the three major cell types undergoing senescence in regenerating muscle. By far, three cell populations: SCs, FAPs, and MCs, which constituted a major part of $SPiDER^{+}$ cells. We confirmed these findings by tissue immunostaining with $p16^{INK4a}$ and γH2Ax labelling and established the levels of these populations in this order: SCs<FAPs<MCs. Although we also identified other cell types (B/T/NK cells, endothelial cells, antigen-processing cells, and neutrophils) in the $SPiDER^{+}$ fraction, their levels were scarce, not allowing their full characterization. Further study of minor senescent populations remains to be performed by adding sequencing power in future investigations. Another thing to bear in mind is that we chose to look for the early senescent populations at 3 DPI, which is only a snapshot of the complex regeneration process. Distinct muscle-residing populations are kinetically organized, with some populations appearing in early or very advanced regeneration steps. Thus, we cannot discard that senescent tenocytes, Schwann cells, smooth muscle cells, and other cell types do not occur in the regenerating muscle. Assessing the heterogeneity of senescent cells at different stages of regeneration should be performed by future studies.

Senescent cells maintain their lineage-specific signatures and gain new features with ageing

A deeper characterization of the major senescent populations showed that senescent cells still conserve their linage-related traits. Thus, senescent cells resemble their origins more than a common description of senescence, as suggested by the PCA clustering and gene expression. This tendency was already

observed in the previous *in vitro* studies, showing that senescent melanocytes, fibroblasts, and keratinocytes were rather clustering according to their lineage and not their senescent state[127]. Interestingly, senescent cells acquired new traits with ageing, with pathways associated with cellular plasticity and development. Whether these data indicate loss of identity or a new role of senescent cells with ageing, remains to be answered by future functional assays. Some studies suggest a controversial role of cellular senescence in cellular reprogramming. While cellular senescence impedes the reprogramming of the cell, the SASP promotes the reprogramming of neighbour cells in a paracrine fashion[194,195,197,259]. Interestingly, aged tissues are more efficiently reprogrammed, in line with the accumulation of senescent cells and our findings[195]. Thus, it might be interesting to investigate whether the reprogramming efficiency can be further boosted by the senescent cells generated in older tissues. In addition, geriatric senescent cells exhibited a new set of pathways related to inflammation, suggesting that aged senescent cells might express an exacerbated pro-inflammatory phenotype, further hampering muscle regeneration.

Senescent cells are generated in response to high levels of injury-induced oxidative stress

Another aim of our research was to understand the mechanisms of senescence entry in distinct populations in the regenerative muscle context. We observed a variety of damage-associated pathways enriched in the senescent populations, with some of them related to DNA damage signalling and oxidative stress. Indeed, high levels of ROS production occur during the earliest stages of muscle regeneration, promoting muscle residing cells activation, recruitment of immune cells and clearance of debris among others[260]. However, high levels of ROS produced by neutrophils can worsen the state of the muscle, damaging previously intact myofibers[19,50,51,260,261]. Moreover, several studies reported the beneficial effects of antioxidant treatments in muscle regeneration and DMD[262–266]. Thus, we presumed that the levels of oxidative stress might be the determining factor for some cells to undergo cellular senescence instead of other fates. Our data showed that DNA damage and ROS levels were increased in all cells in regenerating muscle as compared to the resting state. These levels were even higher in the senescent cells than in the non-senescent ones. Moreover, we showed that ROS^{High} populations, isolated prior to the appearance of senescent cells, were more prone

to enter cellular senescence in the following days. Noticeably, reducing ROS levels with an antioxidant NAC abrogated this tendency. In addition, DNA damage and oxidative stress are increased with ageing, suggesting that this priming might be the cause of the higher senescence burden observed in the regenerating muscle of old animals. Thus, we conclude that although regeneration-induced oxidative stress is needed for several functions, it can also lead to some collateral damage, such as the generation of senescent cells. This effect is further exaggerated with ageing, due to the accumulation of damage in resting conditions.

Senescent cells maintain two highly conserved hallmarks: inflammation and fibrosis

An additional major aim of our study was to identify a core signature of cellular senescence *in vivo*. Searching for the "holy grail" of cellular senescence has been one of the major goals in the field. We observed that 47 genes behaved in the same fashion in most senescent populations, some of which had been previously linked to cellular senescence by other studies. Such is the case for the canonical SASP genes *Ccl2*, *Ccl8*, and *Igfbp4*, identified by both, single-cell and low-input RNA-seq approaches. On the other hand, downregulation of the *Cenpa* gene was shown to induce cellular senescence *in vitro*, also correlating with our findings[245,246]. In addition, most of the genes identified as commonly regulated in our analysis are included in the SeneQuest database, a platform developed by the International Cell Senescence Association (ICSA) that integrates all transcriptomic data of previous *in vitro* works[135]. Of note, we did not observe the most illustrious markers of senescence $p16^{INK4a}$ nor $p21^{CIP1}$ genes in our list, in line with previous statements[127]. Thus, our data majorly reproduced previous findings performed *in vitro*. It is important to note that, even though our list of genes suits most senescent populations, it does not work for 100% of them. This observation is not surprising, given the highly heterogeneous state of cellular senescence, even *in vitro*[127]. Thus, we relied on a pathway enrichment analysis in an attempt to find a common description for senescent cells *in vivo*. We identified that two hallmarks—inflammation and matrix remodelling—are conserved in all senescent populations, ages, and time points. Two major hallmarks were also echoed in the SASP description. Similar to the global pathway analysis, the SASP majorly exhibited pro-inflammatory and pro-fibrotic functions. Of note, a recent multiomics study of senescent cells *in vitro* showed progressive accumulation of pathways related to

inflammation, lipid metabolism, cellular stress and downregulation of pathways related to cell cycle and DNA repair, highly correlating with our findings[238]. Further transcriptomic profiling analysis in senescent cells *in vivo* revealed evidence for an association between the TFs NFκB, Smad, IRF1/3, and C/EBPβ, and for the induction of inflammatory cytokines, matrix proteins, and interferon-response genes. These TFs have been reported to be master regulators of the SASP program (reviewed in Kumari et al., 2021[267]), further supporting our data. Thus, we conclude that the cellular senescence phenomenon is too heterogeneous to share expression at a gene level. Rather than a list of conserved genes, we identified a pattern of expression at a pathway level, with common traits related to matrix remodelling and inflammation.

Senescent cells restrain muscle regeneration throughout life

The prevailing view in the field is that senescent cells have a beneficial role in transient processes, such as embryo development, wound healing, and tissue regeneration. As we previously mentioned, cellular senescence occurs transiently during muscle regeneration as well. Although some research has been done on senescent cells from regenerating muscle, the exact contribution of senescent cells to the process has never been shown. In fact, senescence-targeting approaches have been performed before regeneration induction, but never during muscle regeneration, where the burden of senescent cells reaches its maximal levels[212,225]. These observations show that systemic elimination of senescent cells that accumulate with ageing both rejuvenates and restores the regenerative capacity, but fail to unravel the direct contribution of senescent cells to muscle regeneration. In our study, we employed different strategies to conclude that targeting senescent cells accelerates muscle regeneration. Both senolytics and GCV treatments in p16-3MR mice were effective for targeting senescent cells in regenerating muscle, leading to increased fiber size of newly formed fibers. We also observed increased muscle force, an important parameter for muscle function, in mice treated with either senolytics or GCV. Surprisingly for us, targeting senescent cells was advantageous not only in old mice but even in young ones, challenging the prevailing view in the field. Further, transplanting senescent cells into young regenerating muscle delayed the normal course of regeneration, mimicking age-associated decline and further supporting our previous observations.

Distinct senescent populations equally restrain muscle regeneration

We also questioned whether a particular subtype of senescent cells was responsible for the detrimental effect on muscle regeneration. Indeed, distinct senescent populations are targeted by senolytics or GCV treatments. Thus, we first played with niche-residing and infiltrating populations by combinations of whole muscle graft experiments. We observed that muscle regeneration was improved in all combinations involving partial or total $p16^{INK4a}$-expressing cell removal. Similarly, transplantation experiments showed that all three major senescent cell types—SCs, FAPs, and MCs—induced delayed muscle regeneration in young animals. These results excluded the possibility of one particular cell population being responsible for the observed detrimental effect on muscle regeneration, indicating that a common trait of different senescent populations restrains muscle regeneration.

Senescent cells play a detrimental role in muscle regeneration irrespective of their chronic/transient presence

Another aim of the study relied on the juxtaposition of the acute and chronic presence of senescent cells in muscle tissue. For that, we chose mdx animals with chronic regenerative/degenerative cycles occurring in their muscles. Indeed, senescent cells could be detected for months by different approaches, coexisting with continuous damage in the dystrophic animals. We targeted senescent cells with months-long treatments with senolytics in mdx animals and observed ameliorated disease progression. Similarly, treatment with GCV induced reduced fibrosis and increased fiber size and force in mdx mice crossed with the p16-3MR model. Comparable data were reported by other studies, showing the detrimental role of senescent cells in DMD rats, where senescent cells were targeted with ABT263 senolytic and genetic interventions[228]. Thus, we concluded that senescent cells play a detrimental role in both acute and chronic scenarios, suggesting that muscle tissue does not follow the transient/persistent rule established in the field.

The SASP hinders the proliferative capacity of neighbouring SCs

Cellular senescence is characterized by high metabolic activity and secretion of proactive molecules. Hence, we focused on the SASP to unveil the mechanism behind the regulation of muscle regeneration by senescent cells. Strikingly, the SASP of young senescent cells strongly resembled the state of inflammageing,

suggesting that senescent cells create an "aged-like" niche even in young animals[251–253]. Transcriptomic and proteomic characterization of the SASP demonstrated the pro-inflammatory and pro-fibrotic nature of the secreted molecules, such as CCL2, IL-1a, and MMP2 among others. Importantly, a recent study has shown a negative impact of excessive pro-inflammatory CCR2-CCL2 signalling on muscle regeneration[110]. Further L-R analysis based on the SASP of senescent cells unveiled pro-inflammatory and pro-fibrotic signalling towards non-senescent cells, as indicated by TNFα and TGFβ pathways. In agreement with these data, targeting senescent cells with senolytics or GCV led to a decreased fibrotic load and reduced expression of pro-inflammatory cytokines in regenerating muscle. Moreover, transplantation of senescent cells induced higher infiltration of $CD11b^+$ cells and increased fibrotic area in the regenerating niche. Thus, we established that senescent cells delay muscle regeneration in both young and geriatric animals by promoting inflammation and fibrosis.

Another interesting aspect of the SASP signalling is its ability to induce secondary senescence in a paracrine fashion, termed the senescence bystander effect[140]. Curiously, we detected the "cellular senescence" response among the activated signalling obtained by L-R analysis and SPIA prediction, so we further explored it. Transplantation of senescent cells into pre-injured muscle resulted in a higher number of SA-β-gal^+ cells in the engrafted niche. Moreover, transplantation of *in vitro* induced senescent C2C12 cells into the pre-injured muscles of p16-3MR receptor animals led to higher luciferase signal, suggesting higher abundancy of $p16^{INK4a}$-expressing cells. We also tested the ability of senescent cells to influence the non-injured muscle niche. Interestingly, we observed higher DNA damage levels in SCs that were in close proximity to the engrafted senescent populations. Thus, one of the mechanisms of action of senescent cells might be the induction of secondary senescence in the niche cells, such as SCs.

Muscle regeneration is a complex process involving many different cell populations that must play their role in a timely, organized matter. SCs play the most prominent role in this process, as the generation of the new fibers relies on them. To rapidly and efficiently restore the muscle following insult, SCs must activate and proliferate to generate enough progeny for subsequent differentiation and fusion into fibers. Inhibited proliferation was induced in the receptor SCs, as indicated by L-R analysis coming from the different SASP molecules, suggesting that the SASP may interfere with the SCs proliferation. Indeed, SCs proliferation was higher both

in vivo and *in vitro* upon senescent cells' targeting with GCV. Also, the transwell experiment showed a decreased proliferative rate of receptor SCs in presence of senescent cells and their SASP. This approach was particularly enlightening since senescent cells were physically separated from the receptor SCs, allowing the selective permeability of secreted molecules and small vesicles (the SASP). In summary, these data show that senescent cells restrain SCs proliferation by the SASP signalling during muscle regeneration.

CD36 regulates the SASP production of *in vivo*-generated senescent cells

We and others[127,143] showed that both senescent cells and their SASPs are highly heterogeneous. Inhibiting each of the SASP molecules to further validate our mechanism was unfeasible within the framework of this thesis. Thus, we opted to interfere with SASP production rather than targeting it. A modified version of the computational method FunRes identified the *Cd36* gene upstream NFκB, MAPK, and IRF signalling and SASP-related genes, such as *Il6*, *Tgfb1*, *Mmp3*, *Ccl2*, and *Igfbp5*. Importantly, lipid transport and particularly *Cd36* presented stable upregulation in all senescent populations and conditions. The levels of CD36 were also higher at a protein level in the senescent populations compared to the non-senescent ones. Of note, a recently published multiomics study identified *Cd36* as one of the genes with increased transcription in senescent cells[238]. *In vitro* studies of CD36 suggest its involvement in SASP production[239,240]. Here, we tested the CD36 potential as a senomorphic *in vivo*, by systemic treatment with an antibody. Although we did not observed a reduction in the number of senescent cells, treatment with an anti-CD36 antibody reduced SASP secretion in senescent cells. Interestingly, anti-CD36 antibody treatment affected several SASP components that were previously identified by RNA-seq and FunRes network, including *Ccl2*, *Mmp3*, *Il10*, and *Hgf*, confirming the potential senomorphic role of CD36 *in vivo*. Most importantly, the mice treated with an anti-CD36 antibody presented signs of accelerated muscle regeneration at young and old age. Strikingly, treatment with the anti-CD36 antibody-induced increased fiber size and force and reduced inflammation and fibrotic deposition in regenerating muscle, mimicking the beneficial effects observed with senolytics and GCV strategy. Of note, silencing *Cd36* in senescent cells only was sufficient to neutralize the detrimental role of cellular senescence on muscle regeneration: *siCd36*-treated senescent cells did not delay regeneration in engrafted receptor muscles. However, previous research

indicated an important role of CD36 in muscle regeneration, as total ablation of CD36 induced delayed muscle regeneration in the CD36 KO mice[241]. These apparent differences may arise from different strategies employed. While a total CD36 KO may have a strong effect on whole-body metabolism and skeletal muscle, even in homeostasis, we opted for a short-term treatment of a few days with an anti-CD36 antibody, which most likely had a milder whole-body effect. Moreover, treatment with *siCd36*, prior to the engraftment of the senescent fraction, unequivocally showed CD36 importance in cellular senescence, further confirming our hypothesis. Hence, these data further establish that the detrimental influence of senescent cells is propagated through their SASP and proved the regulatory potential of the SASP by the CD36 receptor (Figure 46).

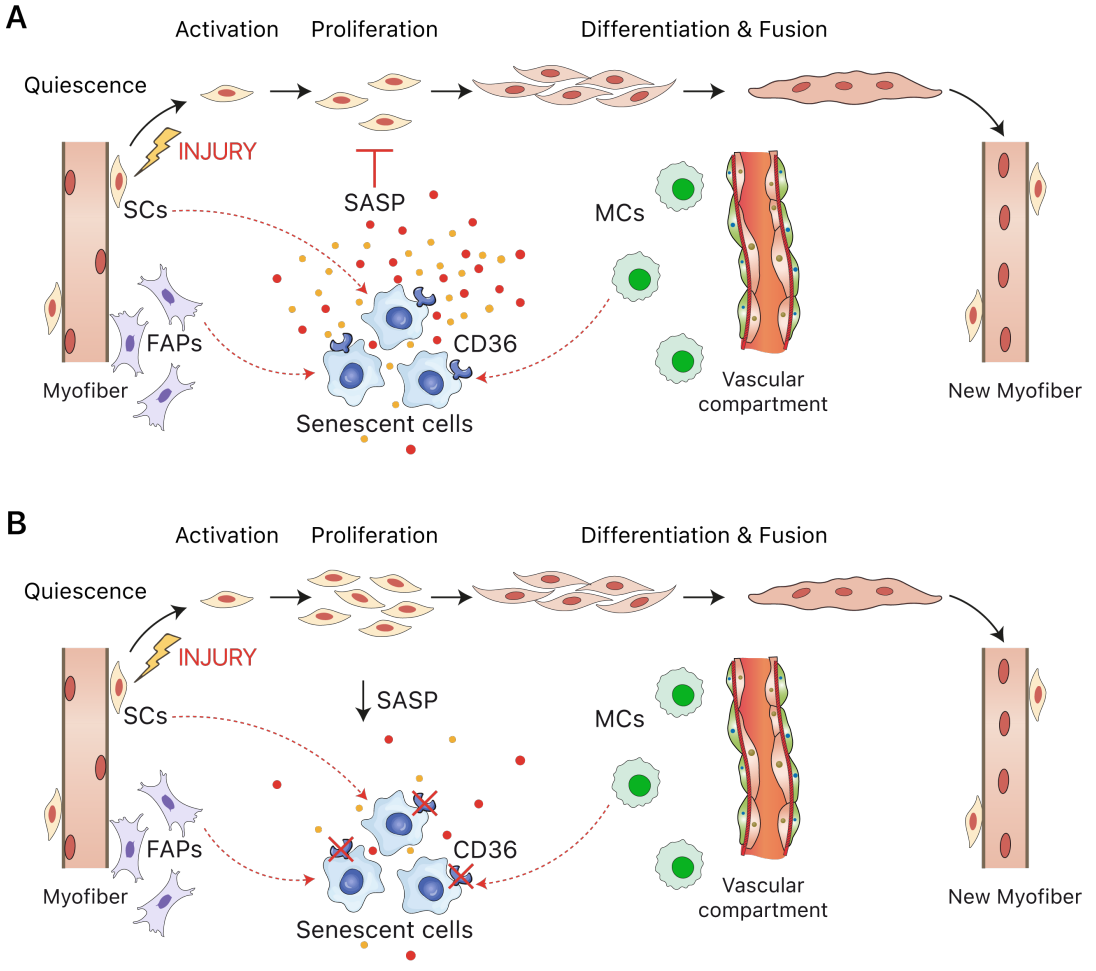

Figure 46. Proposed mechanism.
A) In response to injury, senescent cells are generated from niche-residing cells. The SASP, composed of pro-inflammatory and pro-fibrotic factors, restrains SCs proliferation and muscle regeneration. **B**) CD36 receptor regulates the SASP production in senescent cells. When CD36 is inactivated, the SASP levels are drastically reduced, unleashing the repressive effect on SCs proliferation and promoting muscle regeneration. Figure created with BioRender.

CONCLUSIONS

1) Senescent cells appear transiently during muscle regeneration of young and geriatric animals. The burden of senescent cells is higher and more prolonged in aged mice as compared to young ones.

2) SPiDER-β-gal strategy allows efficient separation of senescent cells from complex tissues, correlating with well-established markers of senescence.

3) Senescent cells arise from the major niche-residing populations (namely, SCs, FAPs and MCs) in the context of muscle regeneration.

4) *In vivo*-generated senescent cells have highly heterogeneous profiles and maintain lineage-specific signatures. Senescent population gain additional traits with ageing, related to cell plasticity and inflammation.

5) Senescent cells are generated in response to high oxidative stress and DNA damage upon injury.

6) Senescent cells maintain two common hallmarks related to inflammation and matrix remodelling/fibrosis, rather than a set of conserved genes.

7) The SASP of senescent cells is highly pro-inflammatory and pro-fibrotic and is regulated by NFκB, Smad, C/EBPβ, as well as by other master regulator TFs.

8) Senescent cells play a detrimental role in muscle regeneration in young and geriatric mice, through pro-inflammatory and pro-fibrotic signalling.

9) Targeting senescent cells can ameliorate DMD progression. Thus, cellular senescence negatively impacts acute and chronic muscle regeneration.

10) Senescent cells restrain proliferation of muscle stem cells through their SASP signalling.

11) CD36 regulates the SASP production in senescent cells, and its inactivation leads to reduced SASP signalling and accelerated muscle regeneration.

MATERIALS AND METHODS

Animal models

C57Bl/6 (WT), p16-3MR (kindly donated by J. Campisi)[168], dystrophic mdx (DBA/2 background)[268] and p16-3MR/mdx (dystrophic DBA/2-mdx mice crossed with p16-3MR mice) were bred and aged at the animal facility of the Barcelona Biomedical Research Park (PRBB), housed in standard cages under 12-hour light-dark cycles and fed *ad libitum* with a standard chow diet. The Catalan Government approved the work protocols, following applicable legislation. Both male and female mice were used in each experiment unless stated otherwise. Live colonies were maintained and genotyped as per Jackson Laboratories' guidelines and protocols. Mice were housed together, health was monitored daily for sickness symptoms (not age-related weight loss, etc), and euthanized immediately at the clinical endpoint when recommended by veterinary and biological services staff members. No statistical methods were used to predetermine the sample size.

Genotyping of mice

For PCR genotyping the following primers were used:

p16-3MR-1: 5′-AACGCAAACGCATGATCACTG-3′ and p16-3MR-2: 5′-TCAGGGATGATGCATCTAGC-3′. Positive animals show a band at 202 bp.

Human biopsies

Human muscle biopsies from the vastus lateralis muscle of patients undergoing surgery were obtained via the Tissue Banks for Research from Vall d'Hebron and Sant Joan de Deu Hospitals (Barcelona) and Arnau de Vilanova/Hospital Clinic Hospitals (Valencia), and especially via the EU/FP7 Myoage Consortium. A portion of the muscle tissue was directly frozen in melting isopentane and stored at -80 °C until analysed. The age of the individuals was 81±7.5 years old. Damaged areas were identified by morphological criteria, based on the presence of infiltrating mononuclear cells. Data are from female patients aged 69, 82, 80, 89, and 85 years/old. The average age was 81±7.5 years.

***In vivo* treatments**

Quercetin (USP, #1592409; 50 mg/kg) and dasatinib (LC Laboratories, #D-3307; 5 mg/kg) were administered orally (gavage). Control mice were administered with an equal volume of vehicle (10 % ethanol, 30 % polyethilenglicol, and 60 % phosal). Ganciclovir (GCV, Sigma-Aldrich, #G2536-100MG; 25 mg/kg) was injected intraperitoneally (i.p.). Anti-CD36 antibody (Cayman Chemical, #10009893; 10 μg

or 20 μg in young and 20 μg in old mice) diluted in phosphate buffered saline (PBS) was administered via i.p., control mice received an equal dose of IgA control antibody (Southern Biotech/Bionova, #0106-14). Treatments with GCV, senolytics, and CD36 were administered daily for 4-7 consecutive days as indicated in the figure legends. N-acetylcysteine (NAC, Sigma-Aldrich, #A9165; 0.01 g/ml) was added into drinking water (exchanged every three days) one week before muscle injury and was prolonged until sacrifice. For long-term treatments, 3 months old mdx and p16-3MR/mdx mice were administered with quercetin plus dasatinib (Q+D) or GCV respectively twice a week for 2 months.

Muscle regeneration

Mice were anaesthetized with ketamine-xylazine (80 and 10 mg/kg respectively; i.p.) or isoflurane. Regeneration of skeletal muscle was induced by intramuscular injection of cardiotoxin (CTX, Latoxan, #L8102; 10 μM) as previously described[269]. At the indicated times post-injury, mice were euthanized, and muscles were dissected, frozen in liquid-nitrogen-cooled isopentane, and stored at -80°C until analysis.

Heterografting

Heterografting was performed as previously described[270]. EDL muscle was removed from the anatomical bed of either p16-3MR or WT and was transplanted onto the surface of the TA muscle of the p16-3MR or WT recipient mouse or *vice versa*. Muscle grafts were collected on day 7 after transplantation.

Muscle force measurement

Ex vivo force measurements of EDL muscles were assessed as previously described[271]. Briefly, mice were sacrificed, and muscles were immediately excised and placed into a dish containing oxygenated Krebs-Henseleit solution. Muscles were mounted vertically in a temperature-controlled chamber and immersed in a continuously oxygenated Krebs-Ringer bicarbonate buffer solution, with 10 mM glucose. One end of the muscle was linked to a fixed clamp, while the other end was connected to the lever arm of a force transducer (300B, Aurora Scientific) using a nylon thread. The optimum muscle length (Lo) was determined from micromanipulations of muscle length to produce the maximum isometric twitch force. The maximum isometric-specific tetanic force was determined from the plateau of the curve of the relationship between specific isometric force with a

stimulation frequency ranging from 1 to 300 Hz. Force was normalized per muscle area, determined by dividing the muscle mass by the product of length and muscle density of (1.06 mg/mm^3), to calculate the specific force (mN/mm^2).

p16-3MR Renilla luciferase reporter assay

In vivo Renilla luciferase activity was measured in TA, quadriceps (QA), and gastrocnemius (GC) muscles from p16-3MR mice. Anaesthetized mice were injected intramuscularly with coelenterazine H (PerkinElmer, #760506) and immediately subjected to measure with the IVIS Lumina III (PerkinElmer). *In vitro*, Renilla luciferase activity was measured from the cryopreserved diaphragm and TA muscles using the Dual-Luciferase Reporter Assay Kit (Promega Corporation, #E1910). Signal was measured with the luminometer Centro LB 960 (Berthold Technologies GmbH & Co. KG) and values were normalized to total protein extracted measured by Bradford method (Protein Assay, Bio-Rad, #500-0006) and damaged area measured after H&E staining.

Cell isolation by flow cytometry

Muscles were mechanically disaggregated and incubated in Dulbecco's Modified Eagle's medium (DMEM) containing liberase (Roche, #177246) and dispase (Gibco, #17105-041) at 37°C with agitation for 1-2 hours. When required, SPiDER-β-gal reagent (Dojindo, #SG02; 1 μM) was added during the second hour. The supernatant was then filtered and cells were incubated in lysis buffer (BD Pharm Lyse, #555899) for 10 min on ice and resuspended in PBS with 2.5% foetal bovine serum (FBS). MCs were isolated as CD45$^+$ and F4/80$^+$, SCs as α7-integrin$^+$, CD45$^-$, F4/80$^-$ and CD31$^-$ and FAPs as Sca-1$^+$, CD45$^-$, F4/80$^-$, α7-integrin$^-$ and CD31$^-$. SPiDER-β-gal was employed to isolate SPiDER$^+$ from SPiDER$^-$ of each cell type (see Figure 18 for gating strategy). Cells were sorted using a FACS Aria II (BD).

Table 2. List of antibodies employed for FACS.

Antibody	Dilution	Brand	Reference number
BV711-conjugated anti-CD45	1/200	BD	#563709
APC-Cy7-conjugated anti- F4/80	1/200	Biolegend	#123118
PE-conjugated anti-α7-integrin	1/200	Ablab	#AB10STMW215
APC-conjugated anti-CD31	1/200	eBioscience	#17-0311-82
PE-Cy7-conjugated anti-Sca-1	1/200	Biolegend	#108114
PE-Cy7-conjugated anti-CD45	1/200	Biolegend	#103114
PE-Cy7-conjugated anti-CD31	1/200	Biolegend	#102418
APC-conjugated anti-Sca-1	1/200	Biolegend	#108111

To isolate ROS^{High} and ROS^{Low} populations, the digested muscle was stained with CellRox Green reagent (Invitrogen, #C10444; 5 μM) according to manufacturer's protocol and a mix of antibodies to separate SCs (α7-integrin^{+}, CD45^{-} and CD31^{-}) and FAPs (Sca-1^{+}, CD45^{-}, α7-integrin^{-} and CD31^{-}) (Figure 47). CellRox^{High} and CellRox^{Low} cells were sorted using a FACS Aria II (BD). Isolated cells were used for cell cultures and proliferation assays.

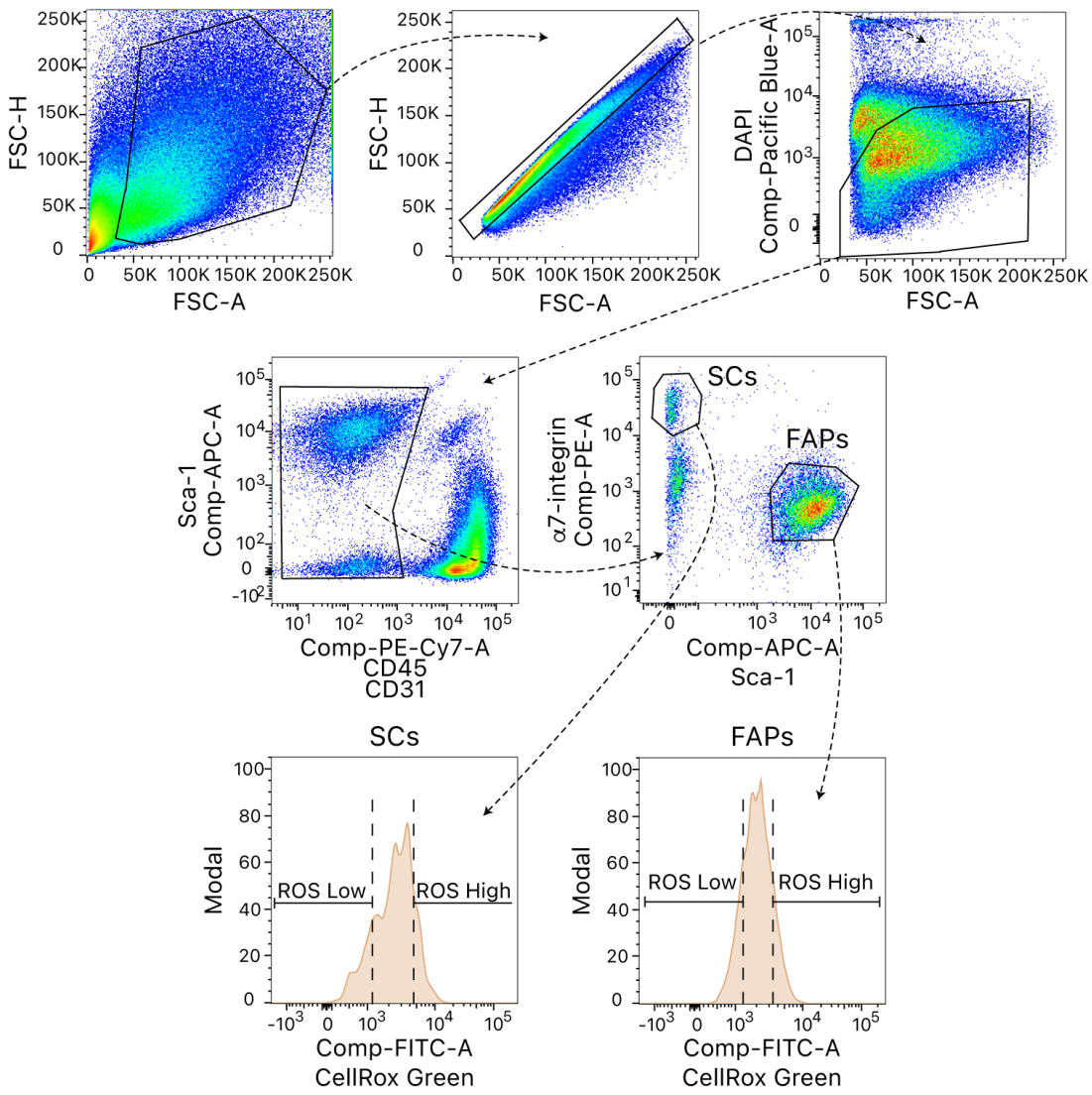

Figure 47. Gating strategy employed for ROS^{High} and ROS^{Low} isolation of SCs and FAPs.

Isolated cells were used either for RNA extraction, cell cultures, engraftments, proliferation assays or plated on glass slides (Thermo Scientific, #177402) for immunostaining and SA-β-gal analysis.

Senescent cells transplantation

Cells transplants were performed as previously described[91]. FACS-isolated SPiDER^{+} and SPiDER^{-} cells were collected, resuspended in 20% FBS DMEM medium, labelled with Vybrant Dil Cell Labelling solution (Invitrogen, #V22889) according to manufacturer instructions, and injected into TA muscles of uninjured or previously injured with the freeze crush method two days before recipient mice[272]. The cell-type proportions of MCs, SCs, and FAPs were controlled in the transplanted SPiDER^{+} and SPiDER^{-} populations. Each TA muscle was engrafted with 10.000 cells, except when each senescent cell type was transplanted separately, where 5.000 cells were engrafted. Engrafted muscles were collected and processed for muscle histology 4 days after cell transplantation.

RNA interference

Freshly sorted cells or C2C12 cells were transfected with siRNA targeting *Cd36* (On-Target plus SmartPool, Dharmacon, #L-062017-00-0005; 5 nM) or unrelated sequence as control (On-Target plus non-targeting siRNA Pool, Dharmacon, #D-001810-10-05; 5 nM) using the DharmaFect protocol (Dharmacon, #T-2003-02). Target sequences for Cd36 siRNA were:
5′-CCACAUAUCUACCAAAAUU-3′, 5′-GAAAGGAUAACAUAAGCAA -3′,
5′-AUACAGAGUUCGUUAUCUA-3′, 5′-GGAUUGGAGUGGUGAUGUU-3′.
Freshly sorted cells were incubated with siRNAs for three hours, washed and engrafted.

Cytokine array

Cytokine antibody arrays (R&D Systems, #ARY028; Abcam, #ab193659) were used according to the manufacturer's protocol. For cells, freshly sorted cells were cultured for 24h in serum-free DMEM. Cell culture supernatants were collected, centrifuged, and incubated with the membranes precoated with captured antibodies. For tissue interstitial fluid, skeletal muscles of mice were dissected and slowly injected with a PBS solution with a Complete Mini EDTA-free protease inhibitor cocktail (Roche, #11836170001). The PBS exudate was then recovered centrifuged and incubated with the membranes precoated with captured antibodies. Then membranes were incubated with detection antibodies, streptavidin-HRP, and Chemi Reagent Mix. The immunoblot images were captured and visualized using the Chemidoc MP Imaging System (Bio-Rad, Hercules, USA)

and the intensity of each spot in the captured images was analysed using the publicly available ImageJ software.

Proliferation assays

To assess proliferation *in vivo*, muscles were injured by local CTX injection, and mice were administered with ethynyl-labelled deoxyuridine (EdU, Invitrogen, #A10044; 25.5 mg/kg; i.p.) two hours before the sacrifice at 4 DPI. Muscles were collected and processed for immunofluorescence staining in tissue slides or cell isolation by FACS. EdU-labelled cells were detected using the Click-iT EdU Imaging Kit (Invitrogen, #C10086). EdU-positive cells were quantified as the percentage of the total number of cells analysed. *In vitro* proliferation was quantified on freshly sorted SCs, seeded in 20% FBS Ham's F10 medium supplemented with bFGF (Peprotech, #100-18B-250UG; 2.5 ng/ml) in collagen-coated plates. After 3 days of culture, SCs were pulse-labelled with bromodeoxyuridine (BrdU, Sigma-Aldrich, #B9285-1G; 1.5 μg/ml) for 1 h. BrdU-labelled cells were detected by immunostaining using rat anti-BrdU antibody (Abcam, #AB6326; 1:500) and a specific secondary biotinylated donkey anti-rat antibody (Jackson Inmunoresearch, #712-066-150; 1:250). Antibody binding was visualized using Vectastain Elite ABC reagent (Vector Laboratories, #PK-6100) and 3,3′-Diaminobenzidine (DAB). BrdU-positive cells were quantified as the percentage of the total number of cells analysed.

Transwell assay

SCs were freshly isolated from regenerating muscle tissue at 3 DPI and plated on 24-well plates (Falcon, #353047) in 20% FBS DMEM supplemented with b-FGF. Subsequently, medium or freshly sorted SPiDER^{+} and SPiDER^{-} cell populations (Fig. 5i) or etoposide-induced senescent C2C12 cells were seeded on 0.4 μm pore size cell culture insert (Falcon, #353495) using the same medium. After 3 days of culture, a proliferation assay was performed on SCs with BrdU labelling as described above.

***In vitro* treatments**

ROS^{High} and ROS^{Low} SCs and FAPs were freshly isolated from regenerating muscle at 24 hours post-injury, seeded, and cultured in presence of NAC (10 mM) or vehicle for 3 days. After the treatment, cells were fixed and further processed for staining. C2C12 cells maintained in 10% FBS DMEM, were treated with etoposide

(Sigma-Aldrich, #E1383, 1 μM) for 5 days to induce senescence and collected for RNA extraction and RT-qPCR. Cells were stained with β-galactosidase staining kit (as described below) to confirm their senescent state.

Cell staining

SA-β-galactosidase (SA-β-gal) activity was detected in freshly sorted cells and cell cultures using the senescence β-galactosidase staining kit (Cell signalling, #9860), according to the manufacturer's instructions. Lipid droplets were stained with Oil Red O (Sigma-Aldrich, #O0625) according to manufacturer instructions. ROS levels were measured by immunofluorescence using CellRox Green reagent (Invitrogen, #C10444; 5 μM) according to instructions. TUNEL assay was performed with In Situ Cell Death Detection Kit, Fluorescein (Roche, #11684795910), cells treated with DNase were employed as a positive control of the staining according to the manufacturer's description. ImageJ software was used to perform image analysis.

Muscle histology, immunofluorescence, and immunoFISH

Muscles were embedded in OCT solution (TissueTek, #4583), frozen in isopentane cooled with liquid nitrogen, and stored at -80 °C until analysis. 10 μm muscle cryosections were collected and stained for SA-β-gal, H&E, Sirius Red or used for immunofluorescence (Table 3).

- Haematoxylin & Eosin (H&E, Sigma-Aldrich, #HHS80 and #45235). Briefly, slides were immersed in haematoxylin solution and then washed with tap water. Following, the slides were rapidly submerged in acid ethanol 2 times, and then in eosin. The slides were dehydrated with ethanol, put in xylol and mounted.
- Sirius Red (Sigma-Aldrich #365548). Briefly, sections were covered with Bouin solution o/n. Next, the sections were washed with tap water for 5 minutes, and then incubated with a picric acid solution (90mL of saturated picric acid + 10mL of 1% direct red80 diluted in water). After that, the slides were washed rapidly in 2% acetic acid and dehydrated with ethanol. Finally, they were cleared with xylol and mounted.
- eMHC staining. Briefly, sections were treated with 3% of H_2O_2 for 30 minutes to inactivate endogenous peroxidase. Then, they were washed with PBS and blocked with MOM blocking solution (Vector #MKB-2213) for 1 hour at RT. Next, the slides were incubated with an anti-eMHC antibody at 4°C o/n. After that,

slides were washed with PBS and covered with a biotinylated secondary antibody for 30 minutes at RT. Then, slides were embedded in a solution of avidin-biotin complex (Vector, #PK-6100) for 30 minutes at RT, and incubated with DAB solution until optimal reaction. Finally, slides were dehydrated with increasing concentrations of ethanol and mounted in DPX.

- SA-β-gal staining. The slides were fixed with 4% paraformaldehyde (PFA) and 0.2% glutaraldehyde, washed with PBS and incubated with PBS (pH=6.0) for 1 hour at RT. Following, the sections were incubated with an X-gal-containing solution at pH=6.0 for 2 days at 37°C. After that, the sections were washed with PBS, re-fixed with 1% PFA for 30 minutes. Finally, the sections were washed and mounted with glycerol.

CSA on H&E and eMHC stained sections, percentage of muscle area positive for Sirius Red staining, and number of SA-β-gal^{+} were quantified using Image J software. Double immunofluorescence was performed by the sequential addition of each primary and secondary antibody using positive and negative controls. The sections were air-dried, fixed, washed on PBS, and incubated with primary antibodies (Table 3) according to the standard protocol after blocking with a high-protein-containing solution in PBS for 1h at room temperature. Subsequently, the slides were washed with PBS and incubated with the appropriate secondary antibodies and labelling dyes. Telomere immunoFISH was performed after γH2Ax immunofluorescence staining with Telomeric PNA probe (Panagene, #F1002-5) as described[273].

Table 3. Antibodies used in this study.

Antibody	Brand	Reference	Dilution
nGFP	Invitrogen	#A6455	1:400
eMHC	DSHB	#F1.652	Ready to use
p16^{INK4a}	Invitrogen	#MA5-17142	1:100
TCF4	Cell Signalling	#2569S	1:80
CD11b	eBioscience	#14-0112-85	1:100
Lamin B1	Abcam	#ab16048-100	1:100
CD36	Invitrogen	#MA5-14112	1:100
γH2Ax	Cell Signalling	#2577S	1:50
Pax7	Abcam	#ab34360	1:20
Ki67	Abcam	#ab15580	1:100

Digital image acquisition

Digital images were acquired using: an upright DMR6000B microscope (Leica) with a DFC550 camera for immunohistochemical colour pictures; a Thunder imager 3D live-cell microscope (Leica Microsystems) with AFC (hardware autofocus control) and a Leica DFC9000 GTC sCMOS camera, using HC PL FLUOTAR ×10/0.32 PH1 ∞/0.17/ON257C and HC PL FLUOTAR ×20/0.4 CORR PH1 ∞/0-2/ON25/C objectives; a Zeiss Cell Observer HS with a ×20 and x40 air objective and Zeiss AxioCam MrX camera; and a Leica SP5 confocal laser-scanning microscope with HCX PL Fluotar ×40/0.75 and ×63/0.75 objectives; the different fluorophores (three or four) were excited using the 405, 488, 568 and 633 nm excitation-lines. The acquisition was performed using the Leica Application v3.0 or LAS X v1.0 software (Leica) or Zeiss LSM software Zen 2 Blue.

RNA isolation and RT-qPCR

Total RNA was isolated from snap-frozen muscles or cells using miRNAeasy Mini Kit (Qiagen, #1038703) and analysed by RT-qPCR. For qPCR experiments, DNase digestion of 10 mg of RNA was performed using 2U DNase (Qiagen, #1010395). Complementary DNA (cDNA) was synthesized from total RNA using the SuperScript™ III Reverse Transcriptase (Invitrogen, #18080-044). For gene expression analysis in freshly sorted SCs, FAPs and MCs, RNA extraction was performed with PicoPure kit (Thermo Scientific, #KIT0204) and cDNA was pre-amplified using the SsoAdvanced PreAmp Supermix (Biorad, #172-5160) following the manufacturer's instructions. Real-time PCR reactions were performed on a LightCycler 480 System using Light Cycler 480 SYBR Green I Master reaction mix (Roche Diagnostic Corporation, #12767000) and specific primers (Table 4). Thermocycling conditions were as follows: an initial step of 10 min at 95 °C, then 50 cycles of 15 s denaturation at 94 °C, 10 s annealing at 60 °C, and 15 s extension at 72 °C. Reactions were run in triplicate, and automatically detected threshold cycle values were compared between samples. Transcript of the Rpl7 housekeeping gene was used as endogenous control, with each unknown sample normalized to Rpl7 content.

Table 4. Primers used in this study.

Gene	Forward	Reverse
$p16^{INK4a}$	5′-CATCTGGAGCAGCATGGAGTC-3′	5′-ATCATCATCACCTGAATCGGGG-3′
mRFP	5′-GACCTCGGCGTCGTAGTG-3′	5′-AAGGGCGAGATCAAGATGAG-3′
$p19^{ARF}$	5′-TGAGGCTAGAGAGGATCTTGAGA-3′	5′-GCAGAAGAGCTGCTACGTGAA-3′
$P21^{CIP1}$	5′-CCAGGCCAAGATGGTGTCTT-3′	5′-TGAGAAAGGATCAGCCATTGC-3′
Il-6	5′-GGTGACAACCACGGCCTTCCC-3′	5′-AAGCCTCCGACTTGTGAAGTGGT- 3′
Il-1b	5′-CCAAAATACCTGTGGCCTTGG-3′	5′-GCTTGTGCTCTGCTTGTGAG-3′
PAI-1	5′-CCGATGGGCTCGAGTATGA-3′	5′-TTGTCTGATGAGTTCAGCATCCA-3′
TNFα	5′-CGCTCTTCTGTCTACTGAACTT-3′	5′-GATGAGAGGGAGGCCATT-3′
IFNγ	5′-AGCGGCTGACTGAACTCAGATTGTAG-3′	5′-GTCACAGTTTTCAGCTGTATAGGG-3′
Il-12	5′-TCCAGCGCAAGAAAGAAAA-3′	5′-AATAGCGATCCTGAGCTTGC-3′
Ccl12	5′-CCCACTCACCTGCTGCTACT-3′	5′-TCTGGACCCATTCCTTCTTG-3′
Il-18	5′-CTGGCTGTGACCCTCTCTGT-3′	5′-ATCTTCCTTTTGGCAAGCAA-3′
Ccl2	5′- CACTCACCTGCTGCTACTCA-3′	5′-GAGCTTGGTGACAAAAACTACAGC-3′
Ccl8	5′-ACGCTAGCCTTCACTCCAAA-3′	5′-GTGACTGGAGCCTTATCTGG-3′
Cxcl10	5′-TGCCCACGTGTTGAGATCAT-3′	5′-AAGGAGCCCTTTTAGACCTTTT-3′
Apoe	5′-CTCCCAAGTCACACAAGAACTG-3′	5′-CCAGCTCCTTTTTGTAAGCCTTT-3′
Igfbp4	5′-TGAGAGCGAACATCCCAACAA-3′	5′-TGTCCCCACGATCTTCATCTT-3′
Igfbp7	5′-TGCGAGCAAGGGTCTCTGAT-3′	5′-GTTGGGATCCCGATGACCTC-3′
Col3a1	5′-TGACTGTCCCACGTAAGCAC-3′	5′-GAGGGCCATAGCTGAACTGA-3′
Col6a3	5′-CCAACAGCATGGAGTCATGG-3′	5′-GCATTGAAGTTGGATGGCCC-3′
Timp2	5′-TGCAATGCAGACGTAGTGAT-3′	5′-ATAGATGTCATTCCCGGAAT-3′
Rpl7	5 ′-GAAGCTCATCTATGAGAAGGC-3′	5 ′-AAGACGAAGGAGCTGCAGAAC-3′

RNA-seq sample and library preparation

Sequencing libraries were prepared directly from the lysed cells, without a previous RNA extraction step. RNA reverse transcription and cDNA amplification were held using the SMART-Seq v4 Ultra Low Input RNA Kit for Sequencing from Clontech Takara. The Illumina "Nextera XT" kit is used for the preparation of the libraries from the amplified cDNA. Libraries were sequenced by the Illumina HiSeq 2500 sequencer (51 bp read length, single-end, ~20M reads).

Bulk RNA-seq Data Pre-processing

Sequencing reads were pre-processed employing the nf-core/rnaseq 1.2 pipeline. Read quality was assessed by FastQC 0.11.8. Trim Galore 0.5.0 was used to trim sequencing reads, eliminating Illumina adaptor remains, and discard reads that were shorter than 20 bp. The resulting reads were mapped onto the mouse genome (GRCm38, release 81) using HiSAT2 2.1.0 and quantified using featureCounts 1.6.2. Reads per kilobase per million mapped reads (RPKM) and transcripts per million (TPM) gene expression values were calculated from the trimmed mean of

M-values (TMM)-normalized counts per million (CPM) values using Bioconductor package edgeR 3.30.0 and R 4.0.0. Differential gene expression analysis and PCA were performed using Bioconductor package DESeq2 1.28.1. Variance-stabilizing transformation of count data was applied to visualize the sample-to-sample distances in PCA. Genes were considered as differentially expressed if showed an adjusted p-value < 0.05.

Single-cell RNA-sequencing and analysis

scRNA-sequencing was performed using the Chromium Single Cell 3′ GEM, Library & Gel Bead Kit v3, 16 rxns (10X genomics, #PN-1000075), following the manufacturer's instruction and targeting a recovery of 5,000 cells/dataset. Each dataset was obtained with a sample size of 2 mice replicates. Libraries were constructed as instructed in the manufacturer's protocol and sequenced using the MGI DNBSEQ-Tx sequencer platform. The average read depth across the samples was 15551/cell. Sequencing reads were processed with STARsolo 2.7.3a using the mouse reference genome mm10 (GENCODE vM23).

From the filtered barcode and count matrices downstream analysis was carried out with R version 4.0.3 (12-10-2020). Quality control, filtering, data clustering and visualization, and the differential expression analysis was carried out using Seurat version 4.0.3 and DoubletFinder version 2.0 R packages [Hao, 2021 #220;McGinnis, 2019 #221]. Datasets were processed following Seurat standard integration protocol as per tutorial instructions. Genes expressed in less than 3 cells and cells with fewer than 500 features, less than 2000 transcripts and more than 20% reads mapping to mitochondrial genes as well as cells identified as doublets by DoubletFinder were removed. PCA was performed for dimensionality reduction and the first 30 components were used for UMAP embedding and clustering.

Functional profiling of cell subpopulations

Functional enrichment analysis of the subsets of differentially expressed genes was performed using g:Profiler web server with g:SCS significance threshold, "Only annotated" statistical domain scope and canonical pathway KEGG, Reactome, and Wiki Pathways sets. For each gene subset, the top five significant gene sets were selected for representation.

Gene Set Enrichment Analysis (GSEA)

RPKM matrix after removal of low count genes (edgeR 3.30.0) served as an input for GSEA 4.0.3 software. We used the signal-to-noise metric to rank the genes, 1000 permutations with the gene set permutation type, and weighted enrichment statistics. Gene set sizes were chosen as 15-500 for MSigDB 7.0 Gene Ontology biological processes (GO:BP) and 10-1000 for MSigDB 7.0 canonical pathways (BioCarta, KEGG, PID, Reactome, and WikiPathways). Gene sets passing false discovery rate (FDR) < 0.25 threshold were subjected to further analysis. Network representation and clustering of GSEA results were performed using EnrichmentMap 3.2.1 and AutoAnnotate 1.3.2 for Cytoscape 3.7.2 with the Jaccard coefficient set to 0.25.

Functional profiling of SASP

We checked whether upregulated genes (DESeq2 adjusted p-value < 0.05 and log2FoldChange > 0) from each Sen_vs_NSen comparison can be expressed in a form of secreted proteins by combining the evidence from multiple data sources: Gene Ontology cellular component (GO:CC), Uniprot, VerSeDa, Human Protein Atlas and experimental data reporting SASP[143,274]. The genes, which occur to be extracellular (GO:CC) and/or secreted (other sources) with evidence from at least 1 source were included in the final list of SASP genes (1912 in total). Functional enrichment analysis was performed using g:Profiler web server with g:SCS significance threshold, "Only annotated" statistical domain scope, and canonical pathway sets from KEGG, Reactome, and Wiki Pathways. Gene sets passing FDR<0.05 threshold were subjected to further analysis. Network representation and clustering of g:Profiler results were performed using EnrichmentMap 3.2.1 and AutoAnnotate 1.3.2 for Cytoscape 3.7.2 with the Jaccard coefficient set to 0.25.

Comparative enrichment analysis of senescent cells and previously published ageing datasets

We used the minimum hypergeometric test implemented in R package mHG 1.1 for the comparative enrichment analysis of senescent cells and previously published ageing datasets: mouse[253], rat (GSE53960), African turquoise killifish (GSE69122), and human (GTEx v6p). Data processing and analysis were performed as described before[253] with the following modifications: (1) to assess the differential expression for rat, killifish, and human datasets the DESeq2 1.28.1 package version was used (instead of DESeq2 1.6.3), (2) both genders were analysed for human dataset, (3)

conversion to human orthologs was performed before the enrichment with MSigDB 5.1 hallmarks for all datasets except the Brunet's mouse tissues, for which we took previously published enrichment results[253].

Transcription factor analysis and activity prediction

For the analysis of transcription regulation we combined the results of several methods: (1) motif enrichment analysis of differentially expressed genes with TRANSFAC_and_JASPAR_PWMs and ENCODE_and_ChEA_Consensus_TFs_from _ChIP-X libraries using R package EnrichR 2.1; (2) Upstream Regulator Analysis of differentially expressed genes using the commercial QIAGEN's Ingenuity Pathway Analysis (IPA, QIAGEN Aarhus, Denmark) software; (3) analysis of transcription regulators differential expression using DESeq2 1.28.1.

Functional profiling of transcription factor target gene regulation

For each transcription factor, we merged the target genes from EnrichR and IPA results split them into upregulated and downregulated, and subjected them to functional enrichment analysis of canonical pathways (KEGG, Reactome) and GO:BP using R package gprofiler2 0.1.9 with the following parameters: correction method "FDR", "custom_annotated" domain score consisting of target genes for all studied transcription factors. Electronic GO annotations were excluded. Gene sets passing FDR < 0.05 threshold were subjected for further analysis. For GO:BP we selected the ones having term size > 15 and < 500 genes.

For functional profiling, we took the clusters of gene sets created using AutoAnnotate Cytoscape App based on GSEA results. We retained all the terms present in these clusters and extended the lists with terms from gprofiler2 enrichment results, adding them by semantic and functional similarity. As result we had a library of terms grouped by clusters, which allowed us to match them with gprofiler2 results and, thus, to map transcription factors to main functional clusters from GSEA/Cytoscape analysis.

Functional profiling of transcriptional regulation of SASP

For each transcription factor upregulated target genes from EnrichR and IPA results were merged and intersected with the list of SASP genes. For SASP genes we extracted Gene Ontology molecular function (GO:MF) terms, clustered them into 12 categories ("Adhesion molecule", "Chemokine", "Complement component", "Cytokine", "Enzyme", "Enzyme regulator", "Extracellular matrix constituent",

"Growth factor", "Hormone", "Ligand", "Proteinase" and "Receptor") and estimated the enrichment of GO:MF clusters with a hypergeometric test using R function "phyper". Correction for multiple comparisons was performed using the Benjamini-Hochberg procedure.

Analysis of lipid metabolism gene set

For the analysis of lipid metabolism, we constructed a gene set using data from multiple sources: KEGG pathway maps ("Fatty acid degradation", "Cholesterol metabolism", "Regulation of lipolysis in adipocytes"), WikiPathways ("Fatty acid oxidation", "Fatty Acid Beta Oxidation", "Mitochondrial LC-Fatty Acid Beta-Oxidation", "Fatty Acid Omega Oxidation", "Fatty Acid Biosynthesis", "Triacylglyceride Synthesis", "Sphingolipid Metabolism (general overview)", "Sphingolipid Metabolism (integrated pathway)", "Cholesterol metabolism (includes both Bloch and Kandutsch-Russell pathways)", "Cholesterol Biosynthesis"), literature research[275–277]. We further estimated the expression of these genes by filtering DESeq2 results (adjusted p-value < 0.05 in at least 3 out of 12 comparisons) and extracted log2FoldChange values to plot the difference in expression between senescent and non-senescent cells.

Reconstruction of ligand-receptor mediated cell-cell communication networks and downstream analysis

For reconstructing cell-cell communication networks, we modified a previously published single-cell-based method, FunRes, to account for bulk gene expression profiles[254]. For the functional profiling, we selected ligand-receptor interactions between three senescent cell populations (SCs, FAPs, and MCs) and the non-senescent SC population in geriatric mice at 3 DPI. We used Bioconductor package SPIA 2.40.0 with a reduced set of non-disease KEGG pathways maps to evaluate the activity of pathways downstream ligand-receptor interactions. For each interaction differentially expressed target TFs in non-senescent SC were split into upregulated and downregulated in comparison with senescent SCs. As a reference set of genes, we took a list of target TFs from all the interactions studied. SPIA analysis was performed with 2000 permutations, pPERT and pNDE were combined with Fisher's product method. Pathways were considered as significantly enriched if passing a pGFdr < 0.05 threshold. For each pathway, we calculated the ratio of ligand-receptor interactions that activate or inhibit the pathway to the total number

of interactions analysed. For results representation, we selected 8 activated and 8 inhibited pathways with the highest ratio of interactions.

Statistical analysis

The sample size of each experimental group is described in the corresponding figure caption, and all the experiments were conducted with at least three biological replicates unless otherwise indicated. GraphPad Prism software was used for all statistical analyses except for sequencing-data analysis. Quantitative data displayed as histograms are expressed as mean ± standard error of the mean (represented as error bars). Results from each group were averaged and used to calculate descriptive statistics. Mann–Whitney test (independent samples, two-tailed) was used for comparisons between groups unless otherwise indicated. Statistical significance was set at a P-value <0.05.

REFERENCES

1. Janssen, I., Heymsfield, S. B., Wang, Z. M. & Ross, R. Skeletal muscle mass and distribution in 468 men and women aged 18-88 yr. *J. Appl. Physiol.* (2000) doi:10.1152/jappl.2000.89.1.81.
2. Frontera, W. R. & Ochala, J. Skeletal Muscle: A Brief Review of Structure and Function. *Behavior Genetics* (2015) doi:10.1007/s00223-014-9915-y.
3. Karagounis, L. G. & Hawley, J. A. Skeletal muscle: Increasing the size of the locomotor cell. *International Journal of Biochemistry and Cell Biology* (2010) doi:10.1016/j.biocel.2010.05.013.
4. Flück, M. & Hoppeler, H. Molecular basis of skeletal muscle plasticity--from gene to form and function. *Reviews of physiology, biochemistry and pharmacology* (2003) doi:10.1007/s10254-002-0004-7.
5. Wolfe, R. R. The underappreciated role of muscle in health and disease. *American Journal of Clinical Nutrition* (2006) doi:10.1093/ajcn/84.3.475.
6. Yin, H., Price, F. & Rudnicki, M. A. Satellite cells and the muscle stem cell niche. *Physiol. Rev.* (2013) doi:10.1152/physrev.00043.2011.
7. Cornelison, D. D. W. & Perdiguero, E. Muscle Stem Cells: A Model System for Adult Stem Cell Biology BT - Muscle Stem Cells: Methods and Protocols. in (eds. Perdiguero, E. & Cornelison, D. D. W.) 3–19 (Springer New York, 2017). doi:10.1007/978-1-4939-6771-1_1.
8. Järvinen, T. A. H., Järvinen, T. L. N., Kääriäinen, M., Kalimo, H. & Järvinen, M. Muscle injuries: Biology and treatment. *American Journal of Sports Medicine* (2005) doi:10.1177/0363546505274714.
9. Dumont, N. A., Bentzinger, C. F., Sincennes, M. C. & Rudnicki, M. A. Satellite cells and skeletal muscle regeneration. *Compr. Physiol.* (2015) doi:10.1002/cphy.c140068.
10. Mintz, B. & Baker, W. W. Normal mammalian muscle differentiation and gene control of isocitrate dehydrogenase synthesis. *Proc. Natl. Acad. Sci. U. S. A.* (1967) doi:10.1073/pnas.58.2.592.
11. Giordani, L. *et al.* High-Dimensional Single-Cell Cartography Reveals Novel Skeletal Muscle-Resident Cell Populations. *Mol. Cell* (2019) doi:10.1016/j.molcel.2019.02.026.
12. Oprescu, S. N., Yue, F. & Kuang, S. Single-Cell Isolation from Regenerating Murine Muscles for RNA-Sequencing Analysis. *STAR Protoc.* (2020) doi:10.1016/j.xpro.2020.100051.
13. De Micheli, A. J. *et al.* Single-Cell Analysis of the Muscle Stem Cell Hierarchy Identifies Heterotypic Communication Signals Involved in Skeletal Muscle Regeneration. *Cell Rep.* (2020) doi:10.1016/j.celrep.2020.02.067.
14. Rubenstein, A. B. *et al.* Single-cell transcriptional profiles in human skeletal muscle.

Sci. Rep. (2020) doi:10.1038/s41598-019-57110-6.

15. Petrilli, L. L. *et al.* High-Dimensional Single-Cell Quantitative Profiling of Skeletal Muscle Cell Population Dynamics during Regeneration. *Cells* (2020) doi:10.3390/cells9071723.
16. Dell'Orso, S. *et al.* Single cell analysis of adult mouse skeletal muscle stem cells in homeostatic and regenerative conditions. *Dev.* (2019) doi:10.1242/dev.174177.
17. Sousa-Victor, P., García-Prat, L. & Muñoz-Cánoves, P. Control of satellite cell function in muscle regeneration and its disruption in ageing. *Nature Reviews Molecular Cell Biology* (2022) doi:10.1038/s41580-021-00421-2.
18. Mukund, K. & Subramaniam, S. Skeletal muscle: A review of molecular structure and function, in health and disease. *Wiley Interdisciplinary Reviews: Systems Biology and Medicine* (2020) doi:10.1002/wsbm.1462.
19. Bentzinger, C. F., Wang, Y. X., Dumont, N. A. & Rudnicki, M. A. Cellular dynamics in the muscle satellite cell niche. *EMBO Reports* (2013) doi:10.1038/embor.2013.182.
20. Forcina, L., Cosentino, M. & Musarò, A. Mechanisms Regulating Muscle Regeneration: Insights into the Interrelated and Time-Dependent Phases of Tissue Healing. *Cells* (2020) doi:10.3390/cells9051297.
21. Arnold, L. *et al.* Inflammatory monocytes recruited after skeletal muscle injury switch into antiinflammatory macrophages to support myogenesis. *J. Exp. Med.* (2007) doi:10.1084/jem.20070075.
22. Sartorelli, V. & Juan, A. H. *Sculpting chromatin beyond the double helix: Epigenetic control of skeletal myogenesis*. *Current Topics in Developmental Biology* (2011). doi:10.1016/B978-0-12-385940-2.00003-6.
23. Maesner, C. C., Almada, A. E. & Wagers, A. J. Established cell surface markers efficiently isolate highly overlapping populations of skeletal muscle satellite cells by fluorescence-activated cell sorting. *Skeletal Muscle* (2016) doi:10.1186/s13395-016-0106-6.
24. Roman, W. *et al.* Muscle repair after physiological damage relies on nuclear migration for cellular reconstruction. *Science (80-.).* (2021) doi:10.1126/science.abe5620.
25. Scharner, J. & Zammit, P. S. The muscle satellite cell at 50: The formative years. *Skeletal Muscle* (2011) doi:10.1186/2044-5040-1-28.
26. MAURO, A. Satellite cell of skeletal muscle fibers. *J. Biophys. Biochem. Cytol.* (1961) doi:10.1083/jcb.9.2.493.
27. Tapscott, S. J. *et al.* MyoD1: A nuclear phosphoprotein requiring a Myc homology region to convert fibroblasts to myoblasts. *Science (80-.).* (1988) doi:10.1126/science.3175662.
28. Fong, A. P. & Tapscott, S. J. Skeletal muscle programming and re-programming. *Current Opinion in Genetics and Development* (2013)

doi:10.1016/j.gde.2013.05.002.

29. Puri, P. L. & Sartorelli, V. Regulation of muscle regulatory factors by DNA-binding, interacting proteins, and post-transcriptional modifications. *Journal of Cellular Physiology* (2000) doi:10.1002/1097-4652(200011)185:2<155::AID-JCP1>3.0.CO;2-Z.
30. Rodgers, J. T. *et al.* MTORC1 controls the adaptive transition of quiescent stem cells from G 0 to GAlert. *Nature* (2014) doi:10.1038/nature13255.
31. Crist, C. G., Montarras, D. & Buckingham, M. Muscle satellite cells are primed for myogenesis but maintain quiescence with sequestration of Myf5 mRNA targeted by microRNA-31 in mRNP granules. *Cell Stem Cell* (2012) doi:10.1016/j.stem.2012.03.011.
32. Segalés, J., Perdiguero, E. & Muñoz-Cánoves, P. Regulation of muscle stem cell functions: A focus on the p38 MAPK signaling pathway. *Frontiers in Cell and Developmental Biology* (2016) doi:10.3389/fcell.2016.00091.
33. Kuang, S., Kuroda, K., Le Grand, F. & Rudnicki, M. A. Asymmetric Self-Renewal and Commitment of Satellite Stem Cells in Muscle. *Cell* (2007) doi:10.1016/j.cell.2007.03.044.
34. Chang, N. C. *et al.* The Dystrophin Glycoprotein Complex Regulates the Epigenetic Activation of Muscle Stem Cell Commitment. *Cell Stem Cell* (2018) doi:10.1016/j.stem.2018.03.022.
35. Brack, A. S. & Rando, T. A. Tissue-specific stem cells: Lessons from the skeletal muscle satellite cell. *Cell Stem Cell* (2012) doi:10.1016/j.stem.2012.04.001.
36. Wang, Y. X., Dumont, N. A. & Rudnicki, M. A. Muscle stem cells at a glance. *J. Cell Sci.* (2014) doi:10.1242/jcs.151209.
37. Chal, J. & Pourquié, O. Making muscle: Skeletal myogenesis in vivo and in vitro. *Development (Cambridge)* (2017) doi:10.1242/dev.151035.
38. Liu, N. *et al.* A Twist2-dependent progenitor cell contributes to adult skeletal muscle. *Nat. Cell Biol.* (2017) doi:10.1038/ncb3477.
39. Mitchell, K. J. *et al.* Identification and characterization of a non-satellite cell muscle resident progenitor during postnatal development. *Nat. Cell Biol.* (2010) doi:10.1038/ncb2025.
40. Dellavalle, A. *et al.* Pericytes of human skeletal muscle are myogenic precursors distinct from satellite cells. *Nat. Cell Biol.* (2007) doi:10.1038/ncb1542.
41. Sampaolesi, M. *et al.* Cell therapy of α-sarcoglycan null dystrophic mice through intra-arterial delivery of mesoangioblasts. *Science (80-.).* (2003) doi:10.1126/science.1082254.
42. Fry, C. S. *et al.* Inducible depletion of satellite cells in adult, sedentary mice impairs muscle regenerative capacity without affecting sarcopenia. *Nat. Med.* (2015) doi:10.1038/nm.3710.

43. Lepper, C., Partridge, T. A. & Fan, C. M. An absolute requirement for pax7-positive satellite cells in acute injury-induced skeletal muscle regeneration. *Development* (2011) doi:10.1242/dev.067595.
44. Sambasivan, R. *et al.* Pax7-expressing satellite cells are indispensable for adult skeletal muscle regeneration. *Development* (2011) doi:10.1242/dev.067587.
45. Murphy, M. M., Lawson, J. A., Mathew, S. J., Hutcheson, D. A. & Kardon, G. Satellite cells, connective tissue fibroblasts and their interactions are crucial for muscle regeneration. *Development* (2011) doi:10.1242/dev.064162.
46. Roh, J. S. & Sohn, D. H. Damage-associated molecular patterns in inflammatory diseases. *Immune Network* (2018) doi:10.4110/in.2018.18.e27.
47. Yang, W. & Hu, P. Skeletal muscle regeneration is modulated by inflammation. *Journal of Orthopaedic Translation* (2018) doi:10.1016/j.jot.2018.01.002.
48. Frenette, J., Cai, B. & Tidball, J. G. Complement activation promotes muscle inflammation during modified muscle use. *Am. J. Pathol.* (2000) doi:10.1016/S0002-9440(10)65081-X.
49. Kishimoto, T. K. & Rothlein, R. Integrins, ICAMs, and Selectins: Role and Regulation of Adhesion Molecules in Neutrophil Recruitment to Inflammatory Sites. *Adv. Pharmacol.* (1994) doi:10.1016/S1054-3589(08)60431-7.
50. Pizza, F. X., Peterson, J. M., Baas, J. H. & Koh, T. J. Neutrophils contribute to muscle injury and impair its resolution after lengthening contractions in mice. *J. Physiol.* (2005) doi:10.1113/jphysiol.2004.073965.
51. Dumont, N., Bouchard, P. & Frenette, J. Neutrophil-induced skeletal muscle damage: A calculated and controlled response following hindlimb unloading and reloading. *Am. J. Physiol. - Regul. Integr. Comp. Physiol.* (2008) doi:10.1152/ajpregu.90318.2008.
52. Tidball, J. G. Inflammatory processes in muscle injury and repair. *American Journal of Physiology - Regulatory Integrative and Comparative Physiology* (2005) doi:10.1152/ajpregu.00454.2004.
53. Chazaud, B. *et al.* Dual and beneficial roles of macrophages during skeletal muscle regeneration. *Exercise and Sport Sciences Reviews* (2009) doi:10.1097/JES.0b013e318190ebdb.
54. Villalta, S. A., Nguyen, H. X., Deng, B., Gotoh, T. & Tidbal, J. G. Shifts in macrophage phenotypes and macrophage competition for arginine metabolism affect the severity of muscle pathology in muscular dystrophy. *Hum. Mol. Genet.* (2009) doi:10.1093/hmg/ddn376.
55. Kastenschmidt, J. M., Avetyan, I. & Armando Villalta, S. Characterization of the inflammatory response in dystrophic muscle using flow cytometry. in *Methods in Molecular Biology* (2018). doi:10.1007/978-1-4939-7374-3_4.
56. Kratofil, R. M., Kubes, P. & Deniset, J. F. Monocyte conversion during inflammation

and injury. *Arteriosclerosis, Thrombosis, and Vascular Biology* (2017) doi:10.1161/ATVBAHA.116.308198.

57. Lu, H. *et al.* Macrophages recruited via CCR2 produce insulin-like growth factor-1 to repair acute skeletal muscle injury . *FASEB J.* (2011) doi:10.1096/fj.10-171579.
58. Segawa, M. *et al.* Suppression of macrophage functions impairs skeletal muscle regeneration with severe fibrosis. *Exp. Cell Res.* (2008) doi:10.1016/j.yexcr.2008.08.008.
59. Summan, M. *et al.* Macrophages and skeletal muscle regeneration: A clodronate-containing liposome depletion study. *Am. J. Physiol. - Regul. Integr. Comp. Physiol.* (2006) doi:10.1152/ajpregu.00465.2005.
60. Wosczyna, M. N. & Rando, T. A. A Muscle Stem Cell Support Group: Coordinated Cellular Responses in Muscle Regeneration. *Developmental Cell* (2018) doi:10.1016/j.devcel.2018.06.018.
61. Orekhov, A. N. *et al.* Monocyte differentiation and macrophage polarization. *Vessel Plus* (2019) doi:10.20517/2574-1209.2019.04.
62. Saclier, M. *et al.* Differentially activated macrophages orchestrate myogenic precursor cell fate during human skeletal muscle regeneration. *Stem Cells* (2013) doi:10.1002/stem.1288.
63. Deng, B., Wehling-Henricks, M., Villalta, S. A., Wang, Y. & Tidball, J. G. IL-10 Triggers Changes in Macrophage Phenotype That Promote Muscle Growth and Regeneration. *J. Immunol.* (2012) doi:10.4049/jimmunol.1103180.
64. Ruffell, D. *et al.* A CREB-C/EBPβ cascade induces M2 macrophage-specific gene expression and promotes muscle injury repair. *Proc. Natl. Acad. Sci. U. S. A.* (2009) doi:10.1073/pnas.0908641106.
65. Joe, A. W. B. *et al.* Muscle injury activates resident fibro/adipogenic progenitors that facilitate myogenesis. *Nat. Cell Biol.* (2010) doi:10.1038/ncb2015.
66. Uezumi, A., Fukada, S. I., Yamamoto, N., Takeda, S. & Tsuchida, K. Mesenchymal progenitors distinct from satellite cells contribute to ectopic fat cell formation in skeletal muscle. *Nat. Cell Biol.* (2010) doi:10.1038/ncb2014.
67. Wosczyna, M. N., Biswas, A. A., Cogswell, C. A. & Goldhamer, D. J. Multipotent progenitors resident in the skeletal muscle interstitium exhibit robust BMP-dependent osteogenic activity and mediate heterotopic ossification. *J. Bone Miner. Res.* (2012) doi:10.1002/jbmr.1562.
68. Lees-Shepard, J. B. *et al.* Activin-dependent signaling in fibro/adipogenic progenitors causes fibrodysplasia ossificans progressiva. *Nat. Commun.* (2018) doi:10.1038/s41467-018-02872-2.
69. Eisner, C. *et al.* Murine Tissue-Resident PDGFRα+ Fibro-Adipogenic Progenitors Spontaneously Acquire Osteogenic Phenotype in an Altered Inflammatory Environment. *J. Bone Miner. Res.* (2020) doi:10.1002/jbmr.4020.

70. Mutsaers, S. E., Bishop, J. E., McGrouther, G. & Laurent, G. J. Mechanisms of tissue repair: From wound healing to fibrosis. *Int. J. Biochem. Cell Biol.* (1997) doi:10.1016/S1357-2725(96)00115-X.
71. Kardon, G., Harfe, B. D. & Tabin, C. J. A Tcf4-positive mesodermal population provides a prepattern for vertebrate limb muscle patterning. *Dev. Cell* (2003) doi:10.1016/S1534-5807(03)00360-5.
72. Kopinke, D., Roberson, E. C. & Reiter, J. F. Ciliary Hedgehog Signaling Restricts Injury-Induced Adipogenesis. *Cell* (2017) doi:10.1016/j.cell.2017.06.035.
73. Lemos, D. R. *et al.* Nilotinib reduces muscle fibrosis in chronic muscle injury by promoting TNF-mediated apoptosis of fibro/adipogenic progenitors. *Nat. Med.* (2015) doi:10.1038/nm.3869.
74. Wosczyna, M. N. *et al.* Mesenchymal Stromal Cells Are Required for Regeneration and Homeostatic Maintenance of Skeletal Muscle. *Cell Rep.* (2019) doi:10.1016/j.celrep.2019.04.074.
75. Molina, T., Fabre, P. & Dumont, N. A. Fibro-adipogenic progenitors in skeletal muscle homeostasis, regeneration and diseases. *Open biology* (2021) doi:10.1098/rsob.210110.
76. Uezumi, A. *et al.* Mesenchymal Bmp3b expression maintains skeletal muscle integrity and decreases in age-related sarcopenia. *J. Clin. Invest.* (2021) doi:10.1172/JCI139617.
77. Malecova, B. *et al.* Dynamics of cellular states of fibro-adipogenic progenitors during myogenesis and muscular dystrophy. *Nat. Commun.* (2018) doi:10.1038/s41467-018-06068-6.
78. Lemos, D. R. *et al.* Functionally convergent white adipogenic progenitors of different lineages participate in a diffused system supporting tissue regeneration. *Stem Cells* (2012) doi:10.1002/stem.1082.
79. Cayrol, C. & Girard, J. P. IL-33: An alarmin cytokine with crucial roles in innate immunity, inflammation and allergy. *Current Opinion in Immunology* (2014) doi:10.1016/j.coi.2014.09.004.
80. Kuswanto, W. *et al.* Poor Repair of Skeletal Muscle in Aging Mice Reflects a Defect in Local, Interleukin-33-Dependent Accumulation of Regulatory T Cells. *Immunity* (2016) doi:10.1016/j.immuni.2016.01.009.
81. Heredia, J. E. *et al.* Type 2 innate signals stimulate fibro/adipogenic progenitors to facilitate muscle regeneration. *Cell* (2013) doi:10.1016/j.cell.2013.02.053.
82. Contreras, O. *et al.* Cross-talk between TGF-β and PDGFRα signaling pathways regulates the fate of stromal fibro-adipogenic progenitors. *J. Cell Sci.* (2019) doi:10.1242/jcs.232157.
83. Vumbaca, S. *et al.* Characterization of the skeletal muscle secretome reveals a role for extracellular vesicles and il1α/il1β in restricting fibro/adipogenic progenitor

adipogenesis. *Biomolecules* (2021) doi:10.3390/biom11081171.

84. Moratal, C. *et al.* IL-1β- and IL-4-polarized macrophages have opposite effects on adipogenesis of intramuscular fibro-adipogenic progenitors in humans. *Sci. Rep.* (2018) doi:10.1038/s41598-018-35429-w.
85. Fiore, D. *et al.* Pharmacological blockage of fibro/adipogenic progenitor expansion and suppression of regenerative fibrogenesis is associated with impaired skeletal muscle regeneration. *Stem Cell Res.* (2016) doi:10.1016/j.scr.2016.06.007.
86. Contreras, O., Soliman, H., Theret, M., Rossi, F. M. V. & Brandan, E. TGF-β-driven downregulation of the transcription factor TCF7L2 affects Wnt/β-catenin signaling in PDGFRα+ fibroblasts. *J. Cell Sci.* (2020) doi:10.1242/jcs.242297.
87. Álvarez, D. *et al.* IPF lung fibroblasts have a senescent phenotype. *Am. J. Physiol. - Lung Cell. Mol. Physiol.* (2017) doi:10.1152/ajplung.00220.2017.
88. García-Prat, L., Sousa-Victor, P. & Muñoz-Cánoves, P. Functional dysregulation of stem cells during aging: A focus on skeletal muscle stem cells. *FEBS Journal* (2013) doi:10.1111/febs.12221.
89. Shefer, G., Van de Mark, D. P., Richardson, J. B. & Yablonka-Reuveni, Z. Satellite-cell pool size does matter: Defining the myogenic potency of aging skeletal muscle. *Dev. Biol.* (2006) doi:10.1016/j.ydbio.2006.02.022.
90. Shefer, G., Rauner, G., Yablonka-Reuveni, Z. & Benayahu, D. Reduced satellite cell numbers and myogenic capacity in aging can be alleviated by endurance exercise. *PLoS One* (2010) doi:10.1371/journal.pone.0013307.
91. Sousa-Victor, P. *et al.* Geriatric muscle stem cells switch reversible quiescence into senescence. *Nature* **506**, 316–321 (2014).
92. Hasty, P., Campisi, J., Hoeijmakers, J., Van Steeg, H. & Vijg, J. Aging and genome maintenance: Lessons from the mouse? *Science* (2003) doi:10.1126/science.1079161.
93. Golden, T. R., Hinerfeld, D. A. & Melov, S. Oxidative stress and aging: beyond correlation. *Aging cell* (2002) doi:10.1046/j.1474-9728.2002.00015.x.
94. García-Prat, L. *et al.* Autophagy maintains stemness by preventing senescence. *Nature* (2016) doi:10.1038/nature16187.
95. Conboy, I. H., Conboy, M. J., Smythe, G. M. & Rando, T. A. Notch-Mediated Restoration of Regenerative Potential to Aged Muscle. *Science (80-.).* (2003) doi:10.1126/science.1087573.
96. Day, K., Shefer, G., Shearer, A. & Yablonka-Reuveni, Z. The depletion of skeletal muscle satellite cells with age is concomitant with reduced capacity of single progenitors to produce reserve progeny. *Dev. Biol.* (2010) doi:10.1016/j.ydbio.2010.01.006.
97. Fulle, S., Sancilio, S., Mancinelli, R., Gatta, V. & Di Pietro, R. Dual role of the caspase enzymes in satellite cells from aged and young subjects. *Cell Death Dis.* (2013)

doi:10.1038/cddis.2013.472.

98. Brack, A. S. *et al.* Increased Wnt signaling during aging alters muscle stem cell fate and increases fibrosis. *Science (80-.).* (2007) doi:10.1126/science.1144090.

99. Pessina, P. *et al.* Fibrogenic Cell Plasticity Blunts Tissue Regeneration and Aggravates Muscular Dystrophy. *Stem Cell Reports* (2015) doi:10.1016/j.stemcr.2015.04.007.

100. Biressi, S., Miyabara, E. H., Gopinath, S. D., Carlig, P. M. M. & Rando, T. A. A Wnt-TGF2 axis induces a fibrogenic program in muscle stem cells from dystrophic mice. *Sci. Transl. Med.* (2014) doi:10.1126/scitranslmed.3008411.

101. Chakkalakal, J. V., Jones, K. M., Basson, M. A. & Brack, A. S. The aged niche disrupts muscle stem cell quiescence. *Nature* (2012) doi:10.1038/nature11438.

102. Carlson, M. E., Hsu, M. & Conboy, I. M. Imbalance between pSmad3 and Notch induces CDK inhibitors in old muscle stem cells. *Nature* (2008) doi:10.1038/nature07034.

103. Liu, L. *et al.* Impaired Notch Signaling Leads to a Decrease in p53 Activity and Mitotic Catastrophe in Aged Muscle Stem Cells. *Cell Stem Cell* (2018) doi:10.1016/j.stem.2018.08.019.

104. Wang, Y., Welc, S. S., Wehling-Henricks, M. & Tidball, J. G. Myeloid cell-derived tumor necrosis factor-alpha promotes sarcopenia and regulates muscle cell fusion with aging muscle fibers. *Aging Cell* (2018) doi:10.1111/acel.12828.

105. Oh, J. *et al.* Age-associated NF-κB signaling in myofibers alters the satellite cell niche and re-strains muscle stem cell function. *Aging (Albany. NY).* (2016) doi:10.18632/aging.101098.

106. Lukjanenko, L. *et al.* Aging Disrupts Muscle Stem Cell Function by Impairing Matricellular WISP1 Secretion from Fibro-Adipogenic Progenitors. *Cell Stem Cell* (2019) doi:10.1016/j.stem.2018.12.014.

107. Schüler, S. C. *et al.* Extensive remodeling of the extracellular matrix during aging contributes to age-dependent impairments of muscle stem cell functionality. *Cell Rep.* (2021) doi:10.1016/j.celrep.2021.109223.

108. Wang, Y. *et al.* Aging of the immune system causes reductions in muscle stem cell populations, promotes their shift to a fibrogenic phenotype, and modulates sarcopenia. *FASEB J.* (2019) doi:10.1096/fj.201800973R.

109. Tobin, S. W. *et al.* Delineating the relationship between immune system aging and myogenesis in muscle repair. *Aging Cell* (2021) doi:10.1111/acel.13312.

110. Blanc, R. S. *et al.* Inhibition of inflammatory CCR2 signaling promotes aged muscle regeneration and strength recovery after injury. *Nat. Commun.* **11**, 4167 (2020).

111. Patsalos, A. *et al.* In vivo GDF3 administration abrogates aging related muscle regeneration delay following acute sterile injury. *Aging Cell* (2018) doi:10.1111/acel.12815.

112. Duan, D., Goemans, N., Takeda, S., Mercuri, E. & Aartsma-Rus, A. Duchenne muscular dystrophy. *Nature Reviews Disease Primers* (2021) doi:10.1038/s41572-021-00248-3.
113. Serrano, A. L. & Muñoz-Cánoves, P. Fibrosis development in early-onset muscular dystrophies: Mechanisms and translational implications. *Seminars in Cell and Developmental Biology* (2017) doi:10.1016/j.semcdb.2016.09.013.
114. Jejurikar, S. S. & Kuzon, W. M. Satellite cell depletion in degenerative skeletal muscle. *Apoptosis* (2003) doi:10.1023/A:1026127307457.
115. Dumont, N. A. *et al.* Dystrophin expression in muscle stem cells regulates their polarity and asymmetric division. *Nat. Med.* (2015) doi:10.1038/nm.3990.
116. Huang, P., Zhao, X. S., Fields, M., Ransohoff, R. M. & Zhou, L. Imatinib attenuates skeletal muscle dystrophy in mdx mice . *FASEB J.* (2009) doi:10.1096/fj.09-129833.
117. Gallardo, F. S., Córdova-Casanova, A. & Brandan, E. The linkage between inflammation and fibrosis in muscular dystrophies: The axis autotaxin–lysophosphatidic acid as a new therapeutic target? *Journal of Cell Communication and Signaling* (2021) doi:10.1007/s12079-021-00610-w.
118. Rando, T. A. Role of nitric oxide in the pathogenesis of muscular dystrophies: A 'two hit' hypothesis of the cause of muscle necrosis. *Microsc. Res. Tech.* (2001) doi:10.1002/jemt.1172.
119. Dudley, R. W. R. *et al.* Dynamic responses of the glutathione system to acute oxidative stress in dystrophic mouse (mdx) muscles. *Am. J. Physiol. - Regul. Integr. Comp. Physiol.* (2006) doi:10.1152/ajpregu.00031.2006.
120. Wehling-Henricks, M. *et al.* Arginine metabolism by macrophages promotes cardiac and muscle fibrosis in mdx muscular dystrophy. *PLoS One* (2010) doi:10.1371/journal.pone.0010763.
121. Serrano, M., Hannon, G. J. & Beach, D. A new regulatory motif in cell-cycle control causing specific inhibition of cyclin D/CDK4. *Nature* (1993) doi:10.1038/366704a0.
122. Campisi, J. Aging, Cellular Senescence, and Cancer. *Annu. Rev. Physiol.* (2013) doi:10.1146/annurev-physiol-030212-183653.
123. Hayflick, L. & Moorhead, P. S. The serial cultivation of human diploid cell strains. *Exp. Cell Res.* (1961) doi:10.1016/0014-4827(61)90192-6.
124. Muñoz-Espín, D. & Serrano, M. Cellular senescence: From physiology to pathology. *Nature Reviews Molecular Cell Biology* (2014) doi:10.1038/nrm3823.
125. Roy, A. L. *et al.* A Blueprint for Characterizing Senescence. *Cell* (2020) doi:10.1016/j.cell.2020.10.032.
126. Hernandez-Segura, A., Nehme, J. & Demaria, M. Hallmarks of Cellular Senescence. *Trends in Cell Biology* (2018) doi:10.1016/j.tcb.2018.02.001.
127. Hernandez-Segura, A. *et al.* Unmasking Transcriptional Heterogeneity in Senescent Cells. *Curr. Biol.* **27**, 2652-2660.e4 (2017).

128. Sharpless, N. E. & Sherr, C. J. Forging a signature of in vivo senescence. *Nature Reviews Cancer* (2015) doi:10.1038/nrc3960.
129. Dimri, G. P. *et al.* A biomarker that identifies senescent human cells in culture and in aging skin in vivo. *Proc. Natl. Acad. Sci. U. S. A.* (1995) doi:10.1073/pnas.92.20.9363.
130. De-Carvalho, D. P., Jacinto, A. & Saúde, L. The right time for senescence. *Elife* (2021) doi:10.7554/eLife.72449.
131. Hall, B. M. *et al.* p16(Ink4a) and senescence-associated β-galactosidase can be induced in macrophages as part of a reversible response to physiological stimuli. *Aging (Albany. NY)*. (2017) doi:10.18632/aging.101268.
132. Severino, J., Allen, R. G., Balin, S., Balin, A. & Cristofalo, V. J. Is β-galactosidase staining a marker of senescence in vitro and in vivo? *Exp. Cell Res.* (2000) doi:10.1006/excr.2000.4875.
133. Evangelou, K. *et al.* Robust, universal biomarker assay to detect senescent cells in biological specimens. *Aging Cell* (2017) doi:10.1111/acel.12545.
134. Narita, M. *et al.* Rb-mediated heterochromatin formation and silencing of E2F target genes during cellular senescence. *Cell* (2003) doi:10.1016/S0092-8674(03)00401-X.
135. Gorgoulis, V. *et al.* Cellular Senescence: Defining a Path Forward. *Cell* (2019) doi:10.1016/j.cell.2019.10.005.
136. Freund, A., Laberge, R. M., Demaria, M. & Campisi, J. Lamin B1 loss is a senescence-associated biomarker. *Mol. Biol. Cell* (2012) doi:10.1091/mbc.E11-10-0884.
137. Zhu, Y. *et al.* The achilles' heel of senescent cells: From transcriptome to senolytic drugs. *Aging Cell* (2015) doi:10.1111/acel.12344.
138. Rodier, F. *et al.* Persistent DNA damage signalling triggers senescence-associated inflammatory cytokine secretion. *Nat. Cell Biol.* (2009) doi:10.1038/ncb1909.
139. Coppé, J. P. *et al.* Senescence-associated secretory phenotypes reveal cell-nonautonomous functions of oncogenic RAS and the p53 tumor suppressor. *PLoS Biol.* (2008) doi:10.1371/journal.pbio.0060301.
140. Acosta, J. C. *et al.* A complex secretory program orchestrated by the inflammasome controls paracrine senescence. *Nat. Cell Biol.* (2013) doi:10.1038/ncb2784.
141. Acosta, J. C. *et al.* Chemokine Signaling via the CXCR2 Receptor Reinforces Senescence. *Cell* (2008) doi:10.1016/j.cell.2008.03.038.
142. Kuilman, T. *et al.* Oncogene-Induced Senescence Relayed by an Interleukin-Dependent Inflammatory Network. *Cell* (2008) doi:10.1016/j.cell.2008.03.039.
143. Basisty, N. *et al.* A proteomic atlas of senescence-associated secretomes for aging biomarker development. *PLoS Biol.* (2020) doi:10.1371/journal.pbio.3000599.
144. Hoare, M. *et al.* NOTCH1 mediates a switch between two distinct secretomes during senescence. *Nat. Cell Biol.* (2016) doi:10.1038/ncb3397.

145. Di Micco, R., Krizhanovsky, V., Baker, D. & d'Adda di Fagagna, F. Cellular senescence in ageing: from mechanisms to therapeutic opportunities. *Nature Reviews Molecular Cell Biology* (2021) doi:10.1038/s41580-020-00314-w.
146. Fafián-Labora, J. A. & O'Loghlen, A. Classical and Nonclassical Intercellular Communication in Senescence and Ageing. *Trends in Cell Biology* (2020) doi:10.1016/j.tcb.2020.05.003.
147. Coppé, J. P., Desprez, P. Y., Krtolica, A. & Campisi, J. The senescence-associated secretory phenotype: The dark side of tumor suppression. *Annual Review of Pathology: Mechanisms of Disease* (2010) doi:10.1146/annurev-pathol-121808-102144.
148. Chien, Y. *et al.* Control of the senescence-associated secretory phenotype by NF-κB promotes senescence and enhances chemosensitivity. *Genes Dev.* (2011) doi:10.1101/gad.17276711.
149. Coppé, J. P. *et al.* Tumor suppressor and aging biomarker p16 INK4a induces cellular senescence without the associated inflammatory secretory phenotype. *J. Biol. Chem.* (2011) doi:10.1074/jbc.M111.257071.
150. Rovillain, E. *et al.* Activation of nuclear factor-kappa B signalling promotes cellular senescence. *Oncogene* (2011) doi:10.1038/onc.2010.611.
151. Ohanna, M. *et al.* Senescent cells develop a parp-1 and nuclear factor-κB-associated secretome (PNAS). *Genes Dev.* (2011) doi:10.1101/gad.625811.
152. Kang, C. *et al.* The DNA damage response induces inflammation and senescence by inhibiting autophagy of GATA4. *Science (80-.).* (2015) doi:10.1126/science.aaa5612.
153. Mazzucco, A. E. *et al.* Genetic interrogation of replicative senescence uncovers a dual role for USP28 in coordinating the p53 and GATA4 branches of the senescence program. *Genes Dev.* (2017) doi:10.1101/gad.304857.117.
154. Freund, A., Patil, C. K. & Campisi, J. P38MAPK is a novel DNA damage response-independent regulator of the senescence-associated secretory phenotype. *EMBO J.* (2011) doi:10.1038/emboj.2011.69.
155. Toso, A. *et al.* Enhancing chemotherapy efficacy in pten-deficient prostate tumors by activating the senescence-associated antitumor immunity. *Cell Rep.* (2014) doi:10.1016/j.celrep.2014.08.044.
156. Dou, Z. *et al.* Cytoplasmic chromatin triggers inflammation in senescence and cancer. *Nature* (2017) doi:10.1038/nature24050.
157. Glück, S. *et al.* Innate immune sensing of cytosolic chromatin fragments through cGAS promotes senescence. *Nat. Cell Biol.* (2017) doi:10.1038/ncb3586.
158. Yang, H., Wang, H., Ren, U., Chen, Q. & Chena, Z. J. CGAS is essential for cellular senescence. *Proc. Natl. Acad. Sci. U. S. A.* (2017) doi:10.1073/pnas.1705499114.
159. Herranz, N. *et al.* mTOR regulates MAPKAPK2 translation to control the senescence-

associated secretory phenotype. *Nat. Cell Biol.* (2015) doi:10.1038/ncb3225.

160. Laberge, R. M. *et al.* MTOR regulates the pro-tumorigenic senescence-associated secretory phenotype by promoting IL1A translation. *Nat. Cell Biol.* (2015) doi:10.1038/ncb3195.
161. De Cecco, M. *et al.* LINE-1 derepression in senescent cells triggers interferon and inflammaging. *Nature* (2019).
162. Tasdemir, N. *et al.* BRD4 connects enhancer remodeling to senescence immune surveillance. *Cancer Discov.* (2016) doi:10.1158/2159-8290.CD-16-0217.
163. Aird, K. M. *et al.* HMGB2 orchestrates the chromatin landscape of senescence-associated secretory phenotype gene loci. *Journal of Cell Biology* (2016) doi:10.1083/jcb.201608026.
164. Chen, H. *et al.* MacroH2A1 and ATM Play Opposing Roles in Paracrine Senescence and the Senescence-Associated Secretory Phenotype. *Mol. Cell* (2015) doi:10.1016/j.molcel.2015.07.011.
165. Capell, B. C. *et al.* Mll1 is essential for the senescenceassociated secretory phenotype. *Genes Dev.* (2016) doi:10.1101/gad.271882.115.
166. Boumendil, C., Hari, P., Olsen, K. C. F., Acosta, J. C. & Bickmore, W. A. Nuclear pore density controls heterochromatin reorganization during senescence. *Genes Dev.* (2019) doi:10.1101/gad.321117.118.
167. Gasek, N. S., Kuchel, G. A., Kirkland, J. L. & Xu, M. Strategies for targeting senescent cells in human disease. *Nat. Aging* (2021) doi:10.1038/s43587-021-00121-8.
168. Demaria, M. *et al.* An essential role for senescent cells in optimal wound healing through secretion of PDGF-AA. *Dev. Cell* (2014) doi:10.1016/j.devcel.2014.11.012.
169. Baker, D. J. *et al.* Clearance of p16 Ink4a-positive senescent cells delays ageing-associated disorders. *Nature* (2011) doi:10.1038/nature10600.
170. Xu, M. *et al.* Senolytics improve physical function and increase lifespan in old age. *Nat. Med.* (2018) doi:10.1038/s41591-018-0092-9.
171. Hickson, L. T. J. *et al.* Senolytics decrease senescent cells in humans: Preliminary report from a clinical trial of Dasatinib plus Quercetin in individuals with diabetic kidney disease. *EBioMedicine* (2019) doi:10.1016/j.ebiom.2019.08.069.
172. Justice, J. N. *et al.* Senolytics in idiopathic pulmonary fibrosis: Results from a first-in-human, open-label, pilot study. *EBioMedicine* (2019) doi:10.1016/j.ebiom.2018.12.052.
173. Yosef, R. *et al.* Directed elimination of senescent cells by inhibition of BCL-W and BCL-XL. *Nat. Commun.* (2016) doi:10.1038/ncomms11190.
174. Zhu, Y. *et al.* Identification of a novel senolytic agent, navitoclax, targeting the Bcl-2 family of anti-apoptotic factors. *Aging Cell* (2016) doi:10.1111/acel.12445.
175. Chang, J. *et al.* Clearance of senescent cells by ABT263 rejuvenates aged hematopoietic stem cells in mice. *Nat. Med.* (2016) doi:10.1038/nm.4010.

176. Zhu, Y. *et al.* New agents that target senescent cells: The flavone, fisetin, and the BCL-XL inhibitors, A1331852 and A1155463. *Aging (Albany. NY)*. (2017) doi:10.18632/aging.101202.
177. Fuhrmann-Stroissnigg, H. *et al.* Identification of HSP90 inhibitors as a novel class of senolytics. *Nat. Commun.* (2017) doi:10.1038/s41467-017-00314-z.
178. Triana-Martínez, F. *et al.* Identification and characterization of Cardiac Glycosides as senolytic compounds. *Nat. Commun.* (2019) doi:10.1038/s41467-019-12888-x.
179. Tilstra, J. S. *et al.* NF-κB inhibition delays DNA damage - Induced senescence and aging in mice. *J. Clin. Invest.* (2012) doi:10.1172/JCI45785.
180. Xu, M. *et al.* JAK inhibition alleviates the cellular senescence-associated secretory phenotype and frailty in old age. *Proc. Natl. Acad. Sci. U. S. A.* (2015) doi:10.1073/pnas.1515386112.
181. Bao, J., Chen, Z., Xu, L., Wu, L. & Xiong, Y. Rapamycin protects chondrocytes against IL-18-induced apoptosis and ameliorates rat osteoarthritis. *Aging (Albany. NY)*. (2020) doi:10.18632/aging.102937.
182. Li, J. *et al.* Metformin limits osteoarthritis development and progression through activation of AMPK signalling. *Ann. Rheum. Dis.* (2020) doi:10.1136/annrheumdis-2019-216713.
183. Chen, D. *et al.* Metformin protects against apoptosis and senescence in nucleus pulposus cells and ameliorates disc degeneration in vivo. *Cell Death Dis.* (2016) doi:10.1038/cddis.2016.334.
184. Demirci, D., Dayanc, B., Mazi, F. A. & Senturk, S. The jekyll and hyde of cellular senescence in cancer. *Cells* (2021) doi:10.3390/cells10020208.
185. Storer, M. *et al.* XSenescence is a developmental mechanism that contributes to embryonic growth and patterning. *Cell* (2013) doi:10.1016/j.cell.2013.10.041.
186. Muñoz-Espín, D. *et al.* XProgrammed cell senescence during mammalian embryonic development. *Cell* (2013) doi:10.1016/j.cell.2013.10.019.
187. Davaapil, H., Brockes, J. P. & Yun, M. H. Conserved and novel functions of programmed cellular senescence during vertebrate development. *Dev.* (2017) doi:10.1242/dev.138222.
188. Da Silva-Álvarez, S. *et al.* Cell senescence contributes to tissue regeneration in zebrafish. *Aging Cell* (2020) doi:10.1111/acel.13052.
189. Yun, M. H., Davaapil, H. & Brockes, J. P. Recurrent turnover of senescent cells during regeneration of a complex structure. *Elife* (2015) doi:10.7554/eLife.05505.
190. Kim, K.-H., Chen, C.-C., Monzon, R. I. & Lau, L. F. Matricellular Protein CCN1 Promotes Regression of Liver Fibrosis through Induction of Cellular Senescence in Hepatic Myofibroblasts. *Mol. Cell. Biol.* (2013) doi:10.1128/mcb.00049-13.
191. Krizhanovsky, V. *et al.* Senescence of Activated Stellate Cells Limits Liver Fibrosis. *Cell* (2008) doi:10.1016/j.cell.2008.06.049.

192. Fitzner, B. *et al.* Senescence determines the fate of activated rat pancreatic stellate cells. *J. Cell. Mol. Med.* (2012) doi:10.1111/j.1582-4934.2012.01573.x.
193. Jun, J. Il & Lau, L. F. The matricellular protein CCN1 induces fibroblast senescence and restricts fibrosis in cutaneous wound healing. *Nat. Cell Biol.* (2010) doi:10.1038/ncb2070.
194. Banito, A. *et al.* Senescence impairs successful reprogramming to pluripotent stem cells. *Genes Dev.* (2009) doi:10.1101/gad.1811609.
195. Mosteiro, L. *et al.* Tissue damage and senescence provide critical signals for cellular reprogramming in vivo. *Science (80-.).* (2016) doi:10.1126/science.aaf4445.
196. Li, H. *et al.* The Ink4/Arf locus is a barrier for iPS cell reprogramming. *Nature* (2009) doi:10.1038/nature08290.
197. Ritschka, B. *et al.* The senescence-associated secretory phenotype induces cellular plasticity and tissue regeneration. *Genes Dev.* (2017) doi:10.1101/gad.290635.116.
198. Chiche, A. *et al.* Injury-Induced Senescence Enables In Vivo Reprogramming in Skeletal Muscle. *Cell Stem Cell* (2017) doi:10.1016/j.stem.2016.11.020.
199. Calcinotto, A. *et al.* Cellular senescence: Aging, cancer, and injury. *Physiol. Rev.* (2019) doi:10.1152/physrev.00020.2018.
200. Saul, D. *et al.* Modulation of fracture healing by the transient accumulation of senescent cells. *Elife* (2021) doi:10.7554/elife.69958.
201. Jin, H. *et al.* Epithelial innate immunity mediates tubular cell senescence after kidney injury. *JCI Insight* (2019) doi:10.1172/jci.insight.125490.
202. Bird, T. G. *et al.* TGFβ inhibition restores a regenerative response in acute liver injury by suppressing paracrine senescence. *Sci. Transl. Med.* (2018) doi:10.1126/scitranslmed.aan1230.
203. Ferreira-Gonzalez, S. *et al.* Paracrine cellular senescence exacerbates biliary injury and impairs regeneration. *Nat. Commun.* (2018) doi:10.1038/s41467-018-03299-5.
204. López-Otín, C., Blasco, M. A., Partridge, L., Serrano, M. & Kroemer, G. The hallmarks of aging. *Cell* (2013) doi:10.1016/j.cell.2013.05.039.
205. Krishnamurthy, J. *et al.* Ink4a/Arf expression is a biomarker of aging. *J. Clin. Invest.* (2004) doi:10.1172/jci200422475.
206. Melzer, D. *et al.* A common variant of the p16INK4a genetic region is associated with physical function in older people. *Mech. Ageing Dev.* (2007) doi:10.1016/j.mad.2007.03.005.
207. Jeck, W. R., Siebold, A. P. & Sharpless, N. E. Review: A meta-analysis of GWAS and age-associated diseases. *Aging Cell* (2012) doi:10.1111/j.1474-9726.2012.00871.x.
208. Schafer, M. J. *et al.* The senescence-associated secretome as an indicator of age and medical risk. *JCI Insight* (2020) doi:10.1172/jci.insight.133668.
209. Fabbri, E. *et al.* Aging and the burden of multimorbidity: Associations with inflammatory and anabolic hormonal biomarkers. *Journals Gerontol. - Ser. A Biol.*

Sci. Med. Sci. (2015) doi:10.1093/gerona/glu127.

210. Baker, D. J. *et al.* Naturally occurring p16 Ink4a-positive cells shorten healthy lifespan. *Nature* (2016) doi:10.1038/nature16932.
211. Baar, M. P. *et al.* Targeted Apoptosis of Senescent Cells Restores Tissue Homeostasis in Response to Chemotoxicity and Aging. *Cell* (2017) doi:10.1016/j.cell.2017.02.031.
212. Baker, D. J. *et al.* Opposing roles for p16Ink4a and p19Arf in senescence and ageing caused by BubR1 insufficiency. *Nat. Cell Biol.* (2008) doi:10.1038/ncb1744.
213. Borghesan, M., Hoogaars, W. M. H., Varela-Eirin, M., Talma, N. & Demaria, M. A Senescence-Centric View of Aging: Implications for Longevity and Disease. *Trends in Cell Biology* (2020) doi:10.1016/j.tcb.2020.07.002.
214. Wolstein, J. M. *et al.* INK4a knockout mice exhibit increased fibrosis under normal conditions and in response to unilateral ureteral obstruction. *Am. J. Physiol. - Ren. Physiol.* (2010) doi:10.1152/ajprenal.00378.2010.
215. Grosse, L. *et al.* Defined p16High Senescent Cell Types Are Indispensable for Mouse Healthspan. *Cell Metab.* (2020) doi:10.1016/j.cmet.2020.05.002.
216. Solovyeva, E. M. *et al.* New insights into molecular changes in skeletal muscle aging and disease: Differential alternative splicing and senescence. *Mech. Ageing Dev.* (2021) doi:10.1016/j.mad.2021.111510.
217. Zhang, H. *et al.* NAD+ repletion improves mitochondrial and stem cell function and enhances life span in mice. *Science (80-.).* (2016) doi:10.1126/science.aaf2693.
218. Blagosklonny, M. V. Geroconversion: Irreversible step to cellular senescence. *Cell Cycle* (2014) doi:10.4161/15384101.2014.985507.
219. Zhu, P. *et al.* The transcription factor Slug represses p16Ink4a and regulates murine muscle stem cell aging. *Nat. Commun.* (2019) doi:10.1038/s41467-019-10479-4.
220. Bae, J. H. *et al.* Satellite cell-specific ablation of Cdon impairs integrin activation, FGF signalling, and muscle regeneration. *J. Cachexia. Sarcopenia Muscle* (2020) doi:10.1002/jcsm.12563.
221. Cosgrove, B. D. *et al.* Rejuvenation of the muscle stem cell population restores strength to injured aged muscles. *Nat. Med.* (2014) doi:10.1038/nm.3464.
222. Baker, D. J., Weaver, R. L. & VanDeursen, J. M. P21 Both Attenuates and Drives Senescence and Aging in BubR1 Progeroid Mice. *Cell Rep.* (2013) doi:10.1016/j.celrep.2013.03.028.
223. Yousefzadeh, M. J. *et al.* An aged immune system drives senescence and ageing of solid organs. *Nature* (2021) doi:10.1038/s41586-021-03547-7.
224. Aw, D., Silva, A. B. & Palmer, D. B. Immunosenescence: Emerging challenges for an ageing population. *Immunology* (2007) doi:10.1111/j.1365-2567.2007.02555.x.
225. Dungan, C. M. *et al.* Deletion of SA β-Gal+ cells using senolytics improves muscle regeneration in old mice. *Aging Cell* **21**, e13528 (2022).

226. Mu, X. *et al.* The role of Notch signaling in muscle progenitor cell depletion and the rapid onset of histopathology in muscular dystrophy. *Hum. Mol. Genet.* (2015) doi:10.1093/hmg/ddv055.
227. Le Roux, I., Konge, J., Le Cam, L., Flamant, P. & Tajbakhsh, S. Numb is required to prevent p53-dependent senescence following skeletal muscle injury. *Nat. Commun.* (2015) doi:10.1038/ncomms9528.
228. Sugihara, H. *et al.* Cellular senescence-mediated exacerbation of Duchenne muscular dystrophy. *Sci. Rep.* (2020) doi:10.1038/s41598-020-73315-6.
229. Bigot, A. *et al.* Large CTG repeats trigger p16-dependent premature senescence in myotonic dystrophy type 1 muscle precursor cells. *Am. J. Pathol.* (2009) doi:10.2353/ajpath.2009.080560.
230. Kudryashova, E., Kramerova, I. & Spencer, M. J. Satellite cell senescence underlies myopathy in a mouse model of limb-girdle muscular dystrophy 2H. *J. Clin. Invest.* (2012) doi:10.1172/JCI59581.
231. Young, L. V. *et al.* Loss of dystrophin expression in skeletal muscle is associated with senescence of macrophages and endothelial cells. *Am. J. Physiol. - Cell Physiol.* (2021) doi:10.1152/ajpcell.00397.2020.
232. Chikenji, T. S. *et al.* pl6INK4A-expressing mesenchymal stromal cells restore the senescence- clearance- regeneration sequence that is impaired in chronic muscle inflammation. *Sapporo Med. J.* (2019) doi:10.1016/j.ebiom.2019.05.012.
233. Saito, Y., Chikenji, T. S., Matsumura, T., Nakano, M. & Fujimiya, M. Exercise enhances skeletal muscle regeneration by promoting senescence in fibro-adipogenic progenitors. *Nat. Commun.* (2020) doi:10.1038/s41467-020-14734-x.
234. Martin, C. *et al.* CD36 as a lipid sensor. *Physiol. Behav.* (2011) doi:10.1016/j.physbeh.2011.02.029.
235. Silverstein, R. L. & Febbraio, M. CD36, a scavenger receptor involved in immunity, metabolism, angiogenesis, and behavior. *Science Signaling* (2009) doi:10.1126/scisignal.272re3.
236. Stewart, C. R. *et al.* CD36 ligands promote sterile inflammation through assembly of a Toll-like receptor 4 and 6 heterodimer. *Nat. Immunol.* (2010) doi:10.1038/ni.1836.
237. Lizardo, D. Y., Lin, Y. L., Gokcumen, O. & Atilla-Gokcumen, G. E. Regulation of lipids is central to replicative senescence. *Mol. Biosyst.* (2017) doi:10.1039/c6mb00842a.
238. Chan, M. *et al.* Novel insights from a multiomics dissection of the Hayflick limit. *Elife* (2022) doi:10.7554/elife.70283.
239. Saitou, M. *et al.* An evolutionary transcriptomics approach links CD36 to membrane remodeling in replicative senescence. *Mol. Omi.* (2018) doi:10.1039/c8mo00099a.
240. Chong, M. *et al.* CD 36 initiates the secretory phenotype during the establishment of cellular senescence . *EMBO Rep.* (2018) doi:10.15252/embr.201745274.
241. Verpoorten, S. *et al.* Loss of CD36 protects against diet-induced obesity but results

in impaired muscle stem cell function, delayed muscle regeneration and hepatic steatosis. *Acta Physiol.* (2020) doi:10.1111/apha.13395.

242. Debacq-Chainiaux, F., Erusalimsky, J. D., Campisi, J. & Toussaint, O. Protocols to detect senescence-associated beta-galactosidase (SA-βgal) activity, a biomarker of senescent cells in culture and in vivo. *Nat. Protoc.* (2009) doi:10.1038/nprot.2009.191.
243. Doura, T. *et al.* Detection of LacZ-Positive Cells in Living Tissue with Single-Cell Resolution. *Angew. Chemie - Int. Ed.* (2016) doi:10.1002/anie.201603328.
244. Franceschi, C. & Campisi, J. Chronic inflammation (Inflammaging) and its potential contribution to age-associated diseases. *Journals of Gerontology - Series A Biological Sciences and Medical Sciences* (2014) doi:10.1093/gerona/glu057.
245. Hédouin, S., Grillo, G., Ivkovic, I., Velasco, G. & Francastel, C. CENP-A chromatin disassembly in stressed and senescent murine cells. *Sci. Rep.* (2017) doi:10.1038/srep42520.
246. Maehara, K., Takahashi, K. & Saitoh, S. CENP-A Reduction Induces a p53-Dependent Cellular Senescence Response To Protect Cells from Executing Defective Mitoses. *Mol. Cell. Biol.* (2010) doi:10.1128/mcb.01318-09.
247. Kandhaya-Pillai, R. *et al.* TNFα-senescence initiates a STAT-dependent positive feedback loop, leading to a sustained interferon signature, DNA damage, and cytokine secretion. *Aging (Albany. NY).* (2017) doi:10.18632/aging.101328.
248. Meng, X. M., Nikolic-Paterson, D. J. & Lan, H. Y. TGF-β: The master regulator of fibrosis. *Nature Reviews Nephrology* (2016) doi:10.1038/nrneph.2016.48.
249. Rhinn, M., Ritschka, B. & Keyes, W. M. Cellular senescence in development, regeneration and disease. *Dev.* (2019) doi:10.1242/dev.151837.
250. Prieto, L. I., Graves, S. I. & Baker, D. J. Insights from In Vivo Studies of Cellular Senescence. *Cells* (2020) doi:10.3390/cells9040954.
251. Shavlakadze, T. *et al.* Age-Related Gene Expression Signature in Rats Demonstrate Early, Late, and Linear Transcriptional Changes from Multiple Tissues. *Cell Rep.* (2019) doi:10.1016/j.celrep.2019.08.043.
252. Stegeman, R. & Weake, V. M. Transcriptional Signatures of Aging. *Journal of Molecular Biology* (2017) doi:10.1016/j.jmb.2017.06.019.
253. Benayoun, B. A. *et al.* Remodeling of epigenome and transcriptome landscapes with aging in mice reveals widespread induction of inflammatory responses. *Genome Res.* (2019) doi:10.1101/gr.240093.118.
254. Jung, S., Singh, K. & Del Sol, A. FunRes: Resolving tissue-specific functional cell states based on a cell-cell communication network model. *Brief. Bioinform.* (2021) doi:10.1093/bib/bbaa283.
255. Nazir, S. *et al.* Interaction between high-density lipoproteins and inflammation: Function matters more than concentration! *Advanced Drug Delivery Reviews* (2020)

doi:10.1016/j.addr.2020.10.006.

256. Connelly, M. A., Shalaurova, I. & Otvos, J. D. High-density lipoprotein and inflammation in cardiovascular disease. *Translational Research* (2016) doi:10.1016/j.trsl.2016.01.006.
257. Rigamonti, E., Zordan, P., Sciorati, C., Rovere-Querini, P. & Brunelli, S. Macrophage plasticity in skeletal muscle repair. *BioMed Research International* (2014) doi:10.1155/2014/560629.
258. Desdín-Micó, G. *et al.* T cells with dysfunctional mitochondria induce multimorbidity and premature senescence. *Science (80-.).* (2020) doi:10.1126/science.aax0860.
259. Chiche, A., Chen, C. & Li, H. The crosstalk between cellular reprogramming and senescence in aging and regeneration. *Experimental Gerontology* (2020) doi:10.1016/j.exger.2020.111005.
260. Kozakowska, M., Pietraszek-Gremplewicz, K., Jozkowicz, A. & Dulak, J. The role of oxidative stress in skeletal muscle injury and regeneration: focus on antioxidant enzymes. *Journal of Muscle Research and Cell Motility* (2015) doi:10.1007/s10974-015-9438-9.
261. Powers, S. K., Ji, L. L., Kavazis, A. N. & Jackson, M. J. Reactive oxygen species: Impact on skeletal muscle. *Compr. Physiol.* (2011) doi:10.1002/cphy.c100054.
262. Myburgh, K. H., Kruger, M. J. & Smith, C. Accelerated skeletal muscle recovery after in vivo polyphenol administration. *J. Nutr. Biochem.* (2012) doi:10.1016/j.jnutbio.2011.05.014.
263. Gierer, P., Röther, J., Mittlmeier, T., Gradl, G. & Vollmar, B. Ebselen reduces inflammation and microvascular perfusion failure after blunt skeletal muscle injury of the rat. *J. Trauma - Inj. Infect. Crit. Care* (2010) doi:10.1097/TA.0b013e3181b28a18.
264. Hnia, K. *et al.* L-arginine decreases inflammation and modulates the nuclear factor-κB/matrix metalloproteinase cascade in Mdx muscle fibers. *Am. J. Pathol.* (2008) doi:10.2353/ajpath.2008.071009.
265. Messina, S. *et al.* Flavocoxid counteracts muscle necrosis and improves functional properties in mdx mice: A comparison study with methylprednisolone. *Exp. Neurol.* (2009) doi:10.1016/j.expneurol.2009.09.015.
266. Whitehead, N. P., Pham, C., Gervasio, O. L. & Allen, D. G. N-Acetylcysteine ameliorates skeletal muscle pathophysiology in mdx mice. *J. Physiol.* (2008) doi:10.1113/jphysiol.2007.148338.
267. Kumari, R. & Jat, P. Mechanisms of Cellular Senescence: Cell Cycle Arrest and Senescence Associated Secretory Phenotype. *Frontiers in Cell and Developmental Biology* (2021) doi:10.3389/fcell.2021.645593.
268. Fukada, S. I. *et al.* Genetic background affects properties of satellite cells and mdx phenotypes. *Am. J. Pathol.* (2010) doi:10.2353/ajpath.2010.090887.

269. Suelves, M. *et al*. uPA deficiency exacerbates muscular dystrophy in MDX mice. *J. Cell Biol.* (2007) doi:10.1083/jcb.200705127.
270. Grounds, M. D., Sorokin, L. & White, J. Strength at the extracellular matrix-muscle interface. *Scandinavian Journal of Medicine and Science in Sports* (2005) doi:10.1111/j.1600-0838.2005.00467.x.
271. Del Prete, Z., Musarò, A. & Rizzuto, E. Measuring mechanical properties, including isotonic fatigue, of fast and slow MLC/mIgf-1 transgenic skeletal muscle. *Ann. Biomed. Eng.* (2008) doi:10.1007/s10439-008-9496-x.
272. Le, G., Lowe, D. A. & Kyba, M. Freeze injury of the tibialis anterior muscle. *Methods Mol. Biol.* (2016) doi:10.1007/978-1-4939-3810-0_3.
273. Fumagalli, M. *et al*. Telomeric DNA damage is irreparable and causes persistent DNA-damage-response activation. *Nat. Cell Biol.* (2012) doi:10.1038/ncb2466.
274. Freund, A., Orjalo, A. V., Desprez, P. Y. & Campisi, J. Inflammatory networks during cellular senescence: causes and consequences. *Trends in Molecular Medicine* (2010) doi:10.1016/j.molmed.2010.03.003.
275. Flor, A. C., Wolfgeher, D., Wu, D. & Kron, S. J. A signature of enhanced lipid metabolism, lipid peroxidation and aldehyde stress in therapy-induced senescence. *Cell Death Discov.* (2017) doi:10.1038/cddiscovery.2017.75.
276. Stahl, A. A current review of fatty acid transport proteins (SLC27). *Pflugers Archiv European Journal of Physiology* (2004) doi:10.1007/s00424-003-1106-z.
277. Zani, I. A. *et al*. Scavenger receptor structure and function in health and disease. *Cells* (2015) doi:10.3390/cells4020178.

SUPPLEMENTARY INFORMATION

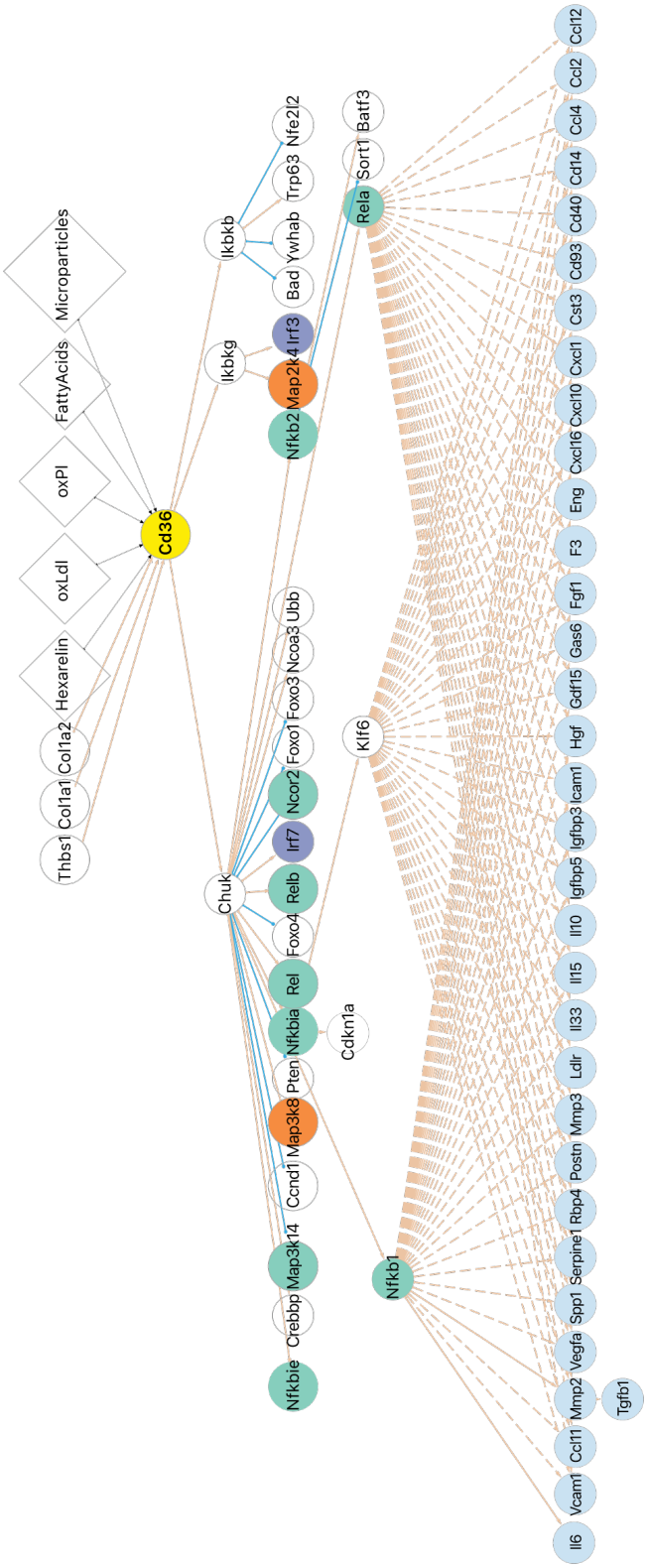

Supplementary Figure 1.

Subnetwork of significant *Cd36* upstream and downstream signalling interactions pulled out from FunRes global signalling interaction network for Sen SCs population at 3 DPI. Green nodes are related to NFκB cascade, orange ones to MAPK signalling and violet to Interferon regulatory factors (IRFs).